No. 3/2017

HIDRAULICA

HYDRAULICS-PNEUMATICS-TRIBOLOGY-ECOLOGY-SENSORICS-MECHATRONICS

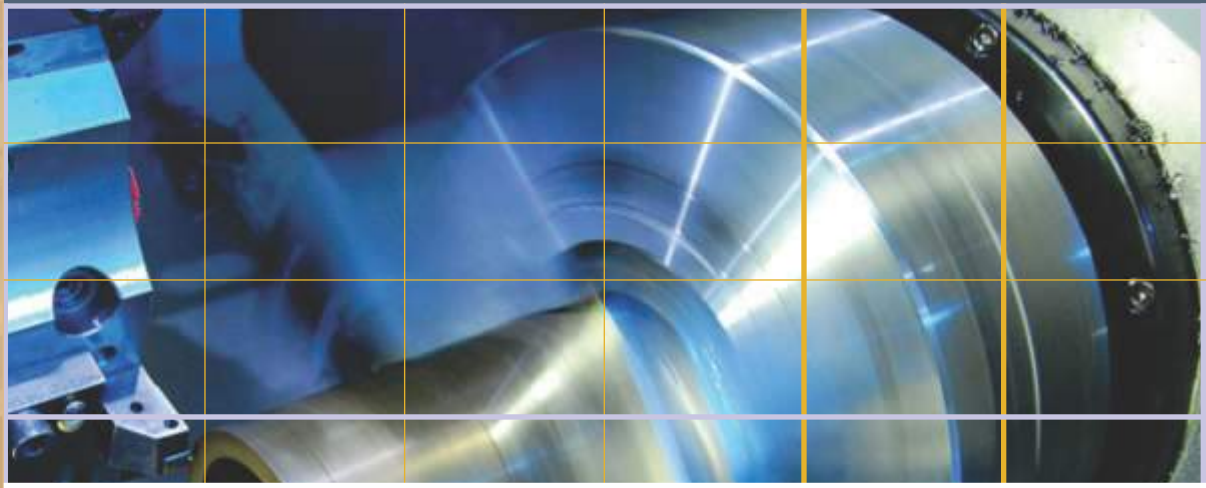

http://hidraulica.fluidas.ro

ISSN 1453 - 7303
ISSN-L 1453 - 7303

CONTENTS

Published by:
Hydraulics and Pneumatics Research Institute, Bucharest-Romania
Address: 14 Cuţitul de Argint, district 4, Bucharest, 040558, Romania
Phone: +40 21 336 39 91; Fax: +40 21 337 30 40; e-Mail: ihp@fluidas.ro; Web: www.ihp.ro
with support from:
National Professional Association of Hydraulics and Pneumatics in Romania - FLUIDAS
e-Mail: fluidas@fluidas.ro; Web: www.fluidas.ro

HIDRAULICA Magazine is indexed by international databases

ISSN 1453 – 7303; ISSN – L 1453 – 7303

EDITORIAL

On Digital Hydraulics

Ph.D.Eng. Petrin DRUMEA
DIRECTOR OF PUBLICATION

Hydraulics, actually hydraulic drives, has experienced a great development as a result of the emergence of new areas where high forces and acceptable maneuverability were required. For a long time specialists have focused on research and development directions which concerned increasing the level of work pressures and the speed of response of the equipment, which has led to a noticeable upgrading of the field over a long period of time.

Likewise, research in the field of hydraulic drives had a long period in which the creative forces have been focused on the setting and tracking systems, which in this case, as well, have been factors of great progress.

Two new directions, initially developed in the fields of electronics and electrotechnics, have caused that in many industrial sub-domains to face the issue of eliminating hydraulic drives as a working technology. These directions were one related to energy efficiency and the other related to digitization of control and drive systems.

Thus, over the past 20 years, research has been made and there can even be reported some industrial achievements related to digital hydraulics as a modern and efficient solution by which hydraulic drives try to meet the new requirements of the industry. In the latest years the research center at IHP Bucharest has joined the research centres specific to the new technical and scientific current existing in Finland, Austria, UK, USA, Japan, Germany and China; although at its beginning, the Romanian center was able to develop a test base in the field of digital hydraulics, to create a team of specialists and to achieve the first practical items of pumps, cylinders and directional control valves.

It is obvious that digital hydraulics is not the only direction to modernize hydraulics, but anyway, it is one of the answers to the great problem of mankind, namely energy efficiency, taking into account the current situation in which hydraulic systems generally have losses ranging between 25% and 65%.

The first remark of the specialists who are part of the newly created team is that there is much reluctance about digital hydraulics, and especially the approaches are still too personal and not very applied. Hopes are quite high, and what has already been achieved can become the basis for major changes in the field of hydraulic drives in years to come.

Remanufacturing of Hydrostatic Systems for Heavy Duty Vertical Lathes

Prof. PhD Eng. **Dan PRODAN**[1]

[1] University POLITEHNICA of Bucharest, prodand2004@yahoo.com

Abstract: *In this paper the author presents a part of the theoretical and experimental research conducted during the remanufacturing of a heavy duty vertical lathe. The remanufacturing of this machine-tool involved the re-design of the hydrostatic system for table suspension. These very heavy machine-tools use hydrostatic systems for supporting the main spindle on bearings, which allows them to take over thrust loads over 100 to at speeds of 50 RPM. In these conditions, the hydrostatic system must be well dimensioned, stable and controllable both in conventional operation mode and especially in CNC operating mode in order to ensure the working parameters.*

Keywords: *heavy vertical lathe, hydrostatic supporting on bearings, CNC machine-tools*

1. Introductory notions

The systems where the load operates on an oil film made and maintained by means of a pressure hydraulic source that necessarily includes a pump [1, 2, 3]. are defined as hydrostatic lubrication systems. If there is also a movement between surfaces, the lubrication system is mixed (hydrostatic and hydrodynamic). In practice there is no clear differentiation of these systems: the hydrostatic lubrication refers to the systems where the lubricating film is obtained from a pump.
The specific elements of the hydrostatic lubrication systems are:

- High stiffness, which allows a steady and accurate position even if there are big variations of the load;
- The wear of elements is non-existent thanks to the permanent film of oil, even during the stop phases;
- The loads are discharged evenly because in a lubrication pocket the pressure is the same anywhere;
- The quality of surfaces is less important than in the case of hydrodynamic lubrication because the load is taken over on a continuous surface rather than in points;
- A good cooling of the moving surfaces is achieved due to the continuous flow.

Among the disadvantages of these systems we can mention:

- The units are expensive, requiring specific devices such as: pumps, pressure valves, filters, throttle valves, flow control valves etc. [4, 5, 6, 7];
- Because of the relatively large number of elements, the reliability of these systems can raise issues.

Solving them involves constructive complications. First, the existence of permanent pressure must be confirmed because its lack could lead to the destruction of the surfaces in contact.
As for the mathematical apparatus used below, it has to be said that it is based on flow equations that are valid only if the thickness of lubricant film is smaller than its length and width. Also, inertial phenomena and temperature variations are neglected.

2. Hydrostatic pockets for heavy duty vertical lathes [1, 8, 9]

In the case of these machine-tools, the hydrostatic pockets are located at the level of the bed and are distributed on one or several rows, in the area of taking over the efforts from the faceplate, as in Figure 1, where it was noted: 1 - zone of pockets, 2 - pockets, 3 - zone for external discharge, 4 - zone for internal discharge.
Hereinafter we take into consideration an unfolded pocket to which the radiuses are neglected as in figure 2, where the following notations were made: L and l - total sizes of pocket, l-2a and L-2b - actual sizes of the pocket of depth e.

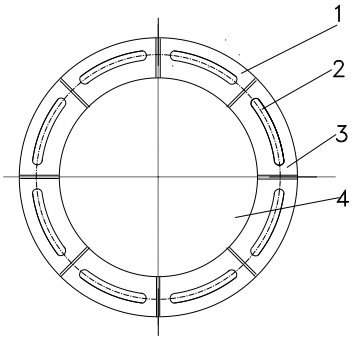

Fig. 1. Location of hydrostatic pockets on heavy duty vertical lathes

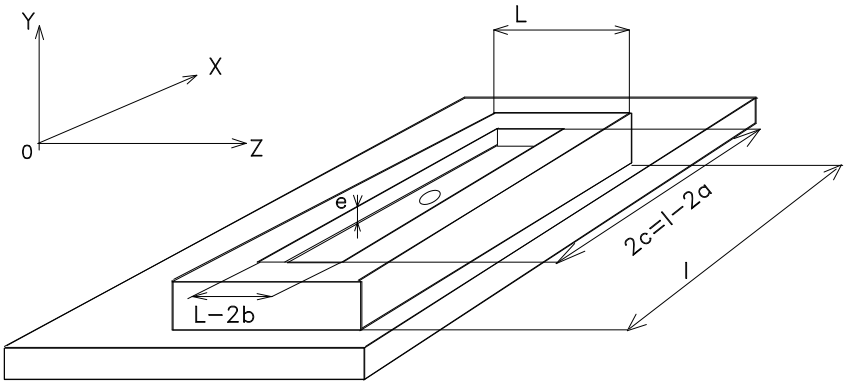

Fig. 2. Geometrical elements of a hydrostatic pocket

The table of the vertical lathe, on which the workpiece is located, is supported on an oil film that has the thickness h, as in Figure 3.

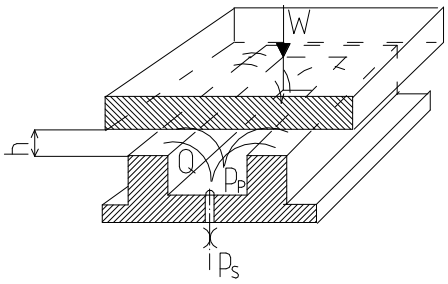

Fig. 3. Defining film thickness

The source of hydrostatic energy is a unit [1, 4, 5, 10] with the pressure p_S; the flow control valve allows the pressure p_P to be adjusted for each pocket. The flow Q, at the level of a pocket, is discharged through the gap h on the surface described on its perimeter [1]. The flow rate of the oil through the gap h depends on a number of factors: speed of table, pressure p_P, flow area characterized by the coordinates (x, y, z), according to Figure 2.
In order to establish the mathematical model it is considered that the principle of superposition can be applied.
For the calculation diagram in Figure 3 one obtains the values of the load W and the required flow Q [1]:

$$W = p_P \cdot S \cdot K_W \tag{1}$$

$$Q = \frac{p_P \cdot h^3}{\mu} \cdot K_Q \tag{2}$$

$$S = L \cdot l \tag{3}$$

In the relations above there are also noted: p_P - pressure in pocket, μ - dynamic viscosity of oil, K_W - load constant of the pocket, K_Q – flow constant of the pocket. K_W and K_Q constants depend on the geometrical sizes that define the pocket [1, 10].
In order for the system to be stable it is necessary that a tendency to return occurs after a movement out of the balance position which was caused by an external force.
This desideratum is achievable if the pressure p_P is properly chosen, depending on film thickness. In the presence of a hydraulic resistor placed between the pressure source and the pocket as in Figure 3, it can be written for the flow rate:

$$Q_f = f(p_S - p_P) \tag{4}$$

The following notations have been used in the relation above: Q_f – flow rate through resistor, considered equal to Q flow of the relation (2); $f(p_s\text{-}p_P)$ - function of definition of pressure drop flow; p_s – source pressure; p_P – pressure in pocket.
If the two expressions of the flow rate are equal, the rigidity λ can be defined as follows:

$$\lambda = -\frac{\partial W}{\partial h} = -\frac{\partial W}{\partial p_P}\frac{\partial p_P}{\partial h} = -\frac{3W}{h}\frac{1}{1-\frac{p_P}{Q}\frac{\partial Q}{\partial p_P}} \tag{5}$$

Rigidity λ depends on the type of resistor chosen. The intended values of rigidity can be obtained by a suitable choice of the resistor. There are used fixed or adjustable resistors.

3. How to adjust the hydrostatic pockets

Capillary tubes, hydraulic resistors (throttle valves) or flow control valves [1]. are commonly used for flow and pressure regulation.
For these systems, in this order, the relation (5) becomes:

$$Q_{f1} = K_1 S_1 (p_S - p_P) \tag{6}$$

$$Q_{f2} = K_2 S_2 \sqrt{p_S - p_P} \tag{7}$$

$$Q_{f3} = K_3 S_3 \tag{8}$$

In the relations (6) - (8) it has been also noted: K_1, K_2, K_3 - specific constants, S_1, S_2, S_3 - flowing surfaces of the respective element. If the subunitary ratio of the pocket pressure is noted by β and the source ratio ($\beta = p_P/p_S$), for the rigidity λ it is obtained:

$$\lambda_1 = -\frac{3S_1K_W}{h} p_S \beta (1-\beta) \tag{9}$$

$$\lambda_2 = -\frac{6S_2K_W}{h} p_S \beta \frac{1-\beta}{2-\beta} \tag{10}$$

$$\lambda_3 = -\frac{3S_3K_W}{h} p_S \beta \tag{11}$$

$$0 \le \beta \le 1 \tag{12}$$

Figure 4 shows, for the three cases, the rigidity dependence on the thickness of oil film. Usually, this film does not exceed 0.5 mm in the case of these machines.

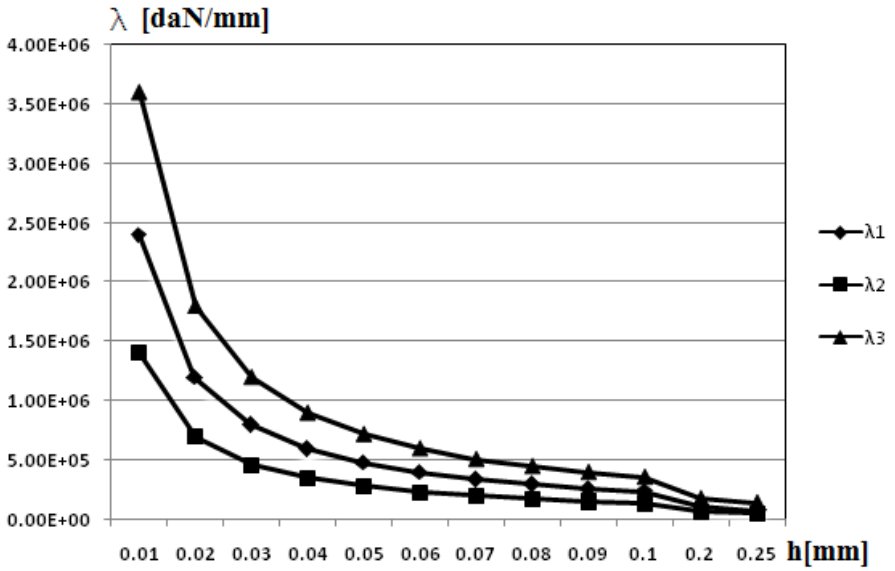

Fig. 4. Rigidity dependence on film thickness

For the lathe to be rebuilt, the intended maximum thickness was 0.15 mm. From the considerations shown above it results that the regulation systems with flow control valves are preferable [3, 4, 7]. for rigidity reasons. The use of serpentines (capillary hydraulic resistors) is a cheap and simple design solution which has however major drawbacks because of the difficulties of adjustment and the risk of clogging with impurities. In the case of clogging, the interventions for repairs last long and involve the change of serpentines and recalibration of the new ones.
The throttle valves are much cheaper than the flow control valves but, as it results from the relations above, the regulated flow rate depends on the load (pocket pressure p_P). This thing influences the accuracy of machine faceplate due to the variations of *h* film thickness, according to the relation:

$$h = \sqrt[3]{\frac{QS\mu K_W}{WK_Q}} \tag{12}$$

The variations of load *W* lead to variations of pressure; these ones change the flow rate which, in its turn, influences the thickness of the film *h*. In order to study the stability of the flow rate and, indirectly, of the film thickness, there were used specialized programs of simulation [11, 12].
Figure 5 shows the influence of pressure variations on the flow rate in the pocket when it is adjusted by a throttle valve.

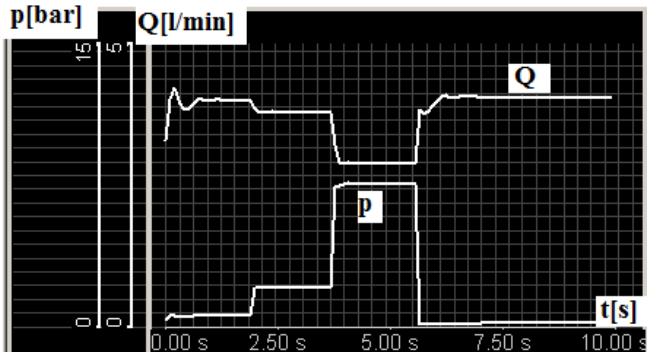

Fig. 5. Influence of pressure variations on the flow rate in the pocket when it is adjusted by a throttle valve

As shown above, the variations of pressure entail uncontrolled modifications of the flow rate and hence of the size *h*.

If a flow control valve is used instead of a throttle valve, one can notice that the pressure variations do not influence the flow rate value within certain limits, according to Figure 6. These limits depend on the adjustment of the flow control valve, on pocket geometry but also on the viscosity and temperature of the oil [1, 2].

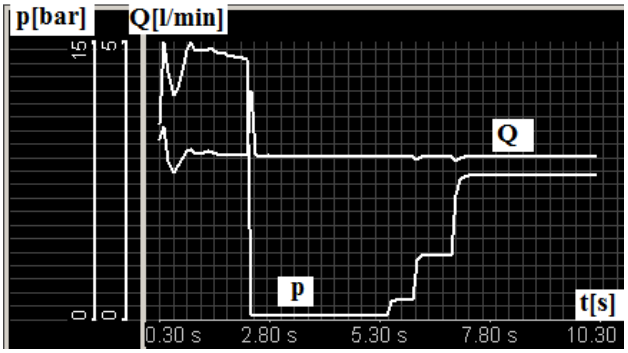

Fig. 6. Influence of pressure variations on the flow rate in the pocket when the flow is adjusted by a flow control valve

The time required for stabilization at start-up is of 3s approximately and is not a problem for a machine-tool in this range.

4. Setting the hydrostatic diagram

The hydraulic diagram in Figure 7 was developed in order to achieve the hydrostatic unit.

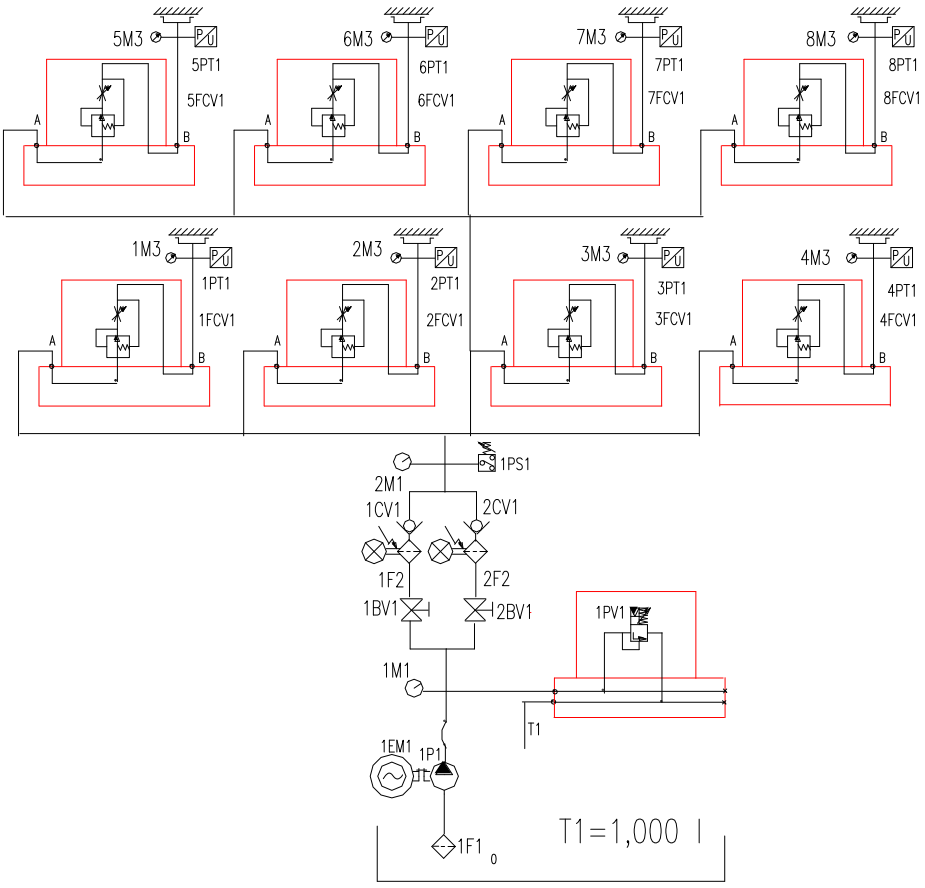

Fig. 7. Hydraulic diagram for the lathe with eight pockets

From the tank T1 the pump 1P1, driven by the electric motor 1EM1, sucks the oil through the suction filter 1F1. The oil is sent through the valves 1BV1 and 2BV1 to the pressure filters 1F2 and 2F2. These ones are provided with clogging electrical indicators. The eight flow control valves 1-8 FCV1 are supplied through the check valves1CV1 and 2CV1. For each pocket there is one manometer 1-8 M3 and one pressure transducer 1-8 PT1. The source pressure is regulated by means of the pressure valve 1PV1, and the value of the maximum pressure is displayed on the manometer 1M1. The filter that operates at a given moment is chosen with the help of the valves 1-2V1. If this filter is clogged, it will be separated by means of the valves and the stand-by filter will be coupled instead. The replacement of the clogged cartridge can be made without having to turn off the machine. The supply pressure of the pockets can be viewed on the manometer 2M1, located near the operator. The pressure required to operate is confirmed by the pressure switch 1PS1. Taking into account the characteristics and performances of the machine, it was chosen a pump with the capacity of q_p = 48 cm^3, driven by an electric motor with the rated speed of n_{EM} = 1470 RPM and a power of P_{EM} = 4 kW.
In these conditions, two-way flow control valves [6] were selected for the eight pockets, with the main features shown in Figure 8.

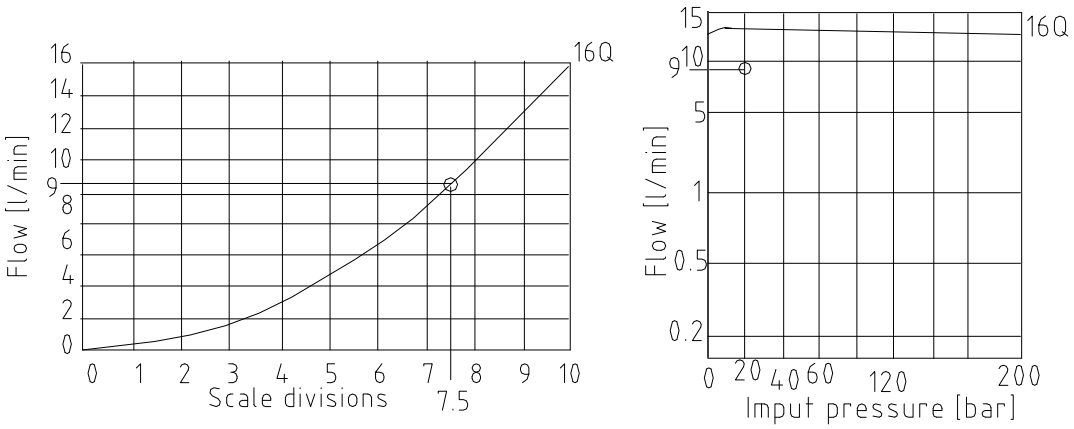

a b

Fig. 8. Operational characteristics of the flow control valve used

In the theoretical case where all eight pockets are identical and the workload is evenly distributed, as per Figure 8a, the flow control valves allow a controllable adjustment from 0 to 7.5 divisions out of 10 at the most. It is estimated that the maximum working pressure shown on the manometer 2M1 will not exceed 20 bar, in which case, according to the characteristics in Figure 8b, it is possible that a maximum flow rate of 16 l/min is adjusted on each pocket. Under these conditions, in conformity with the relation (12), it is estimated that the maximum theoretical thickness of the film will be: $h_{Max} = 0.6\text{mm}$. In fact, a film of 0.15 - 0.2 mm evenly made is the maximum allowed.
To determine the surface *S* in the relation (3) and the constants K_W and K_Q in the relations (1) and (2) we consider the expressions [1]:

$$S = \pi(R_E^2 - R_I^2) \tag{13}$$

$$K_W = \frac{1}{2(R_E^2 - R_I^2)}\left(\frac{R_E^2 - R_2^2}{ln\frac{R_E}{R_2}} - \frac{R_1^2 - R_I^2}{ln\frac{R_1}{R_I}}\right) \tag{14}$$

$$K_Q = \frac{\pi}{6}\left(\frac{1}{ln\frac{R_E}{R_2}} + \frac{1}{ln\frac{R_1}{R_I}}\right) \tag{15}$$

In the relations above there were noted: R_E - outer radius of guideways, R_I - inner radius of guideways, R_1 - inner radius of pockets, R_2 - outer radius of pockets, as in Figure 9.

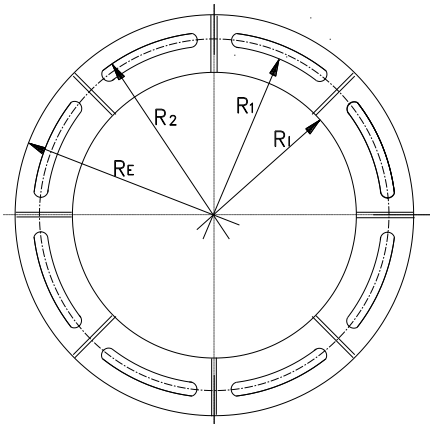

Fig. 9. Geometrical elements defining the hydrostatic pockets

5. Theoretical premises

After the measurement of pockets size of the remanufactured machine, the following values were obtained for the surface *S* and the constants K_W and K_Q: S = 75000 cm^2, K_W = 0.85 [-], K_Q = 21 [-]. The faceplate of the machine has a mass of 20 000 Kg and can bear a workpiece of 100 000 Kg. In these conditions, the required pocket pressures are determined by means of the relation (1) and the necessary flow rate for different values of the film is determined using the relation (2). The theoretical values obtained for two oils with different viscosities are listed in Table 1.

Table 1: The theoretical values obtained for two oils

	W [daN]	p [bar]	h [mm]	Oil v = 46 mm^2/s Q [l/min]	Oil v = 20 mm^2/s Q [l/min]
1	20000	0.4	0.15	4.4	10
2	20000	0.4	0.3	33	76
3	100000	2	0.15	21	48
4	120000	2.5	0.1	8	18
5	120000	2.5	0.15	26	60
6	150000	3	0.15	31	72

For the sizing of the pump 1P1 in the diagram shown in Figure 7 at these flow rates, there were also taken into account the flow rates required for lubricating the feed box, the pinion-ring gear mechanism and the central bearings.
For a certain adjustment of the flow control valves, corresponding to a constant flow rate, the following relation can be used for estimating the dependence of film thickness on the load:

$$p_P h^3 = ct. \tag{16}$$

As shown in Table 1, the necessary flow rate – depending on oil viscosity - for a maximum film of 0.15 mm, at a total load of 120 000 daN, is in the range of 26-60 l/min.
If the intention is to obtain a film of 0.15 mm for a load of 120 000 daN, in idle running without load, according to the relation (16) the film will have a thickness of 0.3 mm. Generally, during the machining operations, the film thickness should be as small as possible so as not to affect the machining accuracy because of the compressibility of the oil. In the case of this machine, it can be considered that the variation of oil thickness Δh due to the variation of vertical forces (including those due to the variations of weight) has the expression below:

$$\Delta h = h \cdot \Delta F \cdot 9 \cdot 10^{-10} \text{ [mm]} \tag{17}$$

In the relation (17) the variation of force ΔF is expressed in daN.
According to Table 1, the capacity of the machine in terms of hydraulic unit makes also possible the takeover of bigger loads, 190 000 daN for example, if the pump flow rate is the necessary one.

In fact, at loads of more than 120 000 daN, the elastic deformations of the mechanical system affect the machining accuracy. Under these conditions, it is recommended to limit the weight of the workpiece at 100 000 daN.
The vertical travel of the faceplate is limited using a system of radial-axial bearings as in Figure 10.

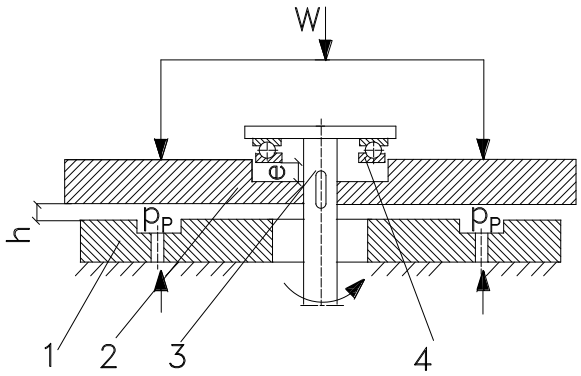

Fig. 10. The system of radial-axial bearings used for limiting the vertical travel of the faceplate

Thanks to pressure p_P in the pockets between faceplate 2 and bed 1, an oil film of thickness *h* is made in presence of the load *W*. The faceplate 2 is driven by the spindle 3. Between the bearing 4 and the faceplate 2 there is the size *e*. If the film *h* grows, at some point the gap *e* may become "0". From now on the surplus of pressure that exceeds the value required for the takeover of the load *W* leads to the emergence of an thrust force that will be discharged onto the bearing. It must not exceed the admissible value, in conformity with the catalogue [6].

6. Experimental results and achievements

The hydraulic unit for suspension was made in the form of a cylindrical tank T1 of 1000 l on which most of the devices were assembled as in Figure 11. The hydraulic devices shown in this figure have the same notations as those in the hydraulic diagram of Figure 7.

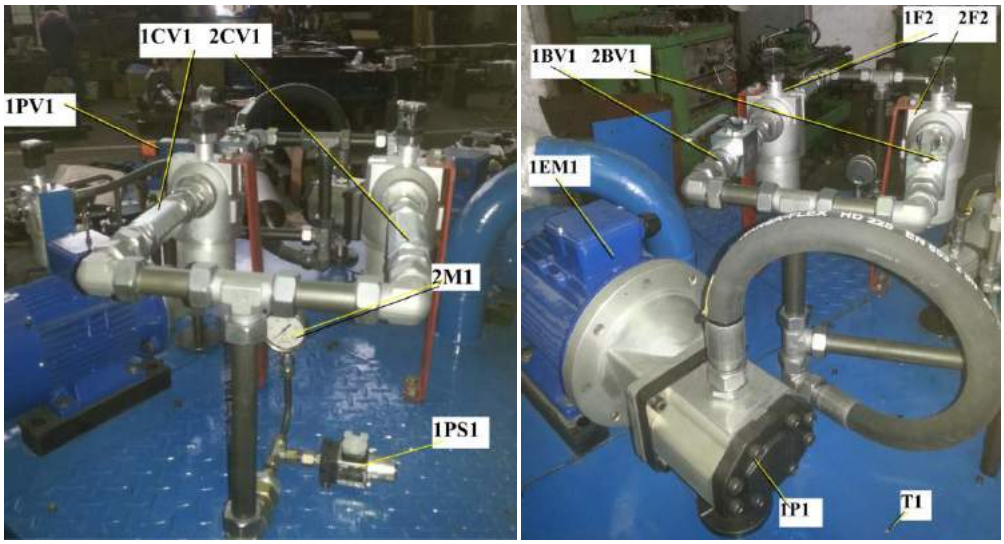

a. b.

Fig. 11. Hydraulic unit for suspension

The hydraulic devices in Figure 7, placed after the pressure switch 1PS1, were located on the machine bed as in Figure 12.

Fig. 12. Location of the control and regulation devices for the pressure in pockets

This equipment is represented by the flow control valves 1-8 FCV1, pressure switches 1-8 PT1 and manometers 1-8 M3. The oil film in the eight pockets can be regulated by means of this equipment. In Figure 13 is shown the location of the eight pockets on the bed of the machine.

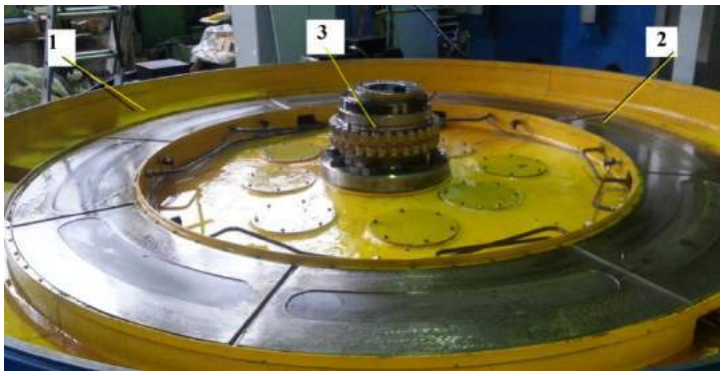

Fig. 13. Location of the real pockets on the bed of the machine

There are eight pocket-type plates 2 clamped to the bed of the machine 1 (made of cast iron); these plates ensure the thrust load discharge. The supporting on bearings 3 makes possible the radial centering of the table.
Initially, a primary adjustment of the flow rate was made in the eight pockets as in Figure 14.

Fig. 14. Primary adjustment of the oil flow rate in the pockets

The unit was started in the absence of the faceplate; then it was checked if columns of liquid 2, approximately equal in height, are made in the eight points controlled. The resulted oil is recovered using the trough 1.

After making equal columns, the hydraulic unit was stopped and the faceplate of the machine was assembled as in figure 15.

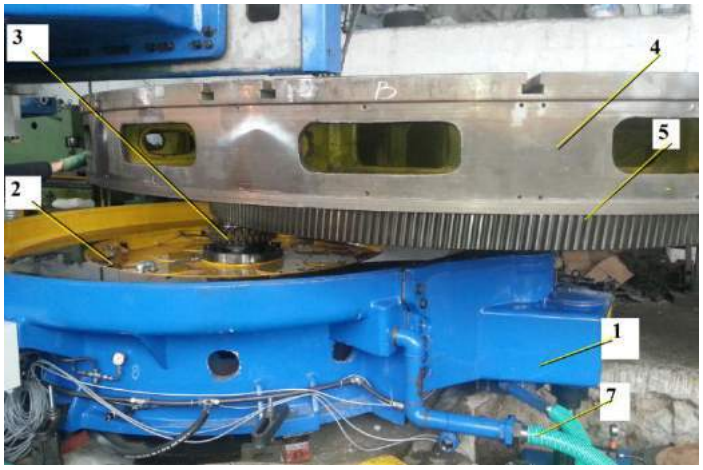

Fig. 15. Assembling of the machine table

On the bed 1 are located the gear box and the driving system of the faceplate 4. This is provided with a driving gear 5 and is centered radials by means of the bearings system 3; it is seated and unloaded axially on the pockets 2. As soon as the faceplate was positioned, the oil film thickness in pockets was adjusted using the eight flow control valves as shown in Figure 16.

a. b.

Fig. 16. Adjusting and checking the thickness of the oil film

The supports of the four dial gauges 3 (positioned every 90^0) were clamped on the bed 1. The dial gauges feel the faceplate 2.
An initial adjustment was made on the occasion of the tests; the faceplate was the only load and it was obtained a uniform film with thickness of 0.15 - 0.17 mm.
The results of the real measurements are shown in Table 2.

Table 2: The results of the measurements

W [daN]	p_{Med} [bar]	h_{Med} [mm]	Q [l/min]
20000	1.8-2.2	0-15-0.17	31

The size *e* was made at the value of 0.2 mm. In this case, the bearing in Figure 10 begins to be stressed only if the pressure of ~2 bar is exceeded under conditions of use, in idle running, of a flow rate higher than 50-55 l/min. This value corresponds to the scale division of ~7.5 on the eight

flow control valves. The force taken by this bearing, with no workpiece on the faceplate, has the approximate value:

$$F = 75\ 000(p_P - 2)K_W \text{ [daN]} \quad (18)$$

In the relation (18) it was noted: p_p - average pressure in pockets [bar], *F* - thrust force transmitted to the bearing [daN].
A specific problem for these machines is the accidental shutdown of the power supply voltage. In this case, if the machine is operating, because of the inertia of the faceplate – workpiece system, there is the risk of seizing occurred due to the disappearance of the oil film. To avoid such accidents, the machine is equipped with an emergency power system that will power the electric motor 1EM1 if needed. There is also a variant where the system is provided with pneumatic-hydraulic accumulators so dimensioned to be able to supply oil to the pockets long enough to allow the faceplate to stop completely [9, 13].

7. Conclusions

The hydrostatic suspension systems are usually used for the heavy duty vertical lathes with faceplate bigger than 5 000 mm.
These systems can operate at constant pressure or constant flow rate. The variant of using flow control valves, namely those operating at constant flow rate, is the preferable option taking into consideration the increased possibilities of adjustment and also the system stability. It should be mentioned that this variant is more expensive than the one which involves adjustments at constant pressure.
In the design phase of the hydrostatic units for these machines, account must be taken of as many factors as possible which may influence the system size. These factors include: minimum and maximum loads that will be put on the faceplate, the intended thickness of the film, maximum revolutions per minute (speed).
Even using specialized programs of calculation and simulation, certain safety margins must be provided due to the complexity of phenomena and variations in sizes as well.
Thus, the viscosity and density of oil – important parameters of calculation – are influenced by the inherent variations of temperature. Exceeding the imposed maximum oil thickness may result in the instability of the system or even its destruction. Thus, forcing the unit by increasing the flow rate in the absence of the load can entail the destruction of the axial - radial bearing located in the centre of the faceplate. The assembling of this bearing is very accurately closed with a chain of sizes determined during the tests phase of the machine.
Special attention must be paid to the oil filtering systems because of the specificity of the hydraulic equipment used. This one comes into contact with the atmosphere of the machining hall and is inevitably clogged. It is recommended to use oversized filters in terms of flow rate and to implement solutions that allow the replacement of filtering cartridges without having to turn off the machine.
The continuous monitoring of the general pressure and of each pocket pressure avoids the seizing which could have particular effects in the case of such machines.
The remanufacturing of this machine, made more than 30 years ago, resulted in a modern machine that is able to compete technically with a brand-new machine.

References

[1] D. Nicolas, "Butées et paliers hydrostatiques", Reference Internet - b5325 Techniques de l'ingénieur;
[2] R.Bassani, B.Piccigallo, "Hydrostatic lubrication", Elsevier Science Publishers B.V., eBook, 1992;
[3] T. Deaconescu, "Hydraulic Drives" („Acţionări hidraulice"), Publishing House of Transilvania University, Brasov, 2007;
[4] B. Perovic, "Machine tools handbook" („Handbuch Werkzeug-Maschinen"), Carl Hanser Verlag, Munchen, 2006;
[5] P. H. Joshi, "Machine tools handbook", McGraw-Hill Publishing House, New Delhi, 2007;
[6] *** SKF, Bosch-Rexroth, Fox, Brevini, Hydac catalogues;

[7] D. Prodan, M. Duca, A. Bucureşteanu, T. Dobrescu, "Hydrostatic drives-machine parts" („Acţionări hidrostatice - Organologie"), AGIR Publishing House, Bucharest, 2005;
[8] L. San Andres, Notes 12(b), Hydrostatic Journal Bearings, Tribology Group/Rotordynamics Laboratory, July 7 2016, Texas A&M University;
[9] D. Prodan, A. Bucuresteanu, E. Bălan, "Using Hydro-Pneumatic Accumulators to Increase the Operation Safety of Heavy Duty Vertical Lathes”, *Advanced Materials Research* Vol. 772 (2015) Trans Tech Publications, Switzerland, pp. 207-211;
[10] D. Prodan, "Heavy machine tools. Mechanical and Hydraulic Systems" („Maşini-unelte grele. Sisteme mecanice si hidraulice"), Printech Publishing House, Bucharest, 2010;
[11] D. Prodan, "Machine-Tools. Modelling and Simulation of Hydrostatic Elements and Systems" („Maşini-unelte. Modelarea şi simularea elementelor şi sistemelor hidrostatice"), Printech Publishing House, Bucharest, 2006;
[12] *** Software package: Automation Studio by Famic Technologies Inc.;
[13] A. Bucuresteanu, "Pneumo-Hydraulic Accumulators. Use and Modeling" („Acumulatoare pneumohidraulice. Utilizare si modelare"), Printech Publishing House, Bucharest, 2001.

Applied Research and Experimental Validation of a TLUD Industrial Solution

PhD. Eng. **Gabriela MATACHE**[1], Prof. PhD. Eng. **Edmond MAICAN**[2],
PhD. Stud. **Ioan PAVEL**[1], PhD. Eng. **Radu Iulian RADOI**[1],
Dipl. Eng. **Mihai-Alexandru HRISTEA**[1]

[1] INOE 2000-IHP Bucharest; fluidas@fluidas.ro

[2] UPB- ISB, e.maican@gmail.com

Abstract: *This paper presents the research carried out by the team of INOE 2000-IHP Institute in collaboration with UPB-ISB, on a hot air generating system to increase the energy independence of greenhouses and solariums aiming to extend the duration of their use by heating with local micro-gasified biomass in TLUD energy modules to increase production safety and reduce production costs. The target was the use of a hot air and forced circulation system equipped with rechargeable, simple, safe, efficient and environmentally friendly energy-saving TLUD modules in which the locally harvested, chopped and dried biomass is thermo-chemically gasified. From the micro-gasification of the biomass with the help of the TLUD type equipment, there resulted about 10% to 15% biochar, the part of carbon not converted into gas, which is a valuable agricultural amendment and contributes to the sequestration of carbon in the soil. These constructive and functional solutions can make an essential contribution to the stepping of agricultural farms from the semi-subsistence level to the commercial level, meaning a strong and stable growth of local crop production in the cold season.*
The paper deals with the research and experimentation of the gasification burning process on the TLUD principle and finalizes with a prototype of a hot air generator system that uses the secondary agricultural production as raw material and is mainly intended for the heating of the greenhouses.

Keywords*: TLUD gasification solutions, energy module*

1. Introduction

The heating systems for greenhouses can use water, steam or hot air as a heat source. The objective of these systems is to achieve a cheap, simple, safe heating that can be purchased by small manufacturers and to pay off quickly enough under limited usage for 3 to 4 months of use. As a result, the hot-air heating solution has been proposed, increasingly used for heating the greenhouses because:

- Ensures very good uniformity of temperature and humidity in the enclosure,
- Provides controlled ventilation that allows very good internal humidity control;
- By recirculation an increase in the energy efficiency of the heated tunnel solarium system is achieved.

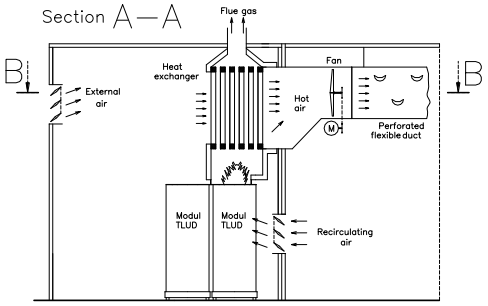

Fig. 1. Functional schematic diagram of a hot-air heated tunnel solarium

Figure 1 shows a functional diagram of a hot-air heated tunnel solarium. The solarium is heated by hot air through a flexible pipe that has slots for hot air distribution jets. A part of the indoor air is recirculated and mixed with the outside air needed for ventilation of the greenhouse. The mixture is heated with a flue gas $\Rightarrow$ air heat exchanger. This functional variant no longer implies periodic

ventilation that can be harmful if it is not well managed. In order to protect the plants from contact with too hot air, the maximum temperature of the jets is limited to 40°C, which implies the use of a constant flow rate for the air that heats the greenhouse. [1]
Figure 2 shows the block diagram of a tunnel solarium heated by a hot air system using two Biomass-Gasification-Module (BGM) thermal modules. The two modules are coupled to the inlet of the heat exchanger which operates at a constant flow of heated air and therefore has an average yield of 90% and a minimum yield of 85%. [2]

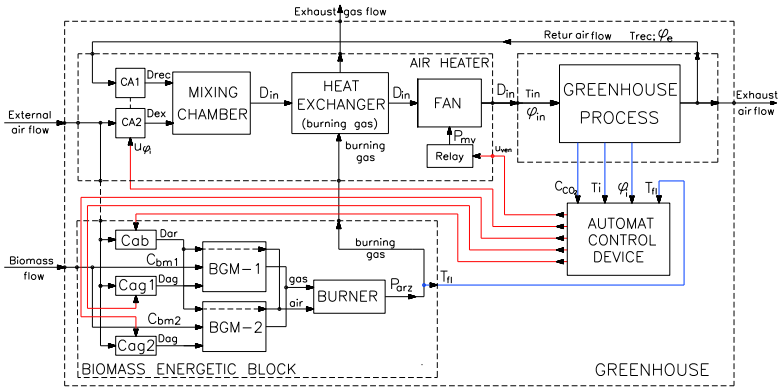

Fig. 2. Block diagram of solarium heated by a hot air system using two BGM thermal modules

2. Presentation of the chosen solution

The biomass is introduced into the reactor and rests on a grill through which the primary air for gasification passes from bottom to top. Rapid pyrolysis reaches a point of incandescence at the top and continues down into the biomass in the reactor. Rapid pyrolysis results in gas, tar and biochar. Tars pass through the incandescent charcoal layer, are cracked and completely reduced due to the heat radiated by the pyrolysis front and the upper flame. The resulting gas is mixed with the secondary combustion air, preheated by the reactor wall, introduced into the combustion zone through the holes disposed at the top of the reactor. The mixture with high turbulence burns with flame at temperatures of about 900°C. The regulation of the thermal power is done by the variation of the primary and secondary air flows. The designed solution shown in Fig. 3 has been filed as Patent application No. A/00286/27.04.2015

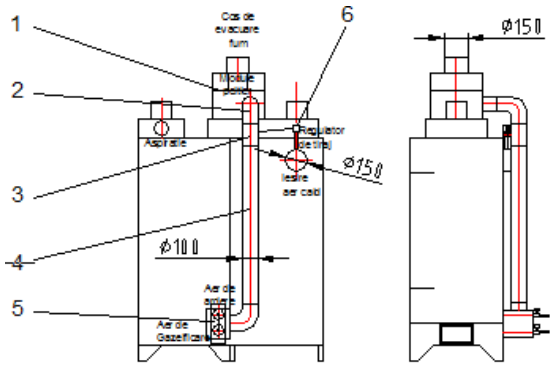

Fig. 3. The designed solution submitted for patenting

3. Numerical simulation of the experimental model

The CFD (Computational Fluid Dynamics) simulation has become a high efficiency technique used in the analysis and comprehension of biomass thermal conversion phenomena. Recovering the biomass and using it in heating stations may represent a cheap source of heating greenhouses and solariums in vegetable farming. This papers aims to develop a CFD simulation of a station which uses biomass in various working conditions, to obtain as good as possible heat transfer between the combustion gases and outside air used for heating greenhouses. The CFD simulation

has been developed on a 3D model of a station, in which a number of technological parameters have been determined experimentally. Technical specifications of the station under simulation, using biomass (pellets) as a source of fuel are presented in Table 1. [3]

Table 1: Technical specifications of the heating station

Features	Specifications
Sizes	1.220 m (l) x 0.5 m (w) x 1.460 m (h)
Area of the heat exchanger	5.2 m^2
Fuel	biomass-pellets (density 200 kg/m^3, average size of pellets 0.025 m)
Combustion time	4 – 6 h

Mathematical model required for the CFD simulation is based on the equations of fluid flowing through the station and the energy equation for heat transfer. Differential equations of continuity and fluid flow are introduced into the calculation algorithm by the relations:

$$\frac{d\rho}{dt} = -\rho(\nabla v) \tag{1}$$

$$\rho\frac{dv}{dt} = \eta\nabla^2 v - \nabla p + \rho g \tag{2}$$

where: ρ fluid density; v fluid velocity; η fluid dynamic viscosity; p pressure; g gravity acceleration.
Differential energy equation for calculating heat transfer is introduced into the calculation algorithm by the relation:

$$\rho\frac{dU}{dt} = \frac{\partial Q}{\partial t} + K\nabla^2 T + \theta \tag{3}$$

where: U internal energy; Q heat flow; K heat transfer global coefficient; T temperature; θ dissipation term.
If the fluid is considered incompressible and unsteady, three equations above shall be simplified accordingly. From the flow conditions according to the formula of Reynolds there has been determined turbulent flow in the heat exchanger. The standard k-ε model is the simplest turbulence model with two transport equations, which are added to the three previous equations, allowing independent assessment of the turbulent velocity and the turbulence length scale. Values of turbulent kinetic energy k and dissipation velocity ε are obtained from the system of transport equations [5]:

$$\rho\frac{Dk}{Dt} = \frac{\partial}{\partial x_i}\left[\left(\mu + \frac{\mu_t}{\mathrm{Pr}_k}\right)\frac{\partial k}{\partial x_i}\right] + G_k + G_b - \rho\varepsilon - Y_M \tag{4}$$

$$\rho\frac{D\varepsilon}{Dt} = \frac{\partial}{\partial x_i}\left[\left(\varpi + \frac{\mu_t}{\mathrm{Pr}_\varepsilon}\right)\frac{\partial \varepsilon}{\partial x_i}\right] + C_{1\varepsilon}\frac{\varepsilon}{k}\left(G_k + G_{3\eta}C_b\right) - C_{2\varepsilon}\rho\frac{\varepsilon^2}{k} \tag{5}$$

where: G_k term for generation of turbulent kinetic energy; G_b floatability term; Y_M compressibility term; Pr_k and Pr_ε turbulent Prandtl numbers for k, and respectively for ε.

Particularizing, the heat flow transmitted between the combustion gases and the air that has entered the heating station in the counter flow fluid-to-fluid heat exchanger, has the following equation:

$$Q = K \cdot S \cdot \Delta T_m \tag{6}$$

and capacity of the heating station shall be calculated using the next equation:

$$P = q_v \cdot \rho \cdot c_p \cdot \Delta T_m \tag{7}$$

where: K global heat transfer coefficient, S heat transfer area, q_v volumetric flow rate, ρ density; c_p specific heat; ΔT_m temperature difference inside the station.

A number of simplifying assumptions have been set so that the impact on the simulation results be minimal. It has been considered that the bed of biomass is a porous medium having a porosity of 0.3, it is homogeneous, constant height and its density does not change during the combustion process. Also, inlet temperature in the furnace is 1100 ºC, constant during combustion. Airflow and combustion gases flow through the heating station walls is considered as null. The condition imposed on combustion gases and hot air exhaust in the atmosphere is outflow, and overpressure is considered as null. Velocities of the combustion air and outside air inlet remain constant; they take values depending on the volumetric flow rate of technological operating parameters, according to Table 2.

Table 2: Technological operating parameters

q_v (m^3/h)	505	375	260
p (Pa)	200	300	400

Air inlet temperatures remain constant, with values of 15ºC for the air needed for combustion and 8ºC for the air brought in from outside with a view to heating inside the station. The volumetric mass and air viscosity have been considered constant for a given temperature.

The simulation results are presented as temperature and velocity fields, and respectively as the trajectory of pathlines in the simulation range of the heating station. The simulation has been developed for three different air flow rates with the ultimate aim to accurately determine the average output temperatures of hot air and combustion gases. The three-dimensional simulation of airflow and heat transfer provides the advantage of an overview very close to the real operation of a heating station when there are known the functional input parameters and temperature developed in the furnace by biomass (pellets) burning.

From numerical simulation there have been obtained the average output temperatures of hot air and resulted combustion gases, Table 3. Knowing the input and output parameters of the heating station, capacity of the heating station has been calculated by using the equation 7, air density and specific heat being considered constant.

Table 3: The values of parameters and heating station capabilities

q_v (m^3/h)	$T_{avg\ combustion\ gases}$ (˚C)	$T_{avg\ hot\ air}$ (˚C)	$T_{int\ outside\ air}$ (˚C)	$T_{int\ combustion\ air}$ (˚C)	P (W)
505	273	68	8	15	22260
375	253	63	8	15	15083
260	226	61.5	8	15	9876

Through the CFD simulation of the heating station, by introducing sequentially the three air supply flows, there results a capacity closed to the one proposed of 20 kW at a maximum flow rate of 505 m^3/h.

The analysis of airflow simulation and temperatures inside the heating station is performed for the maximum flow rate.

The temperature profile in the median plane for the heating station shows an ascending temperature gradient along the burner height, ranging from 80ºC at the bottom till a temperature of 1100ºC at the furnace entry point, (Figure 4).

If the input air required for combustion has the temperature of 15ºC, in the furnace the average temperature of combustion gases exceeds 900ºC. The temperature of combustion gases starts to decrease gradually in the heat exchanger, so that in the first section of the heat exchanger the average temperature is 600ºC, in the second section the gases reach an average temperature of 400ºC, while in the station chimney they are exhausted at the average temperature of 273ºC. The fresh air from the outside at a temperature of 15ºC takes some of the heat of combustion gases in the heat exchanger of the heating station, and it is discharged in order to produce heating at the average temperature of 68ºC.

The velocity profile in the median plane for the heating station shows minimum values near the walls and high values ranging from 3.5 m/s to 5 m/s at hot air and combustion gases output, Figure 5.

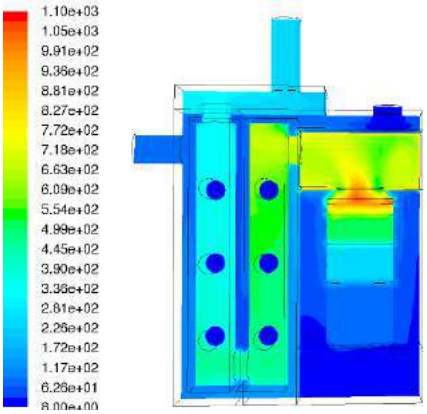

Fig. 4. The profile of temperature field in the median plane of the heating station T (˚C)

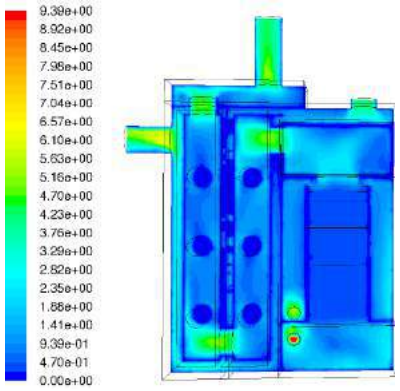

Fig. 5. The profile of velocity field in the median plane of the heating station v (m/s)

Moreover, average values of 4 m/s are recorded in the sections where the combustion gases pass from the furnace to the heat exchanger, from the heat exchanger to the exhaust air chimney, and also in the sections of the heat exchanger. Turbulence increases in these regions as a result of increased velocity and changes in direction, and the heat transfer intensifies. Turbulence level inside the station due to airflow and flow of combustion gases has been assessed by tracing the pathlines according to temperature (Figure 6) and velocity (Figure 7).

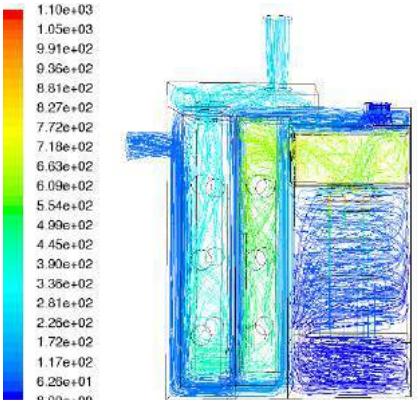

Fig. 6. Airflow and flow of combustion gases traced as path lines in the heating station (color bar - temperature TºC)

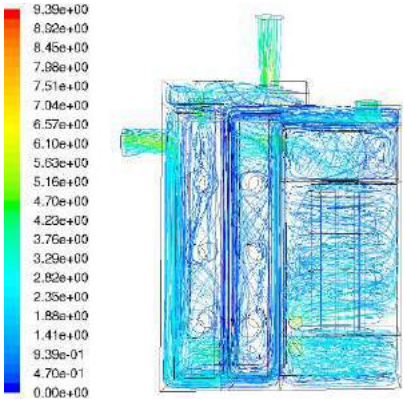

Fig. 7. Airflow and flow of combustion gases traced as path lines in the heating station (color bar - velocity v m/s)

4. Testing of the TLUD prototype

In testing, a 15 kilogram-bag of pellets per test has been used as combustion material. The reactor allows loading two bags of pellets.
The TLUD hot air generator prototype (Figure 8) has been tested in the low power and maximum power operation mode. Tests were conducted at INOE 2000-IHP premises.
Recording the temperature variation at different points of the hot air generator is done with the help of Pt1000 temperature probes. They are connected to a data acquisition board via 4 ... 20 mA amplifiers, the voltage conversion for the analog input of the acquisition board is made with the help of resistors (Figure 9). An application made in LabVIEW is used to display and record the data (Figure10). The application displays numerically and graphically the temperature variation during burning. When the recording stops, the application allows one to save the temperature values over time in a text file. These data can be processed later.

Fig. 8. The hot air generator prototype on the TLUD principle

The LabVIEW application (Figure 11) contains the following functional blocks: program loop with the possibility of setting the data acquisition range, data input block from the acquisition board in which the temperature - output signal scaling is done, numeric display, graph display, running time counter (seconds, minutes, hours), data entry in text file, graph deletion (when starting a new test), and a table display block.

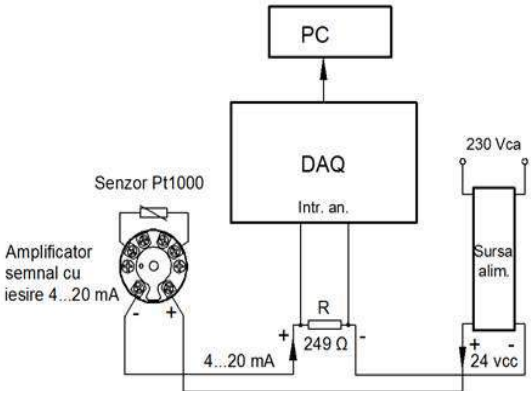

Fig. 9. Connection diagram of the data acquisition system

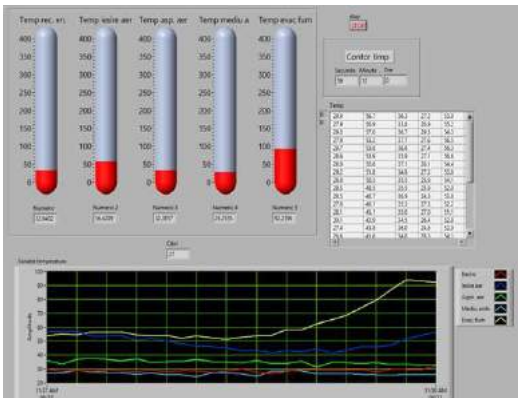

Fig. 10. Graphical interface of the data acquisition software

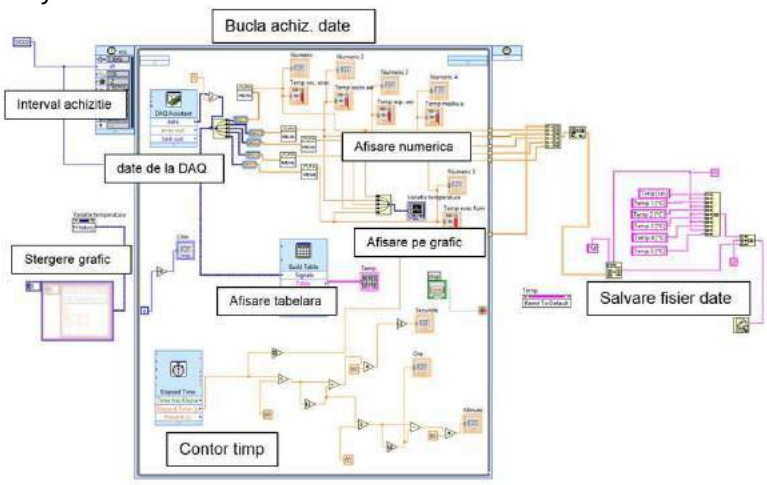

Fig. 11. Diagram in LabVIEW data acquisition software

Test 1 – The variant of gasification and obtaining biochar

The contents of a pellet bag were introduced into the reactor. Initiation of the combustion process was done at the top of the material in the reactor, with commercial fire ignition lighters and it took about 12 minutes from ignition to stabilized gasification mode according to the data acquisition (Figure 12).

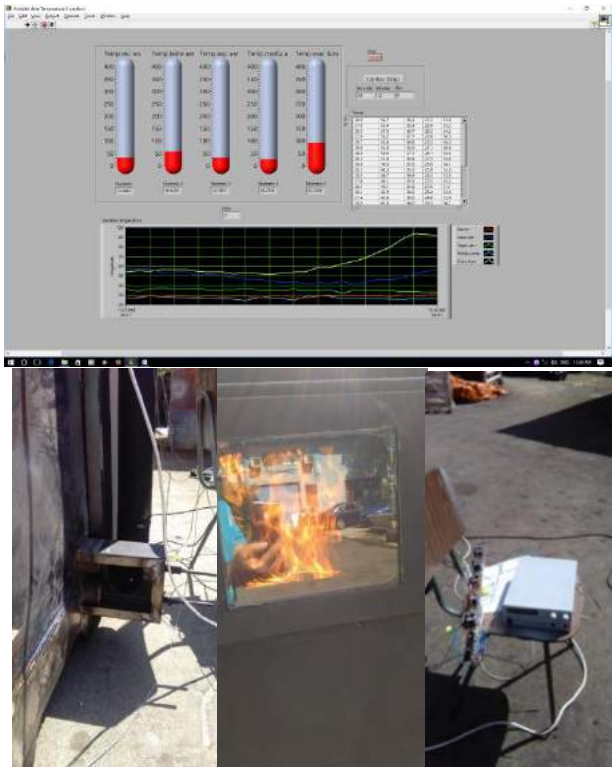

a. b. c.

Fig. 12. Photos during tests (1)

After entering the gasification mode, the flame has moved from the combustion material in the reactor to the burner. The gas produced in the reactor was mixed with the combustion air and a flame similar to the flame from the stove was produced (Fig. 12.b). Several adjustments of the gasification and combustion air intake valves (Fig.12.a) have been made and the adjustability of the hot air generator power has been found. By opening them, the flame grows almost instantaneously. Thus, the correct operation of the TLUD type gasification principle (Top-Lit UpDraft) has been demonstrated.
As a result of the data acquisition (Fig. 12.c) for the entire duration of the operation until the flame is blue and the hot air generator stops (stopping of the fans and opening of the supply door) to get the biochar, the graph in Figure 13 has been achieved.

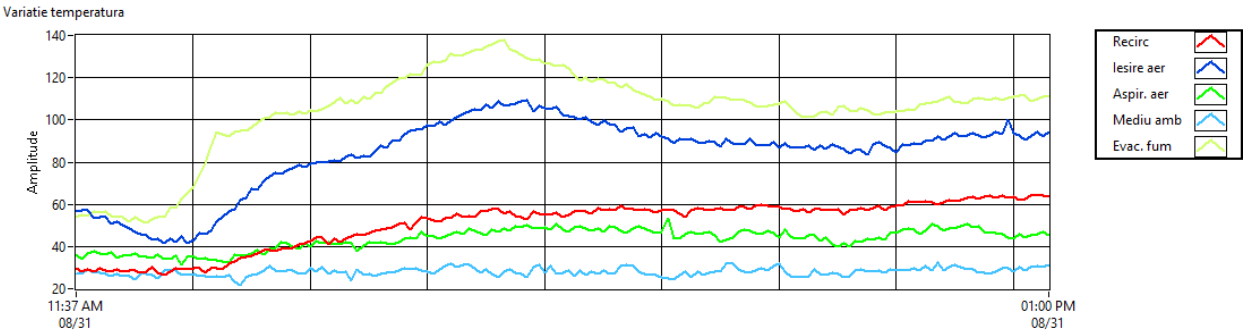

Fig. 13. Variation of temperature with biochar resulted

The burning process lasted 83 minutes for a 15 kg pellet bag under minimum power operating conditions and was interrupted when the flame was blue (signaling that the gasification of the material was complete and the gasification of the biochar is about to start). Thus, approximately ¼ of the volume of the material initially introduced for combustion resulted in biochar (Figure 14).

Fig. 14. Photos during tests (2) - biochar resulted

A good adjustment of power of the hot air generator was achieved by adjusting the combustion air and the gasification air. The temperature of the heating air at the generator outlet for the minimum operating conditions was stabilized at about 90°C and the chimney temperature was about 120°C. The air flaps have been adjusted to approximately 1-2 mm opening.
Under these conditions it can be said that the generator cannot work below the test values, so it has a minimum operating power of 3kW.

Test 2 - The variant of gasification without making biochar, with gasification of the latter
The contents of a pellet bag were introduced into the reactor. The initiation of the combustion process was done with commercial fire ignition lighters and it took about 12 minutes from the ignition to the stabilized operation mode according to the data acquisition (Figure 15).

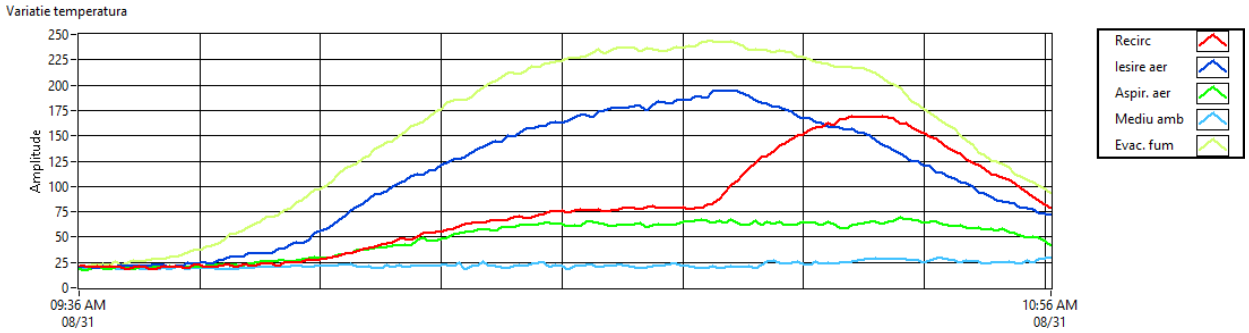

Fig. 15. Variation of temperature without biochar resulted

Under the test conditions at maximum power with combustion air flaps and gasification air flaps open at more than 10 mm, an average heating air temperature of 175°C was obtained and the chimney temperature was approximately 230°C according to the graph of data acquisition.

In Test 2, the burning process was no longer interrupted to obtain biochar (when the flame was blue), and this resulted in longer operating time and an energy amount higher by about ¼ compared to the variant when the reactor was shutted-down and biochar was obtained. The final

result of total burning, including biochar burning, was a very small amount of ash of about 50 g. The generator can work very well in both variants - with obtaining of biochar or burning it and getting energy. In both cases no emissions of smoke or unburned gas were found.
When the pyrolysis front reached near the bottom of the reactor and the thickness of the biochar layer decreased in the conditions of maintaining the flow of gasification air and the minimum resistance created by the material, the burning process accelerated for a short time (until all combustion material including the biochar has been consumed), and after that, although the burning process declined, the generator still supplied hot air for about 20 minutes due to thermal inertia.

5. Conclusions

The prototype tested meets the project objectives, works under different power modes, on the TLUD principle and it can enter into an industrial design process, after which it can be manufactured and delivered to the market.
It has been found that the smoke fan is large for operating conditions less than those obtained at test 1, but for operation at maximum power, as in test 2, it is well-sized. An improvement could be obtained if in the electronic control panel an electronic mount would be provided for the variation of the smoke fan speed. Thus, the hot air generator can be presented as operating from a minimum power of 3 kW up to a maximum power of 24 kW by adjusting the gasification air inlet flaps and combustion air inlet flaps.
If the aim is to introduce hot air into the greenhouse at a lower temperature than that provided by the generator, it is possible to resort to the solution of mixing hot air from the generator with fresh air from the atmosphere until the desired optimal temperature to enter the greenhouse is obtained.

Acknowledgements

Research presented in this paper has been developed with financial support of UEFISCDI (Executive Unit for Financing Higher Education, Research, Development and Innovation) under PCCA 2013 Programme, Financial Agreement no. 67/2014, Project title *Using renewable energy resources to increase the energy independence of mini greenhouses and solariums*, Project acronym *ENERGSER*.

References

[1] E. Murad, E. Maican, C. Dumitrescu, Şt.S Biriş., "Extending the use of hothouses through heating with residual agricultural biomass", *Proc. of 2-nd International Conference of Thermal Equipment, Renewable Energy and Rural Development TE-RE-RD 2013*, Olăneşti, Romania, June 20-22, 2013;
[2] C. Sima, G. Haraga, E. Murad, "Environmentally drying vegetables using greenhouses crop residues"*, Proc. of 2-nd International Conference of Thermal Equipment, Renewable Energy and Rural Development TE-RE-RD 2013*, Olăneşti, Romania, June 20-22, 2013;
[3] P.-M. Carlescu, G. Matache, I. Pavel, R.I. Radoi, I. Ilie, "The transfer simulation in a heating station that uses renewables sources for heating greenhouses*", Proc. of 16th International Multidisciplinary Scientific GeoConference SGEM 2015*, Vol. "Water Resources. Forest, Marine and Ocean Ecosystems" ISBN 978-619-7105-63-6, ISSN 1314-2704, DOI: 10.5593/SGEM2016/B41;
[4] *Contract no. 67/2014* – "Utilizarea resurselor energetice regenerabile pentru cresterea independentei energetice a miniserelor si solariilor", PN-II-PT-PCCA-2013-4-0221;
[5] S.V. Patankar, D.B. Spalding, "A calculation procedure for heat, mass and momentum transfer in three-dimensional parabolic flows", *Int. J. Heat Mass Tran.*, 14, pp. 1787-1806, 1972;
[6] J.P. Vandoormaal, G.D. Raithby, "Enhancements of the simple method for predicting incompressible fluid flows", *Numer. Heat Trans.*, 7, pp. 147-163, 1984;
[7] H.A.M. Knoef (Editor), "Handbook Biomass Gasification Second Edition", BTG Biomass Technologies Group, Netherlands, 2012;
[8] *******, Ansys-Fluent, User Guide, 2010.

Modeling an Automatic Processing Station Using Fluidsim Software

Ph.D. Eng. **Ionel Laurentiu ALBOTEANU**[1]

[1] University of Craiova, Faculty of Electrical Engineering, lalboteanu@em.ucv.ro

Abstract: *Computer-aided design of modern industrial systems contributes to increasing the quality of these systems and reducing the time to obtain the final results.*
The paper presents the results of the modeling of an automated electro-pneumatic processing station using the Festo FluidSIM Pneumatics application. For the chosen operating protocol, both the power part and the electrical and control part were modelled, being generated as well, the state diagram of the processing station cylinders, in a working cycle.

Keywords: *modeling, pneumatic, processing station, FluidSim*

1. Introduction

Modern industrial systems can be designed, modelled, simulated and tested in virtual computer assisted environments, thus increasing the quality of the processes mentioned and shortening development time [1].
We propose to use these new methods in this work for the pneumatic drive system of a piece processing station. The pneumatic drive is modelled and simulated on a personal computer using the Festo FluidSim Pneumatics application [2].

2. Structure of processing station

The processing station consists of a machine tool (MT) with a stock of raw input pieces and a stock of output semi-finished products (Fig.1) and a manipulating robot (MR) transferring the work pieces from the stock Input to the machine tool [3].

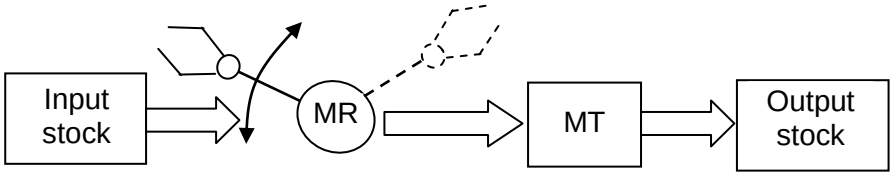

Fig. 1. Structure of processing station

It is considered that the MT performs a single operation (for example, pressing, stamping, drilling, threading, etc.) on a single ingots. It is also considered that both input and output stocks have a limited capacity at a semi-finished product.
The entire structure is integrated in an electro-pneumatic drive system with linear actuators (pneumatic cylinder) and rotary (rotary pneumatic motors), controlled by monostable and bistable valves [4].
Thus, the manipulator robot- MR comprises four modules and machine tool- MT comprises a main processing module and the outlet module machined semi-finished products (Fig. 2).
A complete working cycle of pneumatic drive involves following sequences:

1. Advance C4→ Advance C1→Retraction C4→ Retraction C1;
2. Advance C3→ Left rotation MP2→ Advance C1→ Advance C4;
3. Retraction C1→ Retraction C4→Right rotation MP2→ Retraction C3;
4. Advance C5→ Retraction C5→ Advance C6→ Retraction C6

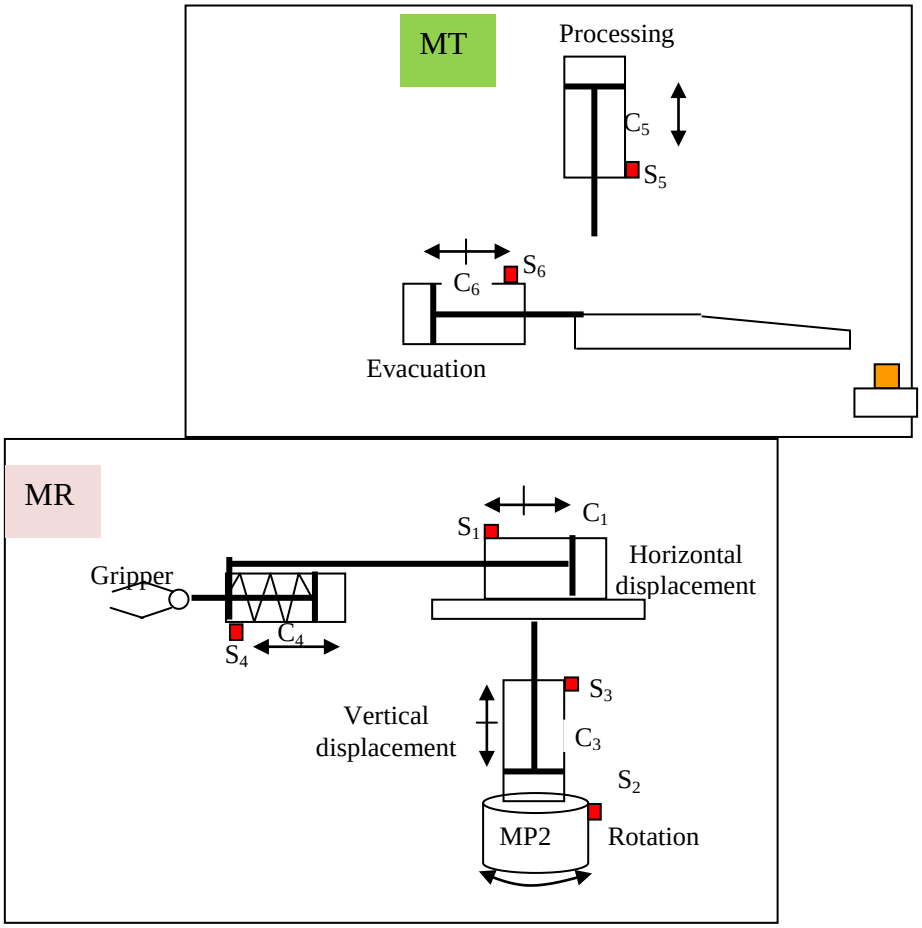

Fig. 2. Structure of the pneumatic drive of the processing station

3. Modeling of processing station

The modeling of the pneumatic actuator consists of two parts: shaping the power (pneumatic) part and shaping the electrical and control part. Both parts of system modeling mainly involve choosing components in the Component Library, placing them on the design sheet, setting parameters, and making connections between components [5].
If the component library is not visible in the workspace, it can be displayed by choosing Total View from the Library menu.

3.1. Modeling of pneumatic part

The model of the pneumatic part of the processing station was divided into three blocks [6] (Figure 3):
- the compressed air preparation unit block;
- the block of the manipulating robot;
- the block of machine tool.

The meaning of the elements used in the model is the following:
D1...D6 – pneumatic valve;
C1...C6 – pneumatic cylinders;
MP2 – rotary pneumatic motor;
DC1...DC11 – one-way flow control valve;
S1...S6 – sensors;
Y1...Y6 – relays valve control

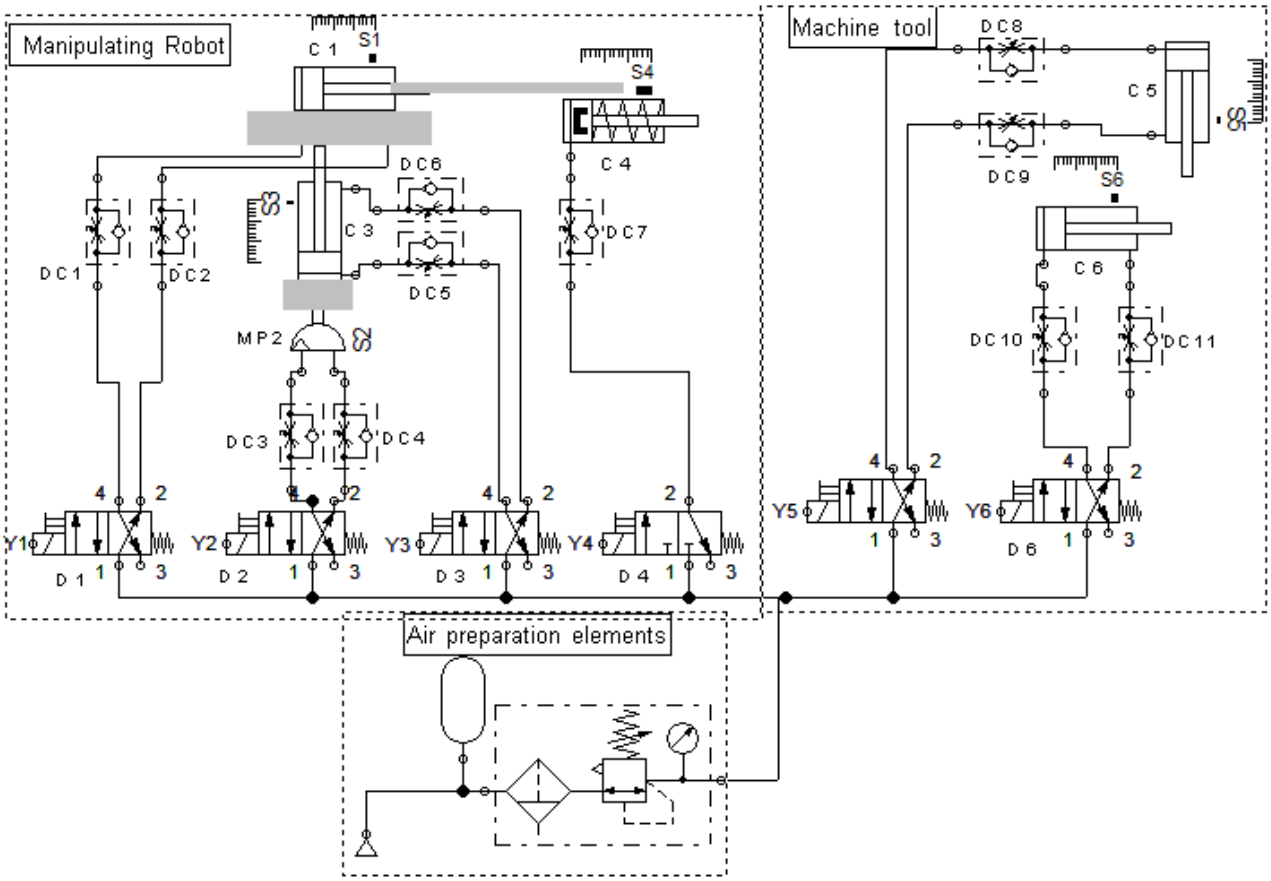

Fig. 3. FluidSim model of the pneumatic part for the processing station

3.2. Modeling of electrical and control part

The next step of the modeling is the realization of the electric circuit incorporating the actual control logic. This circuit is made on the same work sheet, separate from the pneumatic scheme, apparently independent of it [5]. The sequential control scheme proposed for the embodiment is shown in Figure 4.

This scheme requires power supply, contacts (button, contact sensors), relays and interconnections. All parts for the electrical part are located in the same component library.

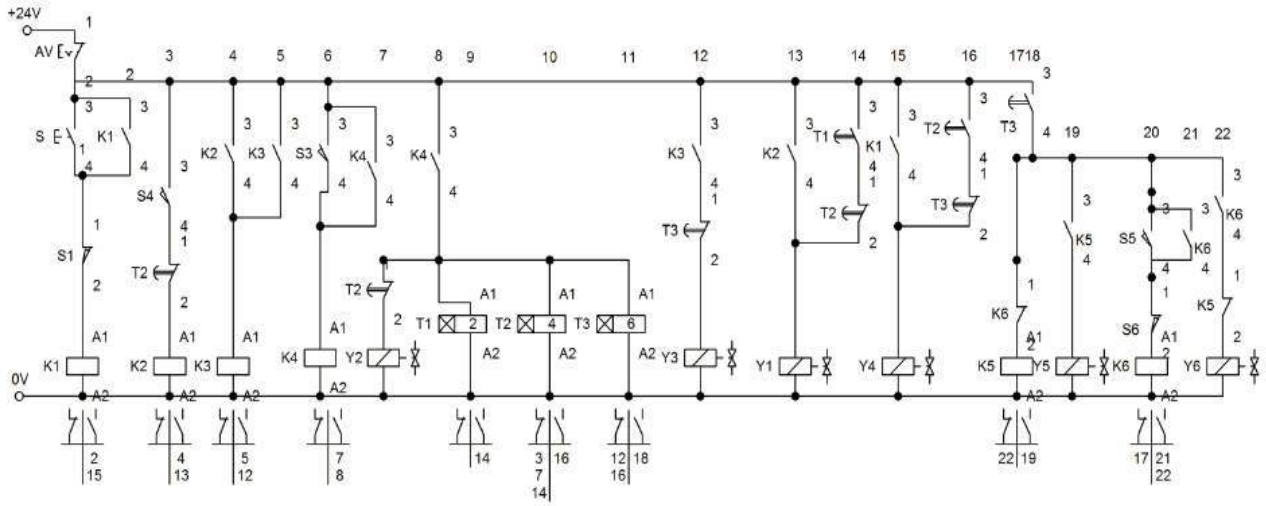

Fig. 4. Sequential control circuit diagram with contacts and relays implemented in FluidSim

4. Simulation results

Following simulation, FluidSim can generate a state diagram of pneumatic drive [7]. The state diagram records the state quntitie of important components and depicts them graphically (Figure 5).

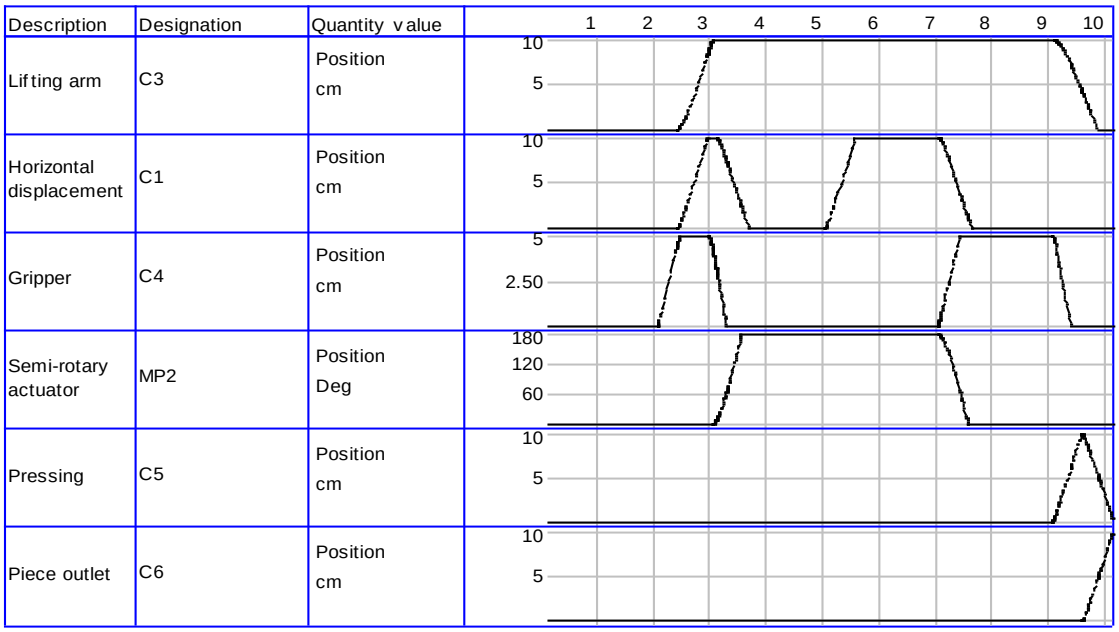

Fig. 5. State diagram of pneumatic components, in a work cycle generated by FluidSim

The state diagram highlights the operating sequences of the execution elements in the pneumatic drive.

5. Conclusions

The paper presents the results of the modeling of an automated electro-pneumatic processing station using the Festo FluidSIM Pneumatics software. FluidSim allows the drawing of electropneumatic circuits and can perform schema simulations based on physical components of the components. It eliminates the gap between drawing a circuit and effectively simulating the pneumatic system.
Both the pneumatic part of performed processing station as well as electrical and command part was proven correct functioning according to the solution and protocol required.
Simulation results showed the evolution of the typical elements of pneumatic drive. The practical and experimental aspects will be presented in a future work.

References

[1] C. Lazăr, O. Păstrăvanu, F. Schonberger, "Computer-assisted management of technical processes" ("Conducerea asistată de calculator a proceselor tehnice"), Matrix Rom Publishing House, Bucharest, 1996;
[2] *** FESTO FluidSIM Pneumatic 4.2, User manual;
[3] M.A. Drighiciu, "Hydro pneumatic drive and automation" ("Acţionări şi automatizări hidropneumatice"), Publishing House of University of Craiova, Craiova, 2003.
[4] B. Robert, van Varseveld and G. M. Bone, ″Accurate Position Control of a Pneumatic Actuator Using On/Off Solenoid Valves″, *″IEEE/ASME Transactions on mechatronics″*, vol. 2, no. 3, September, 1997, pp. 195-204;
[5] I.L. Alboteanu, ″Pneumatic Tracking System for Photovoltaic Panel″, *″Hidraulica″,* No. 1/2015, ISSN 145-7303, pp. 32-39;
[6] I.L. Alboteanu, Gh. Manolea, A. Novac, ″Automation of a pumping station for low power applications″, *″Hidraulica″*, No. 1/2014, ISSN 145-7303, pp. 58-64;
[7] http://www.festo.com/net/startpage/

Testing of the Fertigation Equipment in Operation Conditions

PhD. Eng. **Gheorghe SOVAIALA**[1], Dipl.Eng. **Sava ANGHEL**[1], PhD. Eng. **Gabriela MATACHE**[1], Dipl. Eng. **Alina Iolanda POPESCU**[1]

[1]INOE 2000-IHP Bucharest, sovaiala.ihp@fluidas.ro

Abstract: *The fertigation equipment developed within the FERTIRIG project, PN-II-PT-PCCA-2013-4-0114, financial agreement no. 158/2014, has been tested under real operation conditions at ICDP Pitesti Maracineni, on local irrigation facilities existing in the experimental - demonstrative plots, in fruit trees such as plum, pear and apple, which are fruit species of greatest importance for the Romanian fruit growing.*
It has been designed and developed in accordance with the fertilization / fertigation technologies developed in the previous stages by the specialists in the field of horticulture from the project partners.

Keywords: *Fertigation, injection device, fruit plantations*

1. Introduction

The irrigation system is installed in plantations usually prior to tree planting or immediately after planting, in order to ensure soil watering especially in the rooting area.
Drip irrigation hoses or micro-sprinklers are placed on the soil or near the soil under the rows of trees, and watering is applied more often and with lower watering norms, especially during the first half of the growing season, until rooting is ensured, then irrigation is monitored according to the soil water voltage values given by moisture sensors installed in the parcels since the year of planting the trees.
The plantations fertilizing is based on soil fertility status, established by soil analysis or foliar diagnosis. When applying fertilizer dosages, it should be taken into account that the trees capitalize about 30-40% of the amount administered, and from this a part is blocked in the permanent organs of the tree, and the other part is exported through the harvest, the leaves and the wood that falls to the cutting.
The right moment for fertilizers application is still discussed by the researchers. Phosphorus potassium, organic fertilizers and one third of nitrogen must be applied in the autumn before ploughing, and the rest of the nitrogen, split in two doses, must be applied in spring during blooming and during the intense growth of the sprouts.
The process of nutrients absorption is not an uniform process during the active vegetation period, but it shows certain intensification or slowing-down, depending on several factors, such as: the physiological specificity of the species, the vegetation phenological phases, the light regime, heat and water, the presence of various substances in the soil, soil reaction (the pH) [1].

2. Material and method

The recommended recipes with dosages of the most commonly used soluble fertilizers used worldwide for plum and pear species are presented for plantations equipped with local irrigation installations and soluble fertilizer dispensers [1]. Monthly dosages, or dosages per certain phenological phases of the vegetation season, shall be divided into weekly or, at the most, two-weekly applications. Soluble fertilizers will be applied simultaneously with local irrigation in stages of at least 3 hours each. Of course, the recommendations in Tables 1 and 2 will be adjusted according to the foliar diagnosis. This will be done annually on samples of leaves harvested between July 15 and August 15, within the laboratories of Pedology and Agrochemistry County Offices.

Table 1: Fertilization recipe in plum plantations on fruit

Month	Requirements as to the mineral elements (kg/ha)				Recommended fertilizing (kg/ha)			
	N	P_2O_5	K_2O	MgO	Potassium nitrate	Mono-ammonium phosphate	Ammonium nitrate	Magnesium nitrate
March	5	5	5	0	10	10	5	0
April	10	15	25	5	60	20	0	30
May	25	15	40	5	85	25	10	30
June	30	15	50	15	120	25	5	100
July	30	5	50	15	130	10	5	100
August	25	5	45	10	100	5	25	60
September	5	5	10	5	10	5	0	25
Annual total	130	65	225	55	515	100	50	345

Table 2: Fertilization recipe in pear plantations on fruit

Month	Requirements as to the mineral elements (kg/ha)				Recommended fertilizing (kg/ha)			
	N	P_2O_5	K_2O	MgO	Potassium nitrate	Mono-ammonium phosphate	Ammonium nitrate	Magnesium nitrate
March	12	10	15	0	40	15	20	0
April	20	15	25	5	60	25	15	25
May	35	20	35	10	85	30	0	32
June	40	15	35	15	88	20	40	60
July	25	10	30	10	70	8	8	55
August	6	5	5	8	10	0	0	45
September	8	5	10	5	10	8	0	30
October	10	5	5	0	25	5	15	0
Annual total	156	85	160	53	388	111	98	247

Note: The amount of administered fertilizer is divided into weekly dosages and it is applied for at least 3 hours of irrigation; the recommendations will be adjusted according to the foliar diagnosis.

The ICDP Pitesti Maracineni experimental - demonstrative fields of intensive fruit growing are equipped with irrigation – fertilizing equipment, which administer the water and the fertilizer elements specific of each crop.
The application of water and soluble minerals is done in phases, dosages, moments and phenological phases, specific to the physiological and technological requirements of each fruit crop.

The fertilization is carried out with equipment for injection of the various primary solutions in the irrigation system arranged for a particular crop.
In principle, the technology for irrigation with dripping tube or micro-sprinkler irrigation is limited to local watering, with controlled amounts of water, correlated with the soil absorption capacity and evapotranspiration of the crop in question, distributed around plants, mainly in the root development area. The use of such equipment, facilities and drip irrigation systems or micro-sprinkler systems is particularly suitable for horticultural crops (fruit trees, vineyards, vegetables, flowers), in the field or in protected areas, with availability for a high degree of mechanization.

3. Results

The fertigation facility in ICDP Pitesti-Maracineni, which the tests on the fertigation equipment have been conducted upon, fig. 1, is made up of the supply pipe, connected by a branch pipe (figure 2) to the underground pressure network, the vent valve with tap (fig.3), that is the closing / opening tap for inlet of the irrigation water in the installation, the sand filter (fig.4), mounted on a circuit parallel to the main circuit of the irrigation system (bypass), tap separating the main circuit from the circuit crossing through the sand filter, water meter (figure 5), screen filter (figure 6), the network of pipes distributing the irrigation water to the serviced plots (2 by dropping and 2 by micro-sprinkling) solenoid valves (figure 7) mounted on each distribution network, with control from a supervisor point.

Fig.1 Fertigation system for intensive fruit plantations

Fig. 2. Branch pipe of fertigation system

Fig. 3. Vent valve with tap

Fig. 4. Sand filter

Fig. 5. Water meter

Fig. 6. Screen filter

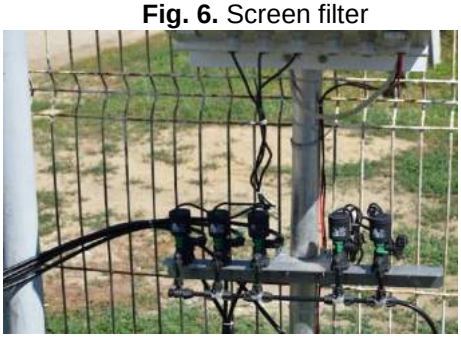

Fig. 7. Solenoid valves for irrigation plot selection

For commissioning of the installation one shall proceed as follows:
- Shut off the tap valve of the main pipeline and open the tap on the vent valve to remove the air from the installation;
- Depending on the turbidity of the irrigation water, a choice is made to introduce it into the distribution network either through the main circuit or through the sand filter circuit, by properly handling the inlet / circuit separation valves;
- The water passes through the meter, which records the volumes of transiting water, the screen filter with 120 μm fineness, which holds the particles in suspension and prevents the clogging of the distribution elements of the installation (dripping devices / micro-sprinklers) and reaches the solenoid valves; the plot to be irrigated is selected by closing / opening these valves.

On the main pipeline, upstream of the water meter there are mounted pressure couplings with ¾ 'tap valves, for branching the injection device, fig. 8, which absorbs the primary solution from the mixing tank, fig. 1.

Fig. 8. Branching of the injection device to the local watering system

The main features of the local irrigation system (including 2/4 distribution networks) are:
- The underground pipeline for water supply to installation = Ø 100 mm
- The pipeline connecting the primary solution injection device = Ø 50 mm
- Distribution hoses on rows of trees = Ø 16 mm
- Distance between dripping devices along the watering hoses = 1 m
- Flow rate of dripping devices = 2 (4) l / h
- The length of the trees rows (of the watering hoses) = 160 m

- Number of hoses (rows) = 35 (45)
- The primary solution dosage will be 80-100 (100-150) l
- The administration time will be within 3 hours, as is the minimum administration duration of a watering standard.

The injection device [2] was tested with a primary solution of 0.2% concentration prepared from the Magnisal* chemical product [3].
*Magnisal is a totally water soluble fertilizer that contains 11% nitrogen as NO_3 and 16% magnesium as MgO; the product solubility is 173 g/100 g water at a temperature of 0°C, 200 g/100 g water at 10°C, 225 g/100 g water at 20°C, 256 g/100 g water at 30°C, 289 g/100 g water at 40°C; concentration (%), pH and electrical conductivity (mS / cm) vary as follows: 0.1/5.56/0.88; 0.2/5.51/1.69; 0.3/5.37/2.52; 1.0/4.85/7.58; 5.0/4.06/29.9.
The main advantages of the product are: Magnisal is a totally water-soluble fertilizer; all nitrogen is in the form most accessible for the plant (NO_3); it is the most effective fertilizer for preventing and treating magnesium deficiency; it is the most recommended magnesium source for foliar spraying.

Table 3: The technical and functional characteristics achieved with the injection device [4]

Pres. in the watering pipe, bar	Working pressure of injection device, bar	Injection pressure, bar	Supply flow of injection device l/min	Discharge flows from drive chambers 1 and 2, l/min	Volume of drive chambers 1 and 2, ml	Control chambers volume of directional valves 1 and 2, ml	Injected flow rate of primary solution, l/min
3.7	3.5	3.6	3.79	1.596/1.444	42/38	11.1/11.6	1.4
Frequency of mobile assembly, double strokes/min	Control chambers flow of directional valves 1 and 2, l/min	Efficiency of injection device $\eta = Q_{inj}/Q_{supply\ of\ inj.\ device}$ %					
38	0.418/0.432	36					

4. Conclusions

On the main pipeline of the irrigation facility, between the points of the connecting pipe of injection device, a tap valve as a diaphragm will be fitted, by means of which pressure drop will be achieved; Δp = pressure drop of the injection device - injection pressure, which will facilitate the injection process of the primary solution, in a continuous operation of the device.
For the control and monitoring of the working parameters, it is necessary to make a hydraulic circuit parallel to the main pipeline of the installation (which is the power supply circuit of the injection device), equipped with specific parts (taps, Y route filters, directional valve, pressure reducer with gauge, flow meter), similar to those in the test stand structure, fig. 9.

Fig. 9. Elements of control and monitoring of the working parameters

The advantages of fertigation

- It makes water, energy and labour force savings;
- As a result of the watering lack for leaves and fruits, the appearance of specific diseases is reduced;
-The low atmospheric humidity reduces the appearance of cryptogamic diseases;
- Applied pesticides are not washed off the leaves with irrigation, thus prolonging their action period;
- There is reduced the density of weeds and their excessive growth as a result of watering / fertilizing lack for the strips between the rows;
- It ensures an increased efficiency of use by the crop plants of the mineral fertilizers, applied simultaneously with irrigation water;
- It does not pollute soil and surface or deep water, due to local administration done in small and frequent dosages of fertilization recipes;
- It ensures an uniform watering and without water and fertilizer losses on slope or uneven ground;
- During the fertilization, other technological works can be applied in orchards;
- Upgrading of the old sprinkler irrigation systems only requires connecting the new equipment of local irrigation to the former.

Economic efficiency

This method of fertilization is the most efficient, both in terms of the yield of the fertilizer mixture use by the crop plants and in terms of energy and water consumption and labour force consumed for the administration of a chemical fertilizer dosage.

Local water distribution, only near the root system of plants, results, for the same balances of water used by plants, in low consumption, namely lower by about 50-60% of water consumption specific to sprinkler irrigation, which implicitly results in reduced costs of water supply.

The application of fertilizer irrigation reduces the labour force involved by more than 50%, and the yield of fertilizer usage by crops is higher than 80%.

Acknowledgments

Research presented in this paper has been developed with financial support of UEFISCDI (Executive Unit for Financing Higher Education, Research, Development and Innovation) under PCCA 2013 Programme, Financial Agreement no. 158/2014, project code PN-II-PT-PCCA-2013-4.

References

[1] D. Sumedrea, I. Isac, M. Iancu, A. Olteanu, M .Coman, I. Dutu, "Trees, fruit trees, strawberry", Technical and economic guide, Ministry of Agriculture and Rural Development, elaborated during the project "Completion of the financial support granted by the European Union for Restructuring of Agriculture in Romania" (CESAR), Pitesti, 2014;

[2] Gh. Șovaială , S. Anghel, G. Matache, A.-M. Popescu, P.-M. Cârlescu, "Injector of primary solutions with hydraulic control", *Scientific Papers, Agronomy series*, Vol . 59/2016, pp. 131-134;

[3] P.-M. Carlescu, G. Matache, Gh. Sovaiala, M. Tudor, Al. Marinescu, "The efficient use of water and fertilizer resources in a fertigation plant", *16th International Multidisciplinary Scientific GeoConference SGEM2016 Conference Proceedings*, ISBN 978-619-7105-61-2 / ISSN 1314-2704, DOI: 10.5593/SGEM2016/B31/S12.095, June 28 - July 6, 2016, Book3, Vol. 1, pp. 727-734;

[4] Gh. Sovaiala, S. Anghel, Scientific and Technical Report - Phase 4 - Project FERTIRIG, PN-II-PT-PCCA-2013-4-0114, financial agreement no. 158/2014.

Hydro Power Solution with Radial Turbine Based on Medium Flow Rate Water Streams

Assistant professor **Fănel Dorel ȘCHEAUA**[1]

[1]"Dunărea de Jos" University of Galați, MECMET RESEARCH CENTER, fanel.scheaua@ugal.ro

Abstract: *It is evident the continuous increase of the energy needs, proportionate to the increase of the number of inhabitants, but also due to the increase of the living standards of the human communities. For providing the necessary energy, the fossil fuels are used in the majority proportion, which bring changes to the environment. In order to avoid this disadvantage, energy obtaining methods based on natural renewable resources that are practically unlimited and most importantly do not bring negative changes to the environment are increasingly taken into account. Thus, besides solar energy, wind power, tidal energy and hydro power are solutions that are currently used all over the world, but which need to be further developed in the future. A turbine model working within a hydro power system is described in this paper aiming to highlight the main working parameters. A CFD analysis is conducted on the virtual model and presented the obtained results regarding fluid velocity, absolute pressure, turbine shaft torque and the total power amount calculated values.*

Keywords*: hydro power, hydraulic energy, water resource, turbine model, fluid flow, 3D modelling, computational fluid dynamics (CFD)*

1. Introduction

There are multiple power solutions available today that can use the renewable resources available, in order to avoid burning fossil fuels and environmental degradation. Renewable resources include solar energy, wind power, tidal and wave strength, as well as the potential of water flows. There are currently areas where these energy-efficient methods are being implemented with good results but must be developed and exploited to the real potential. The water-based energy was considered an environmentally friendly alternative, and has been used since ancient times in mills located directly on a water course before electricity has been discovered. For obtaining a good efficiency in the energy production based on water streams, there must be favourable conditions related to the water flow rate and the difference level. Where these essential conditions are met, hydropower plants have been established in operation. There are countries where a considerable percentage of total energy is produced on the basis of water flow in hydropower plants, such as Norway producing 99% of its energy from hydro power plants, New Zealand 75%, Canada 57%, Switzerland 55%, Sweden 40%, USA 10%. Around 20% of the world's electricity is produced in hydropower plants, but the potential is much higher, especially in countries with a predominantly mountainous relief or major water courses.

2. Construction types of hydraulic turbines

Today's hydropower plants have in use several turbine types, including PELTON, KAPLAN, or Francis models. All these models are using the water flow in order to convert the hydraulic energy into mechanical rotational energy.
PELTON'S turbine model was one of the most efficient types of hydraulic turbine, invented by Lester Allan PELTON in 1870, operating on the basis of the mechanical pulse generated by falling water pressure. These hydraulic turbines are recommended and used for relatively low water flows and high level differences.
The water drop capture unit built for the PELTON turbine model contains the drainage channel made at a considerable level, the turbine mounted in the housing and the downstream water outlet channel, (figure 1). The solution of this hydropower plant can be used both on a large scale and on a small scale as a micro-hydropower having a low water flow rate, but at an optimal level difference.

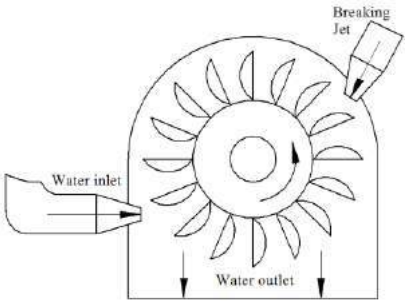

Fig. 1. Schematically representation of PELTON turbine

In ROMANIA, at the LOTRU Hydro Power Plant, PELTON turbines with vertical axis were installed, as well as the DOBREŞTI Hydro Power Plant, built within 1928-1930, equipped with PELTON turbines, which at the moment of commissioning was the highest hydroelectric power plant in Romania. [6]
FRANCIS and KAPLAN turbine models are also in use. The difference between the two constructive types lies in the fact that the water goes differently to the turbine blades: the Francis turbine has water in the radial direction, while the KAPLAN turbine benefits from the inlet of the water in the axial direction, (figure 2).
At the FRANCIS turbine, the blades are fixed, while the KAPLAN turbine blades benefit from angular adjustment in order to modify the rotational speed of the turbine shaft, depending on the intensity of the water flow.
The two types of turbines can operate at a medium water fall difference level and an medium water flow rate for the FRANCIS turbine and a low height but considerable flow rate for the KAPLAN turbine.
Rotational speed is ranging from 50-250 rpm for the FRANCIS turbine, and for the KAPLAN turbine between 200-550 rpm.

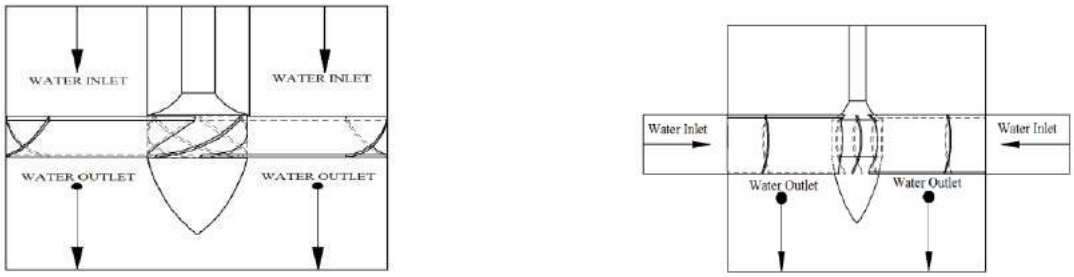

a) KAPLAN model b) FRANCIS model

Fig. 2. Schematically representation of KAPLAN and FRANCIS turbine models

Hydro power system IRON GATES I, built between 1964-1972, use vertical KAPLAN turbines operating on a 20 to 30 meter difference level, depending on the Danube level. [7]

3. Theoretical model of water flow through the hydraulic turbine

Water courses appropriate to geographical differences level are presenting particular importance since it can be used to obtain energy. Each water course can be appreciated after flow rate and drop height. Based on these parameters, the available power can be approximated, considering the flow rate, water density, drop height and gravitational acceleration: [5]

$$P = \rho \cdot g \cdot h \cdot \eta \cdot Q \tag{1}$$

The operation of the water turbine of a power plant depends on the fluid momentum on the turbine which causes the rotational movement of the turbine shaft which is connected to the power generator.

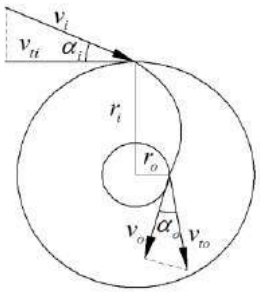

Fig. 3. Turbine blade model

The turbine shaft torque can thus be approximated based on input and output data of the water flow, (figure 3): [9]

$$T = \rho Q_w (r_i v_i - r_0 v_0) \tag{2}$$

The power at the turbine shaft can be approximated on the basis of the difference between the inlet and the outlet angle of the turbine blades: [9]

$$P_t = wT = w\rho Q_w (r_i v_i \cos\alpha_i - r_0 v_0 \cos\alpha_0) \tag{3}$$

4. CFD analysis of water flow through the turbine type system

A tri-dimensional model with a blade turbine is analyzed using the ANSYS CFX program. The system benefits from 4 radial-directional circular inputs that provide direct drive action on the turbine blades. For each entry an input flow rate of 50-100 kg/s was declared. The working fluid is chosen as water. The overall virtual hydro power model is shown in Figure 4.

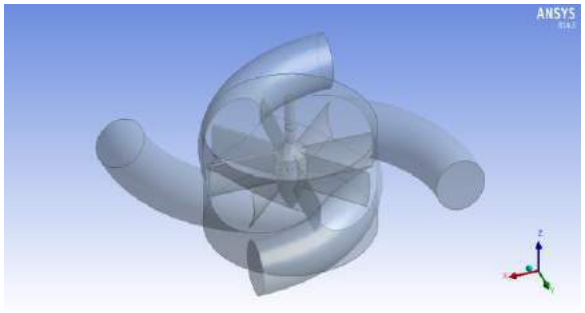

Fig. 4. Adduction channel and turbine model

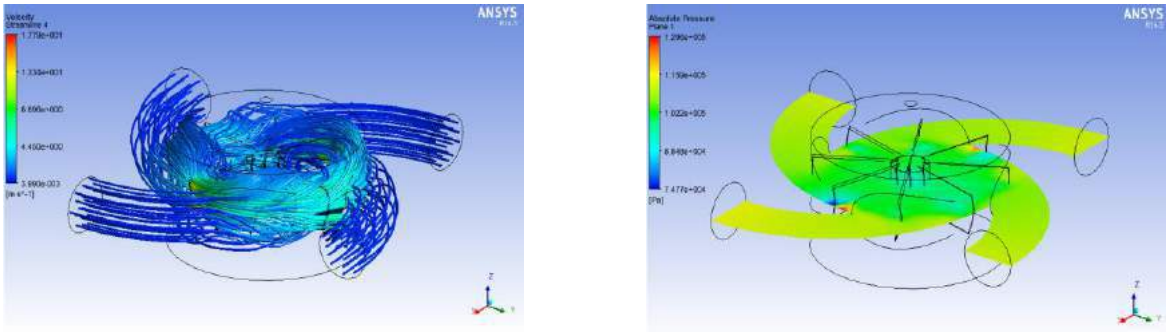

a) water velocity streamlines

b) absolute pressure values

Fig. 5. The result obtained from the flow analysis

Figure 5, shows the fluid velocity and absolute pressure. The results obtained show the direct action of the fluid on the turbine blades. Also, the calculated values for the maximum torque and total power amount that can be obtained using this turbine type are presented in table 1.
The values of the turbine shaft torque and total power were calculated using the values of the input and output velocity of the working fluid obtained from the performed analysis. The volumetric flow rate of the fluid was 0.2 m^3/s and a rotational speed of the turbine shaft of 60 rpm.

Table 1: The values for fluid velocity, torque and power

v_i (m/s)	v_0 (m/s)	T (Nm)	P(W)
10	2.5	1420	8917.6
10.5	3	1479	9288.12
11	3.5	1538	9658.64
11.5	4	1597	10029.16
12	4.5	1656	10399.68
12.5	5	1715	10770.2
13	5.5	1774	11140.72
13.5	6	1833	11511.24
14	6.5	1892	11881.76
14.5	7	1951	12252.28
15	7.5	2010	12622.8

This water-based energy generation system is a small-scaled model that shows the theoretical possibility of obtaining energy by using a low-flow rate water course.

5. Conclusions

This paper shows a hydro power system model with turbine intended for the production of energy using water streams. It is a simple, small-scaled model for which a CFD analysis was performed. Based on the result values obtained from the analysis the turbine shaft torque and the power amount productivity were calculated based on water flow rate.
This model can be a solution to apply in the case of water flows with medium water flow rate and an optimum fall height.

References

[1] Axinti, G., Axinti, A., S., Acționări hidraulice și pneumatice, Editura Tehnica-Info, Chișinău, 2009
[2] Axinti, A., S., Șcheaua, F., D., Introducere în hidraulica industrială, Editura Galați University Press, 2015
[3] Vasilescu, Al., A., Mecanica fluidelor, Ministerul Educatiei și Învățământului, Universitatea din Galați, Galați, 1979
[4] Scheaua, F., D., Aspects Regarding the Special Hydraulic Distributors Operation, Hidraulica Magazine, ISSN 1453-7303, no.4, 2016
[5] https://en.wikipedia.org/wiki/Hydropower
[6] http://www.autogreen.ro/energie/turbina-pelton/
[7] http://hidroelectrica.ro/Details.aspx?page=108&article=116
[8] http://www.green-mechanic.com/2014/03/frances-turbine-vs-kaplan-turbine.html
[9] http://www.mpoweruk.com/hydro_power.htm

Technical Solutions for Digital Hydraulic Cylinders and Test Methods

PhD. Stud. **Ioan PAVEL**[1], PhD.Eng. **Radu Iulian RĂDOI**[1],
Dipl. Eng. **Alexandru-Polifron CHIRIȚĂ**[1], Dipl. Eng. **Mihai-Alexandru HRISTEA**[1],
Dipl. Eng. **Bogdan Alexandru TUDOR**[1]

[1]Hydraulics and Pneumatics Research Institute INOE 2000-IHP; pavel.ihp@fluidas.ro

Abstract: *A cylinder with a continuously variable piston area is considered by many an impossible goal. This paper presents solutions for digital hydraulic cylinders with certain discrete values of multiple surfaces, which, selected by well established rules, can control the force and speed output values although they are supplied with constant pressure and flow. Also hereinafter we present test diagrams for digital pumps and digital switching directional control valves, as well as a test stand model for multiple-area cylinders, their testing methodology and mathematical modeling of a three-area digital cylinder.*

Keywords: *Multiple-area cylinders, digital cylinders, digital hydraulics, digital cylinder test stand, multiple-area cylinder testing methodology*

1. Introduction

Digital Hydraulics refers to systems that use components (actuators or control parts) which have certain discrete values and actively control the system output signal. Digital Hydraulics basically covers most hydraulic equipment: pumps, directional control valves, linear or rotary motors, accumulators [1].
There are two branches in the digital hydraulics:

- Systems based on parallel distribution technology
- Systems based on the switching method.

Parallel distribution systems have a multitude of components (on/off valves) connected in parallel, and the output is controlled by changing the state combination of components. The system has a certain number of discrete output values and it is possible to maintain or adjust the values of the output signal according to well-established rules, most often by a binary code.
Technologies based on the switching method use devices with fast and continuous switching.
There are two main methods by which the input voltage is switched [1]:

- The PWM (Pulse Width Modulation) control
- The PFM (Pulse Frequency Modulation) control.

The PWM (Pulse Width Modulation) control is the most commonly used flow control method, including by the specialists at INOE 2000-IHP. In this method, the ratio between closed and open (pulse width on a frequency step), will vary according to the output requirements of the system. Thus, at constant frequency there are obtained flow variations proportional to the opening time setting for one step.
The PFM (Pulse Frequency Modulation) is based on setting a fixed stationary time on either closed or open from a return period of the valve disk and frequency variation. By varying the frequency, there are flow variations proportional to the adjusted frequency due to the number of fixed stationary stops on or off in the time unit.
PFM can be with two types of initial adjustments:

- On time set constant
- Off time set constant.

A hydraulic cylinder can be actuated with a digital PWM switching directional control valve when targeting speed variation and energy efficiency [2].
There are constantly presented new solutions of digital hydraulic devices or digital hydraulic systems based on digital devices already in series production and existing on the market [3], [4]. The basic idea in promoting and implementing digital hydraulics is to replace the expensive and sensitive servo systems with a multi on/off directional valves assembly or with cheap and reliable switching devices. Parallel connection solution enables good flow control without continuous

switching of directional control valves. Results can be obtained even with slower directional control valves, which reduces the purchase and maintenance price of hydro-powered equipment.
There are some challenges to the switching method that should be addressed, the most important of which are the control method and the switching speed of the digital directional control valves.
Digital technology has the potential to make cheaper, more energy-efficient, and more reliable hydraulic systems, but research and technological development in the field will play a crucial part [4]. The trend was from analog to digital in all areas of technology; now it seems that the turn of Hydraulics came to experience this trend.
In Europe, the concern for scientific research in the field of digital hydraulics is recognized through results disseminated in conferences and papers published in prestigious journals; such results belong to research center at Tampere University of Technology in Finland and Johanes Kepler University Linz, Institute of Machine Design and Hydraulic Drives in Austria [4].
In Romania the foundations of a Digital Hydraulics Laboratory have been laid at INOE 2000-IHP; a team of young researchers perform their activity there; on the basis of several patent applications, they have begun designing and testing digital hydraulic devices. There are thought out new solutions for digital pumps, digital pulse width modulation switching directional valves, multiple-area digital hydraulic cylinders, various schematic diagrams and digital assemblies.

2. Digital hydraulic equipment testing diagrams

A system is considered digital if it has a digital mounting schematic diagram or a digital device that controls the output values of that system [5]. In this regard, at INOE 2000-IHP a specialized laboratory has been established, which is equipped with a 300 l oil tank, two 15 KW and 22 KW electro-pumps and three specialized testing devices for which test diagrams were designed and also auxiliary equipment required for testing digital pumps with various-area piston, digital pulse width modulation switching directional valves and multiple-area digital cylinders.

2.1 Testing diagram for digital pumps (Fig. 1.)

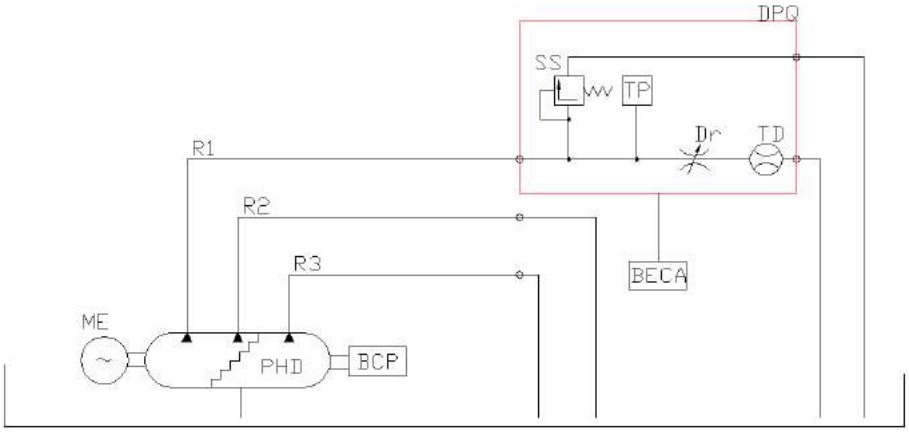

Fig. 1. Testing diagram for a digital pump

Testing the experimental model of the digital pump is done by means of the pressure and flow measurement device which can be mounted on each flow branch - *R1, R2, R3* - of the digital pump and also on combinations of them. The device provides protection against overpressure by means of the *SS* safety valve, pressure monitoring by means of the *TP* transducer, load simulation by means of the *Dr* throttle and flow monitoring by means of the *TD* transducer. Information on pressure and flow values is sent to the *BECA* control and data acquisition unit.
The main objective of these tests is to check the flow at nominal working pressure on each branch of the pump and its ability to provide variable flow by selecting different combinations of branches with different flow rates. There are also monitored the evolution of the flow with the variation of the working pressure, the accuracy of flow control and its pulses.

2.2 Testing diagram for pulse modulation directional control valves (Fig. 2.)

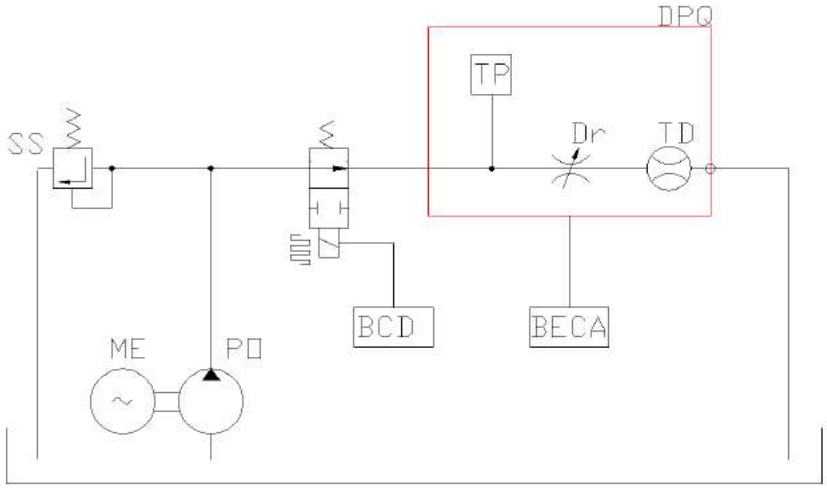

Fig. 2. Testing diagram for pulse modulation directional control valves

For testing digital switching on / off (PWM) directional valves a device (*DPQ*) for measuring the test pressure and flow rate was designed; it consists of a pressure transducer - *TP*, a throttle - *Dr* and a special flow transducer - *TD*. During tests there is also used a control unit for the digital switching hydraulic directional valve - *BCD*. A regular pumping system – *PO* and a safety valve – *SS* are used to supply the directional valve. The parameters to be monitored are pressure and flow depending on the variation of the switching signal.

2.3 Testing diagram for multiple-area digital hydraulic cylinders (Fig. 3.)

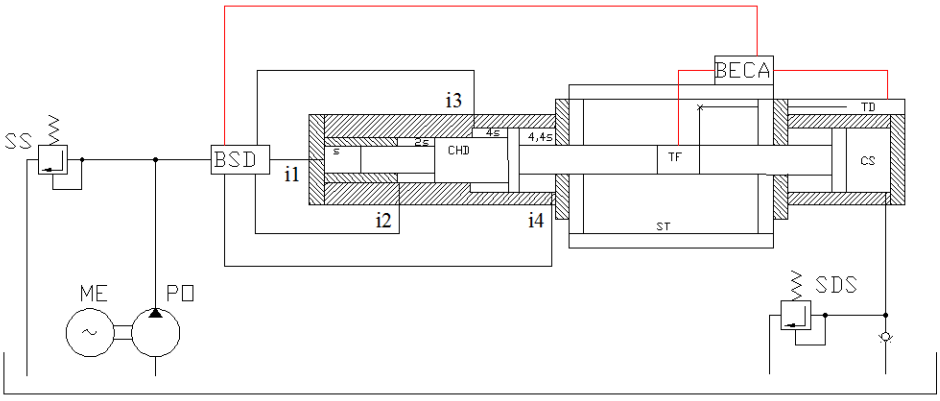

Fig. 3. Testing diagram for multiple-area digital hydraulic cylinders

For testing multiple-area digital hydraulic cylinders a specialized stand is used; it consists of a frame - *ST* which allows to mount the cylinder to be tested - *CHD*, the force transducer - *TF*, the displacement transducer - *TD* and the load cylinder - *CS*. The electronic control and data acquisition unit - *BECA* has the role of acquiring data from the force and displacement transducer and controlling the distribution selection unit - *BSD*. Constant flow and pressure supply is made by using a regular pump - *PO* and a safety valve - *SS*. The load adjustment is done by means of the load valve - *SDS*. Testing of multiple-area digital hydraulic cylinders is done according to the test methodology presented below.

3. Digital hydraulic cylinder test methodology

As a technical means of measuring the quality of the digital hydraulic cylinders we have used the hydraulic stand presented; it is able to provide the test conditions required for subjecting the digital hydraulic cylinders to the defining tests to demonstrate the principle of operation V=f(Ai) at

constant flow, F=f(Ai) at constant pressure and to determine the technical characteristics designed. Functional models of the digital hydraulic cylinders under this study cannot be found in the test standards in force, that is why a set of tests inspired by them is required, through which to verify the technical characteristics of the design and demonstrate the basic idea that at constant pressure and flow supply there are achieved (by selecting combinations of areas) at the digital hydraulic cylinder rod variable force and speed values, repeating as determined by specified graphs.

Testing of multiple-area digital cylinders

Testing of functional models will be done on a specialized stand (Fig. 4), with controlled hydraulic load, equipped with force transducer for active control of the force adjusted on the cylinder under test and for data acquisition, and equipped also with displacement transducer for active control of the speed adjusted on the cylinder under test and for data acquisition.

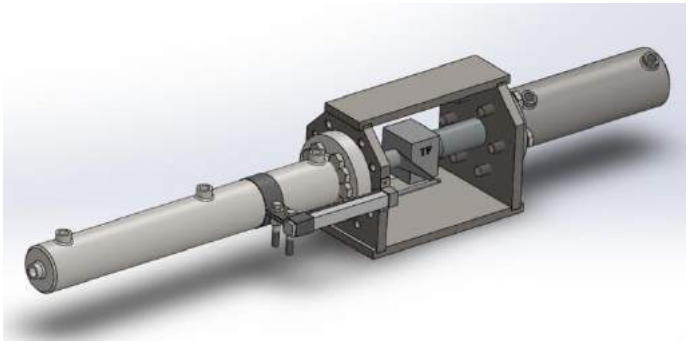

Fig. 4. Multiple-area cylinder test stand

Running tests do not always require tight or fast closing devices. The test schematic diagram can include a standard pumping system and equipment, as shown in Figure 5.b), in which case the number of electromagnets actuated is reduced.

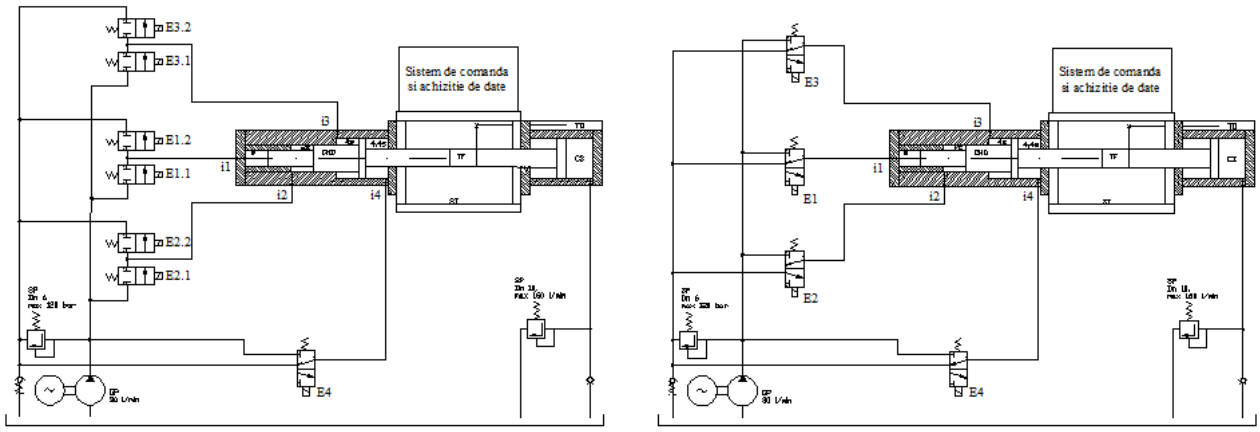

a) b)

Fig. 5. Connection diagram for a three-area CHD test stand
a) on/off directional control valve variant; b) classic directional control valve variant

Caption:
CHD- Digital Hydraulic Cylinder
CS- Load Cylinder
TF- Force Transducer
TD- Displacement Transducer
SP- Pressure Valves
GP- Pumping Unit
ST- Test Stand
E1-4 – Electromagnets

The successive sequences of the tests are as follows:

- re-check that the stand and the equipment mounted on it corresponds to the mounting diagram;
- check exterior tightness;
- check interior tightness;
- check starting pressure and minimum idling pressure;
- force tests are carried out - F=f(Ai) - at constant pressure;
- speed tests are carried out - V=f(Ai) - at constant flow.

The tests on the experimental digital hydraulic cylinder model are performed as follows:

Checking of the exterior tightness is performed to the test pressure of:

- p_{min}
- 0.5 $p_{n,}$ but no more than 50 bar
- 1.25-1.5 $p_{n,}$ but no more than 1.1 p_{max}.

after performing five double strokes at the minimum speed (all areas are active).

During the tests, to the outside of the cylinder behind the sealing and scraping system no visible oil traces shall occur which increase over time. It is admissible an oil film under the condition of not agglomerating in the form of drops on the piston rod. The result of the measurements is listed on the test data sheet.

Checking of the interior tightness is usually done in the extreme positions of the piston and in three to five intermediate points located equidistant along the entire stroke of the piston at the test pressure p_i= 1.25-1.5 p_n but no more than 1.1 $p_{max,}$ for 1 minute for each area of the multiple-area cylinder. For the model being tested, commands corresponding to the control code 1,2 and 4 in the command cyclogram are executed.

For each position the internal losses are estimated by using the indications of the stroke transducer (or comparator) for 1 min. Displacement of the rod is not admissible. The result of the measurement is listed on the test sheet.

Checking of the minimum pressure for uniform and shock-free movement of the piston and checking of the starting pressure are done in idling. The working chambers are filled with oil at the ambient temperature at which the test is carried out, kinematic viscosity ν=35 cSt. All surfaces of the multiple-area cylinder are connected to a source of oil under pressure according to the test scheme. There is recorded the lowest pressure at which the piston displacement with minimum speed occurs and also the pressure for which the piston has a smooth motion without shocks for each surface of the multiple-area cylinder but also on all the summed surfaces, over the entire length of the stroke. For the three-area cylinder, commands corresponding to the control code 1,2,4 and 7 in the command cyclogram are executed. Uniformity of the piston displacement speed is checked with a recorder. The result of the measurement is listed on the test sheet.

Checking of the thrust force is made at constant pressure by selecting combinations of sections of the multiple-area digital cylinder, over the entire length of the stroke. Force is measured by means of force transducers with precision class of at least 1 on a stroke sector corresponding to pressure and force stabilization. The resistance-type load is created by means of a hydraulic cylinder powered by a separate hydraulic installation, low pressure, and it can be continuously varied through the adjustable pressure valve. Measurement is made to determine the force variation depending on the combination of selected areas, F=f(Ai) at constant pressure. Check commands are made according to the command cyclogram, successively for all combinations along the advance rod stroke. The result of the measurement is listed on the test sheet.

Checking of the piston speed is made at constant flow; the displacement must be carried out under load, smoothly and without shocks over the entire length of the stroke. Verification is done for each combination of surfaces of the multiple-area cylinder but also on all the summed surfaces, along the advance rod stroke. Measurement is made to determine the speed variation depending on the combination of selected areas, V=f(Ai) at constant flow. Check commands are made according to the command cyclogram. The result of the measurement is listed on the test sheet.

The command cyclogram to make the graphs of F=f(Ai), at p=ct and V=f(Ai), at q=ct for a three-area CHD - F corresponds to the force obtained with the smallest area at constant pressure, and V corresponds to the speed achieved with constant flow for the smallest section.

The command cyclogram for the three-area cylinder

Control code	Input commands							Output values	
	s		3 s		3.76 s		4.2 s	Force	Speed
	E1.1	E1.2	E2.1	E2.2	E3.1	E3.2	E4		
0	0	0	0	0	0	0	0	0	0
1	1	0	0	1	0	1	0	1F	1V
2	1	0	1	0	0	1	0	3F	0.33V
3	1	0	1	0	0	1	0	4F	0.25V
4	1	0	0	1	1	0	0	4.76F	0.2V
5	0	1	1	0	1	0	0	6.76F	0.16V
6	1	0	1	0	1	0	0	7.76F	0.14V
Retraction	0	1	0	1	0	1	1	4.4F	0.227V
Energy recovery (retraction with external load; secondary control)									
-1	1	0	1	0	0	1	1	0.2F	0.227V
-2	0	1	0	1	1	0	1	0.44F	0.227V
-3	0	1	1	0	0	1	1	1.2F	0.227V
-4	1	0	0	1	0	1	1	3.4F	0.227V

The tests will be performed according to the present testing methodology for multiple-area digital cylinders, using the stand, test schemes, and control system codes. The data will be acquired and a test report for the tests performed will be elaborated. The goal will be to demonstrate the idea that the digital hydraulic cylinder is supplied with constant pressure and flow and there are achieved variable forces and speeds, controllable by selecting surface combinations according to the command cyclogram to plot the graphs of F=f(Ai), at p=ct and V=f(Ai), at q=ct.

4. Solutions for multiple-area digital hydraulic cylinders (Fig. 6, 7, 8, 9, 10)

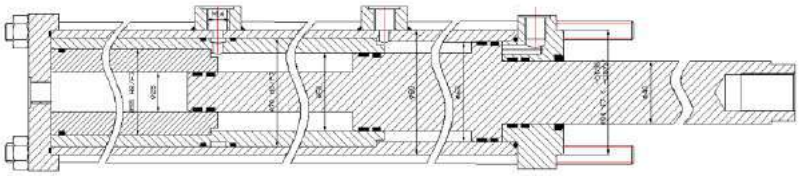

Fig. 6. Solution for a digital hydraulic cylinder with three binary coded areas

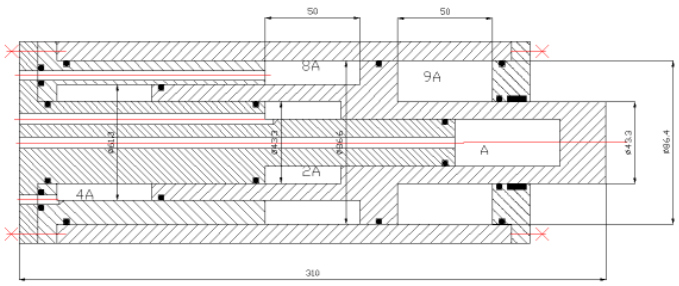

Fig. 7. Solution for a digital hydraulic cylinder with four binary coded areas

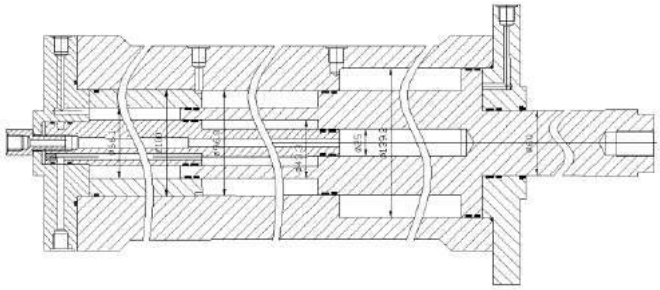

Fig. 8. Own solution for a digital hydraulic cylinder with five binary coded areas

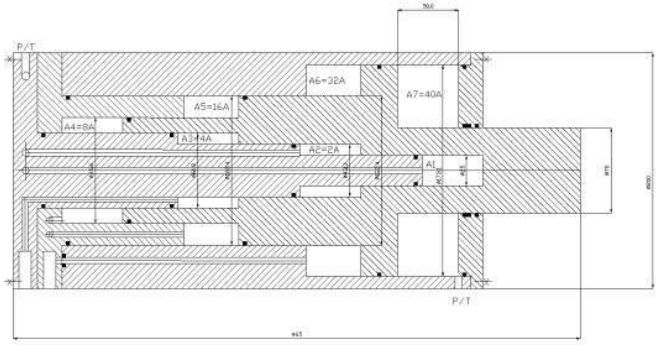

Fig. 9. Own solution for a digital hydraulic cylinder with six binary coded areas

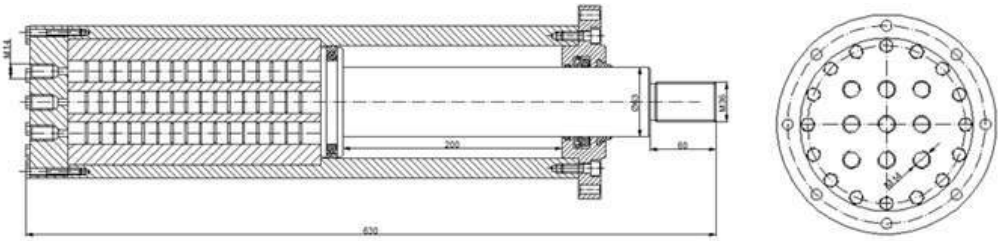

Fig. 10. Solution for a multi-piston digital hydraulic cylinder with nine equal areas (PNM coding)

The result of tests, data acquisition and comparison with mathematical modeling of the three-area CHD will be presented in another paper in a future issue of the magazine.

5. The mathematical model of the three-area digital hydraulic cylinder

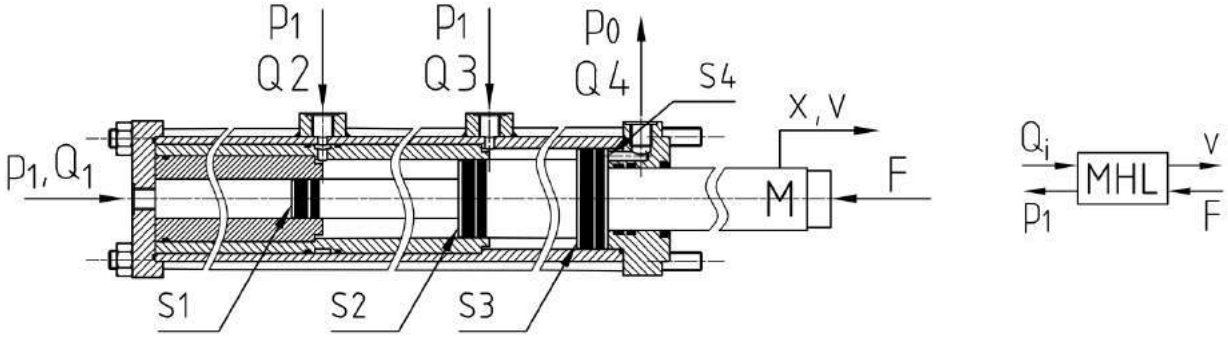

Fig. 11. The physical model

If for the hydraulic cylinder in the figure 11 we consider $p_0 = 0$, the mathematical model is:

$$Q_i = S_i \cdot v + a_M \cdot p_1 + \frac{V_0 + x \cdot S_i}{E} \cdot \frac{dp_1}{dt} \quad (1)$$

$$M \frac{dv}{dt} + b_M \cdot v + c_f \cdot sgn(v) \cdot p_1 \cdot S_i + F = p_1 \cdot S_i \quad (2)$$

In the equations above and in Figure 11 we noted: Q_i – input flow (Q_1, Q_2, Q_3,) [m^3/s], p_1 – motor chamber pressure [N/m^2], v – motor spindle speed [m/s], a_M – linearized coefficient of flow rate losses proportional to pressure [$(m^3/s)/(N/m^2)$], V_0 – the initial volume of fluid on the left of the cylinder chambers [m^3], x – displacement [m], M – moving mass [kg], b_M – linearized coefficient of force losses proportional to speed [N/(m/s)], c_f – coefficient of friction, F – resistance force [N], E – fluid modulus of elasticity [N/m^2].

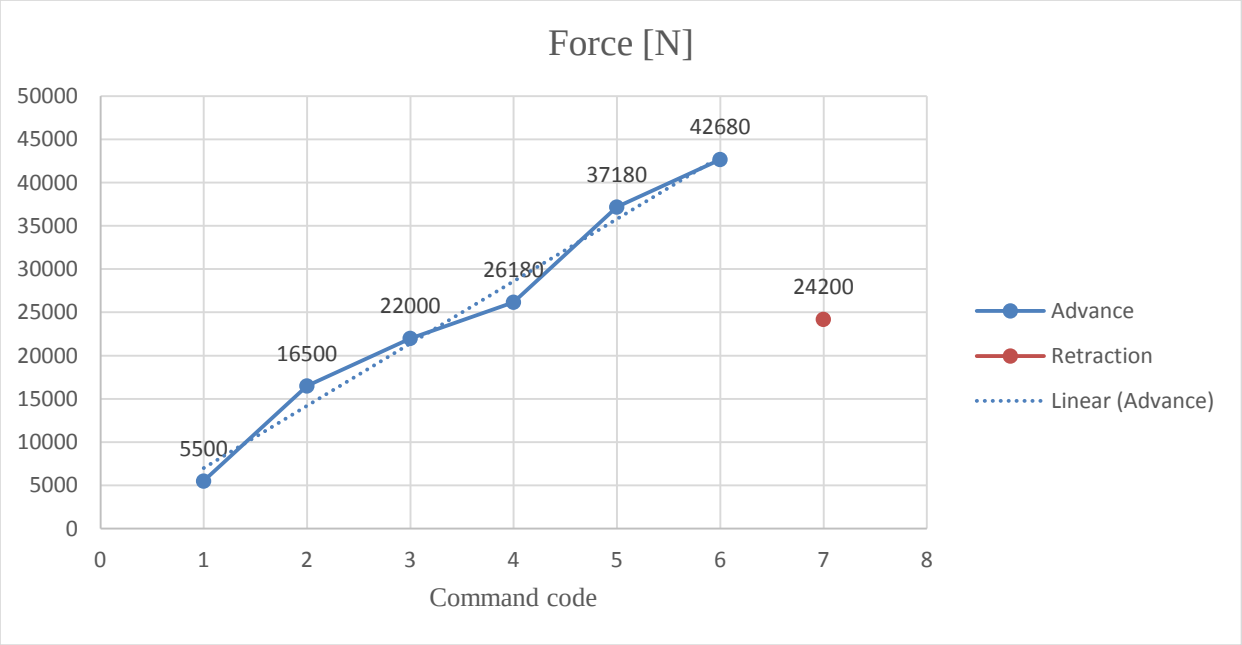

Fig. 12. The forces achieved by the hydraulic cylinder

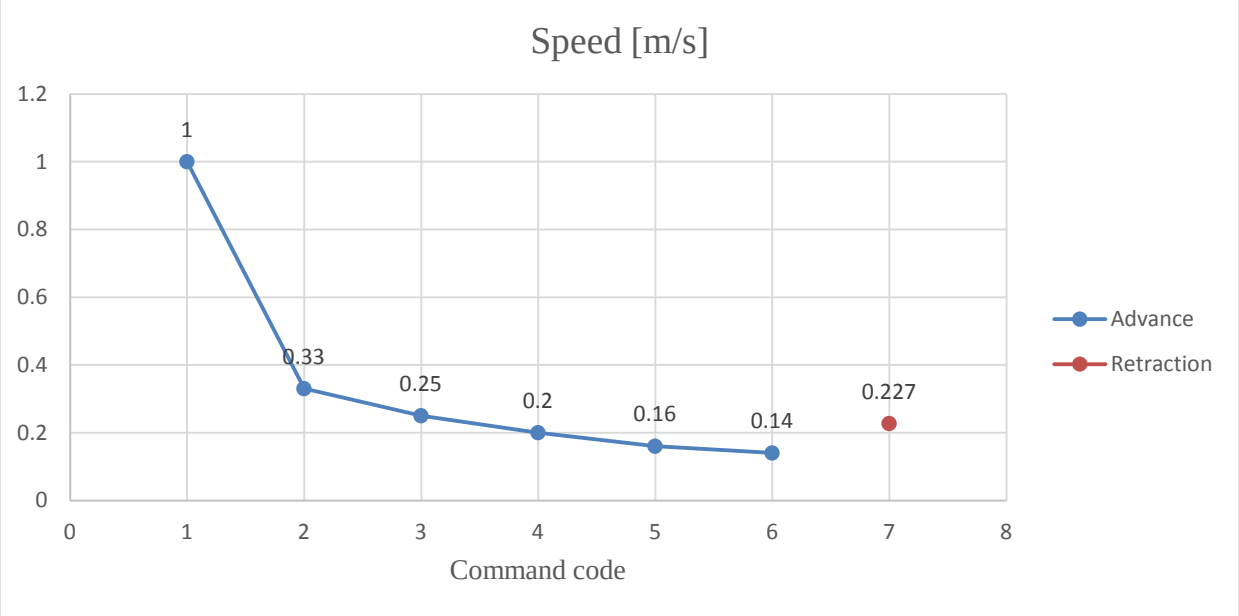

Fig. 13. The speeds achieved by the hydraulic cylinder

In the previous graphs one can see the quasi-linear variation of force and the variation of the hydraulic cylinder speed supplied from a constant flow source.

6. Conclusions

The conclusions arising from this paper are as follows:

- Testing of digital hydraulic equipment can be done on test stands equipped with standard hydraulic devices;
- Electronic control systems are specific to digital hydraulic equipment;
- In our case, test solutions are chosen to determine the correct operation of digital hydraulic equipment, not to determine factors that influence their dynamics;
- The next stage in the research work of the team within INOE 2000-IHP is to improve the functional performance and the manufacturing technology of digital devices, allowing for easy introduction of them into manufacturing on a large scale and reducing their cost price.

Over the next period, cost reductions and increased energy efficiency will be dominant as success factors for any industry. Currently, the hydraulics industry is not fit to meet these requirements: classic hydraulic systems and components are rather expensive and energy-inefficient [6].
Correct dimensioning and choosing the best technical and economic solutions could make the hydraulic systems the fastest and most efficient form of power transmission. Energy savings resulting from the implementation of digital hydraulic solutions can improve the technical and economic performance of the technology lines in which they are used, reflecting ultimately in the execution price of the products put on the market. At the same time, through energy savings and efficient use of resources, they contribute to the foundations of sustainable development.

Acknowledgment

This paper has been developed in INOE 2000-IHP, with financial support of the Ministry of Research and Innovation (MCI), under the national research *Programme NUCLEU-2016,* project name: *Physics of processes for reducing energy losses and developing renewable energy resources by use of high-performance equipment,* phase no.3.1.1, phase name: *Theoretical and experimental research on models of linear hydraulic motors as a digital concept*, project code PN 16-40-03-01, financial agreement no. 5N/2016, Additional act no. 3/2017.

References

[1] R. Scheidl, H. Kogler, B. Winkler, "Hydraulic switching control-Objectives, concepts, challenges and potential applications", *Proc. of 20th International Conference of Hydraulics, Pneumatics, Sealing Elements, Fine Mechanics, Tools, Specific Electronic Equipment & Mechatronics HERVEX 2012*, November 7-9, Calimanesti-Caciulata, Romania, ISSN 1453 – 7303; pp.56-67;
[2] R. Scheidl, G. Hametner, "The role of resonance in elementary hydraulic switching control", *Proc. Instn. Mech. Engrs*., Vol. 217 Part I: J. Systems and Control Engineering, 2003, pp. 469-480;
[3] M. Ketonen, "Implementation of a digital hydraulic valve system with Bosch Rexroth sec valves", *Proc. of the Fifth Workshop on Digital Fluid Power*, October 24-25, 2012, Tampere, Finland; pp.161-174;
[4] M. Linjama, M. Vilenius, "Digital Hydraulics – Towards Perfect Valve Technology", Digitalna Hidravlika, *Ventil - Journal for Hydraulics, Automation and Mechatronics*, 14 (2), 2008; pp.138-148;
[5] M. Linjama, K. Huhtala, "Digital power management system –Towards lossless hydraulics", *Proc. of the Third Workshop on Digital Fluid Power,* October 13-14, 2010, Tampere, Finland; pp.5-22;
[6] M. Linjama, "Digital Fluid Power – State of the Art", *The Twelfth Scandinavian International Conference on Fluid Power*, Volume 2(4), SICFP'11, May 18-20, 2011, Tampere, Finland; pp.331-354.

Simulation of the Flow Processes in the Waste Water Treatment Plant

Prof.PhD.eng. **Mariana PANAITESCU**[1], Prof.PhD.eng. **Fanel-Viorel PANAITESCU**[2]

[1] Constanta Maritime University, marianapan@yahoo.com

[2] Constanta Maritime University, viopanaitescu@yahoo.ro

Abstract: *In order to accomplish the flows from the existing processes simulation in a wastewater treatment plant there has been used a software tool called GPS-X, version 6.1.1.The steps of simulation were the following: it has been designed the flow station wastewater treatment plant; settings have been configured for installation components; subsequently input data have been changed according to the number of inhabitants, interchangeable.*
Through simulation, there has been established loading type and subsistence change input data.
In the end, there runs the process of simulation of waste water treatment plants, listing the values of waste water parameters monitored through simulation, before the evacuation into natural receiver. Through this work one can see that the values of the analyzed parameters did waste water purified; to discharge into natural receiver values are reduced from those set at the input of the plant, making it possible to purify water according to the standards in force. Sustainable development implies the control of environmental pollution through the use of easy and efficient software tools.

Keywords: *Simulation, waste water treatment plant, flow, environment6al pollution, GPS-X software*

1. Introduction

In order to secure there place on the international market all countries seek to implement useful tools for increasing the competitiveness of their products, falling into effective, modern systems of quality assurance.
The International Organization for Standardization has developed and published designs for such schemes in ISO standards series 9000, which currently underlie quality systems implemented in many enterprises and their compliance certification. Currently such certification of conformity to the requirements of ISO 9000 standards is done by international accreditation bodies.
Economic development in the past decades through industrialization, urbanisation materialized on chemical transformation of agriculture, brought the issues related to the impact on the natural environment through increased consumption of natural resources, but also the introduction of disruptive factors, pollutants. The problem of modeling the process of wastewater treatment plant is an important issue, particularly in the field of topical environmental pollution. Sustainable development involves pollution control environment relative to economic growth. The use of complex software tools, such as GPS-X, is a real help in validating the reaction process, generating simulated graphs of parameter variation.
Through this paper one can see that the values of the analyzed parameters did waste water purified; to discharge into natural receiver values are reduced from those set at the input of the plant, making it possible to obtain water purified according to the standards in force.

2. Technological flow design of waste water treatment plant

There has been designed the technological flow for the wastewater treatment plant (WWTP) (Figure 1).

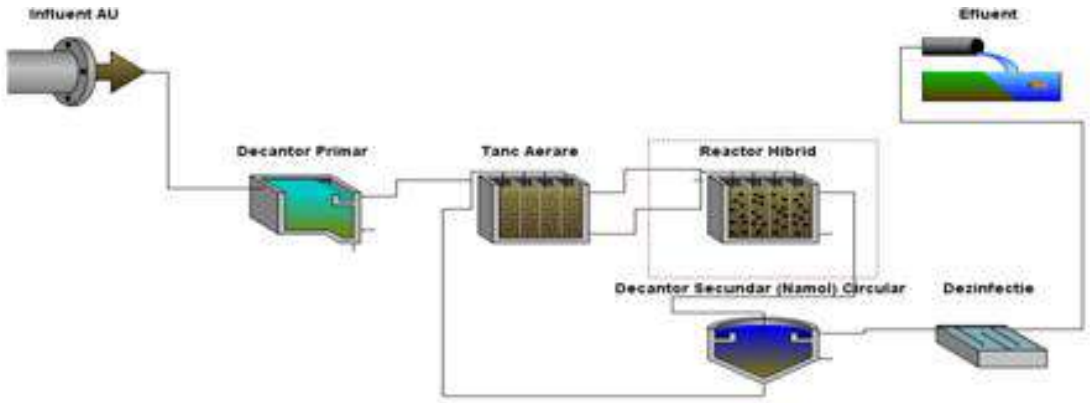

Fig. 1. Technological flow for WWT

Constituents are: Influent-waste water from public network, primary settler (chosen to rectangular), aeration basin, hybrid reactor (anaerobic biodegradation, biogas generation subsequently used as an energy source), secondary settler (radial), and for advanced treatment plant; there are available filtering options (slowly filtration, quickly filtration, sands filters, membrane filtration) and disinfection.
Configure the settings as follows: component installations, initial concentration in primary settler (Fig. 2), aeration basin (Fig. 3), number of reactors in the aeration basin (Fig. 4), number of reactors in the hybrid reactor (Fig. 5) - specific surface of biofilm is 530 l/m, secondary settler (Fig. 6), disinfection (Fig. 7). Aeration basin is a basin of pneumatic aeration with the introduction of air bubbles (1.5-3 mm).

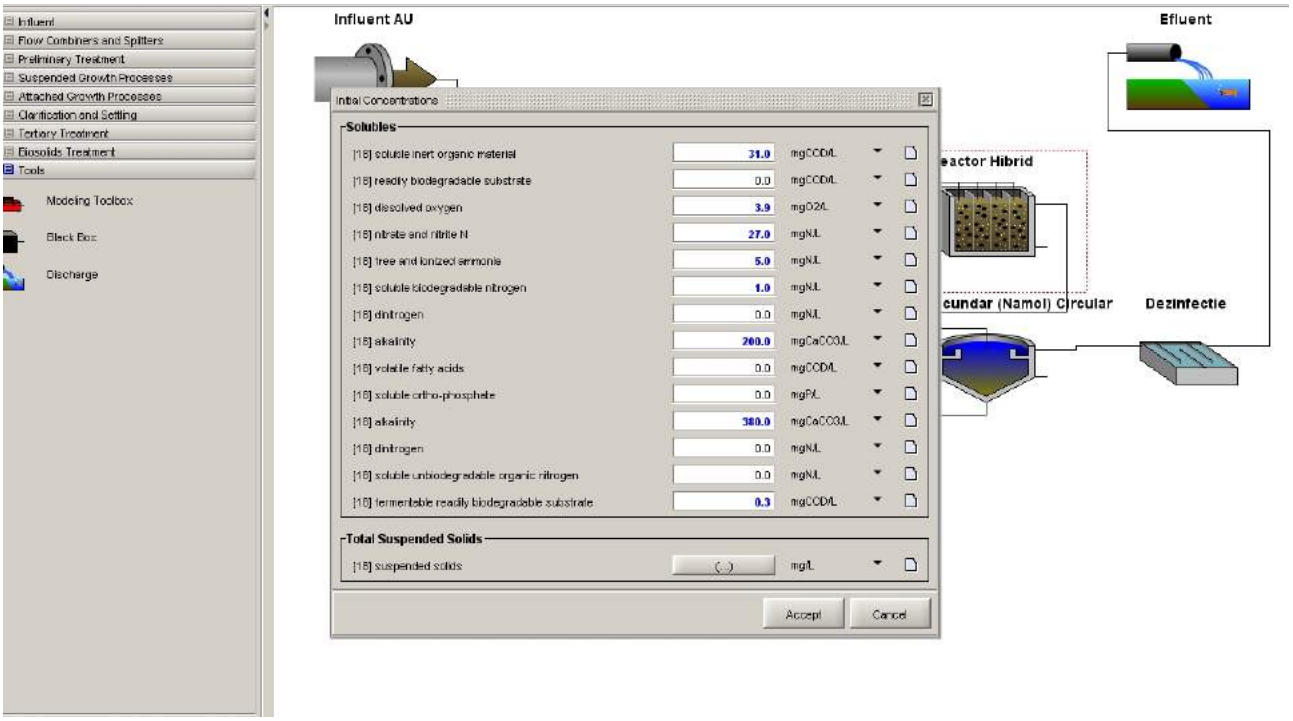

Fig. 2. Initial concentrations

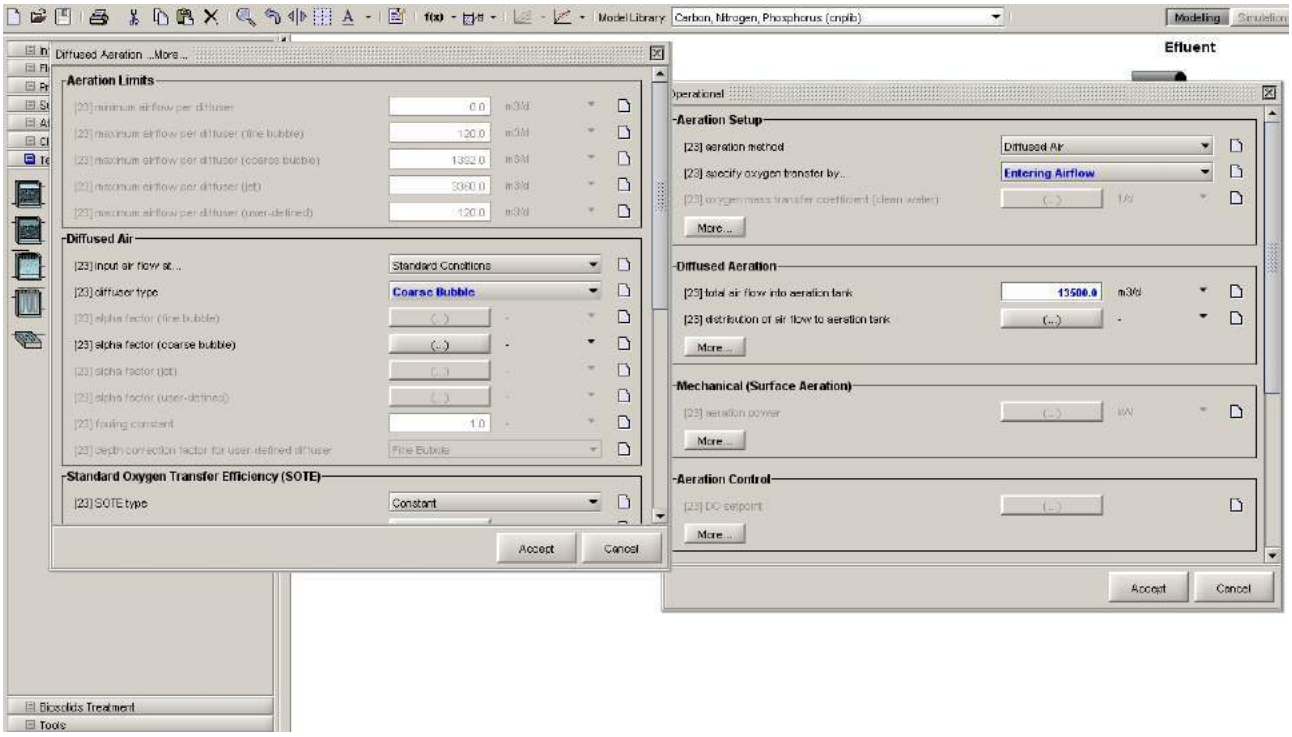

Fig. 3. Aeration setup

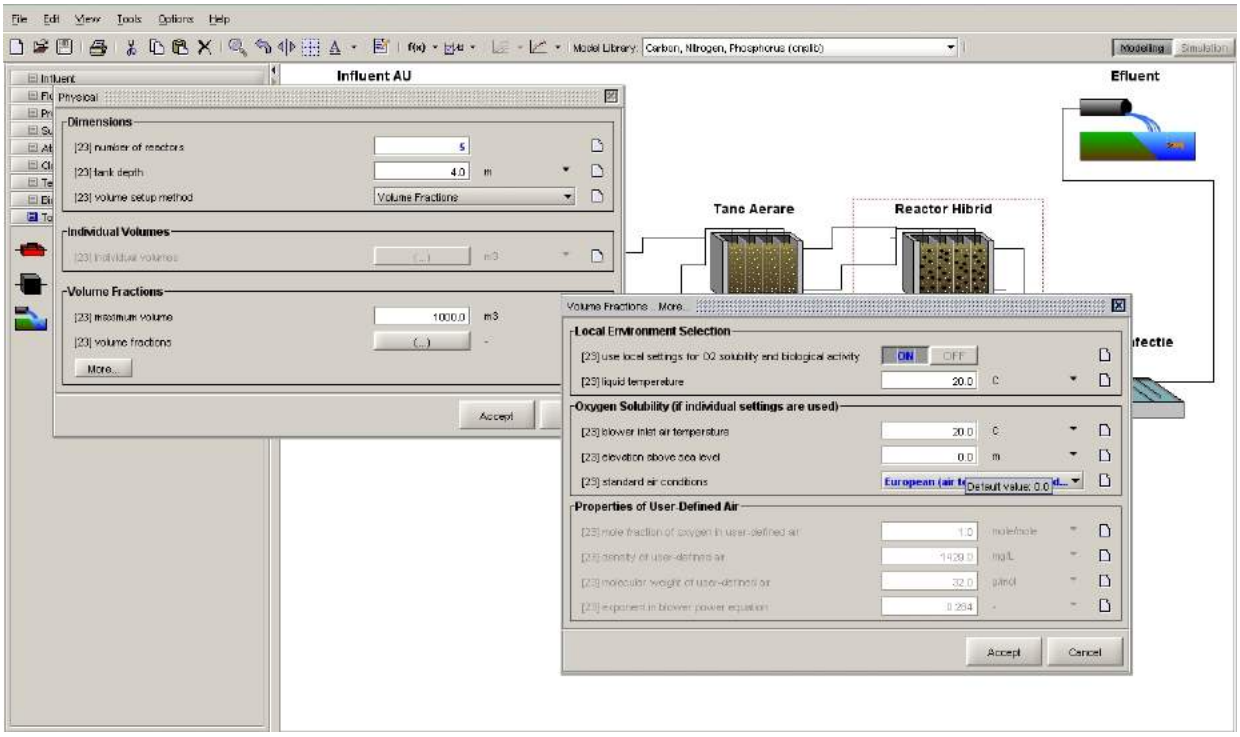

Fig. 4. Number of reactors in the aeration basin-5

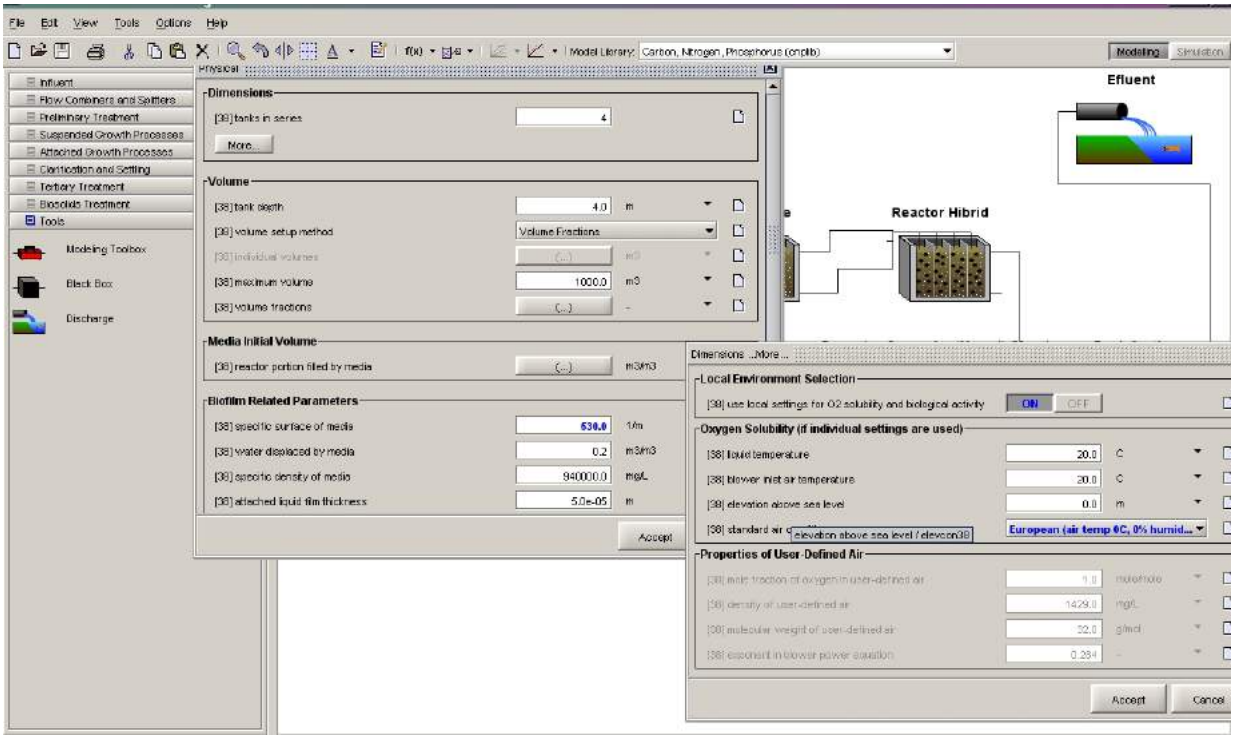

Fig. 5. Number of reactors in the hybrid reactor-4

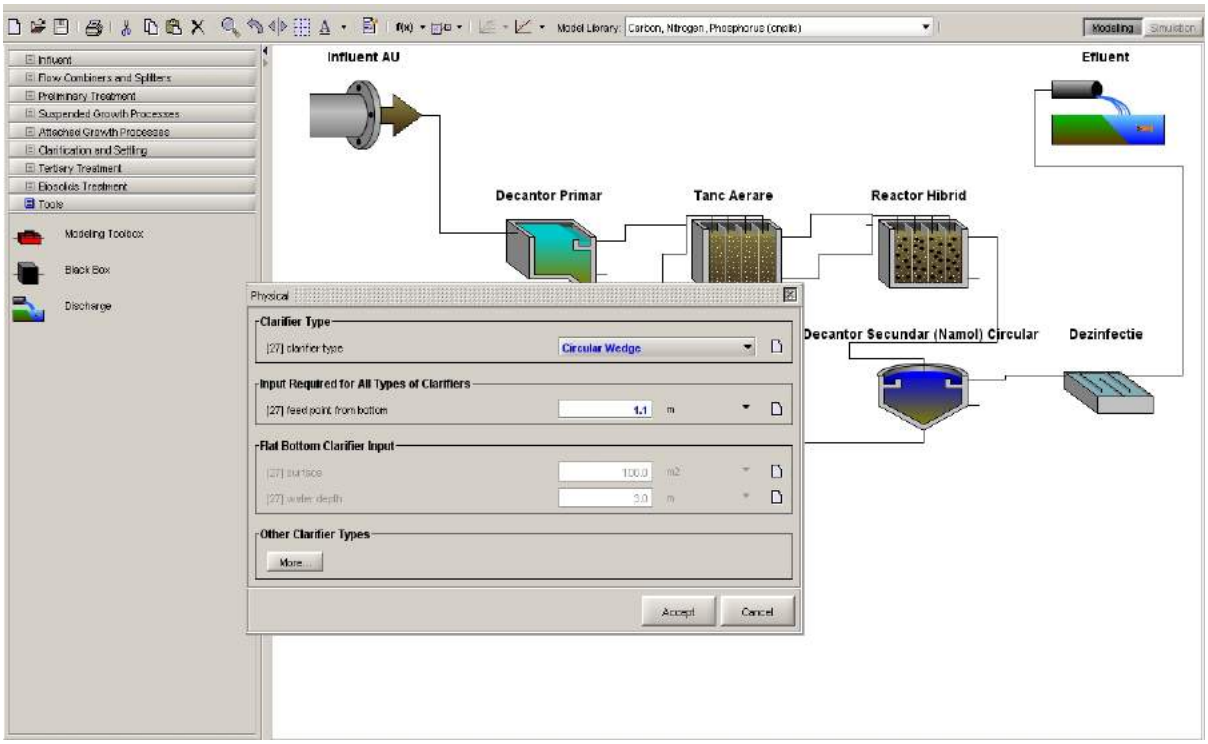

Fig. 6. Circular secondary settler WWT

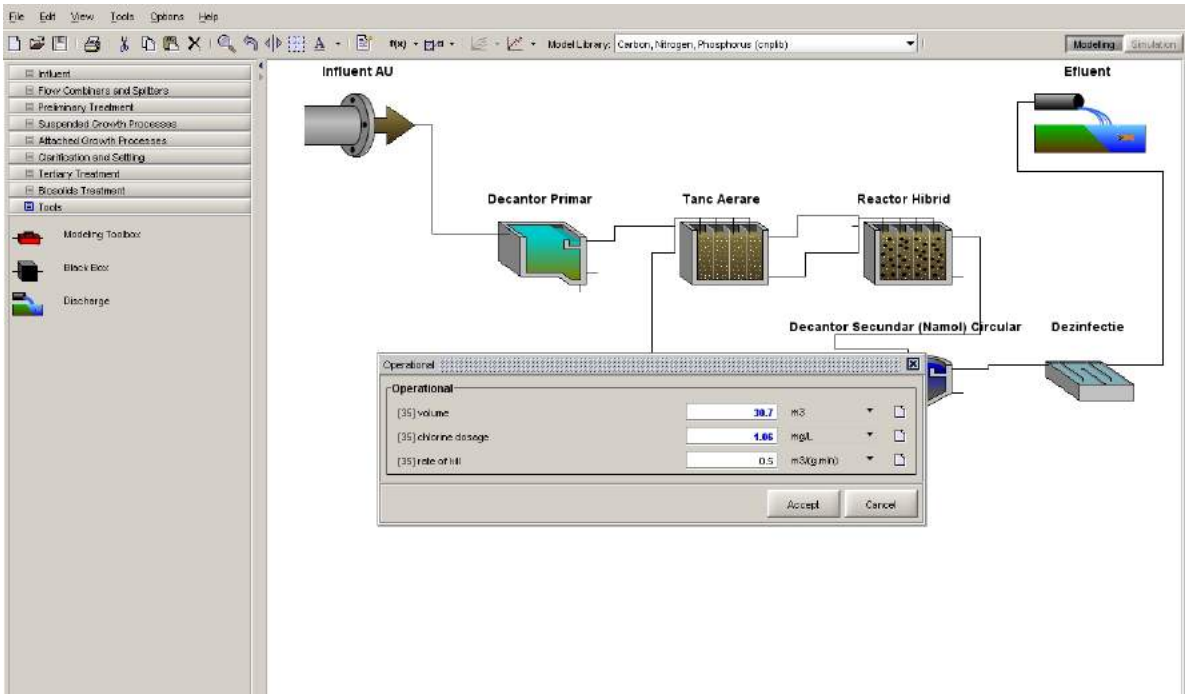

Fig. 7. Disinfection

2.1 Input data

Then introduction/modification of the input data follows (Fig. 8).

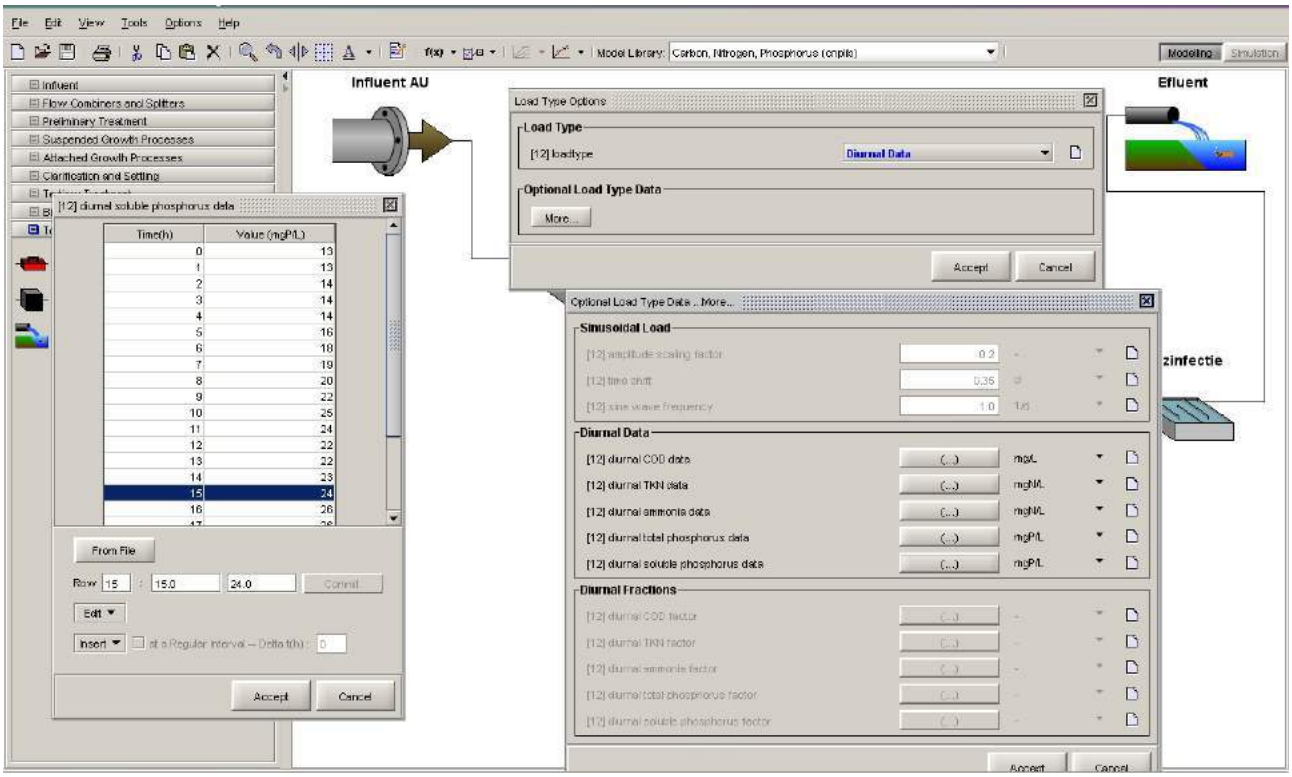

Fig. 8. Diurnal data

Input data are (Fig. 9):

COD – Chemical Oxygen Demand -500 g/m^3; Total Kjeldhal Azoth (TKN)- 40 g/m^3, Total Phosphorus (TP) – 15 g/m^3. The amount of phosphates compounds (Ortho-phosphates soluble)-9 g/m^3, nitrogen compounds- 29 g/m^3, free ammonia and ionized, nitrates and nitrites- 0.2 g/m^3. Influent alkalinity will be 9 moles/m^3.

CCO reports/SSV (volatile suspended solids), Bod5/BOD expanded, SSV/SST (total suspended solids) will have the values of 1.1, 0.53 respectively 0.81. Organic fractions of influence: fraction of inert soluble matter on total CCO-0.05, fraction of biodegradable material, through fermentation from total CCO-0.7, particulate inert fraction from total CCO-0.13. Amount of insoluble solids suspensions -26.7 g/m^3; the soluble inert organic materials-25 g CCO/m^3; easy biodegradable substrate-350 g CCO/m^3; inert organic matter particulata-65 g CCO/m^3; hardly biodegradable substrate-60 g CCO/m^3; quantities of SST, SSW and SSIT (total inorganic solids suspensions)-140.3 g /m^3, 113.6 g/m^3, respectively, 26.7 g /m^3.

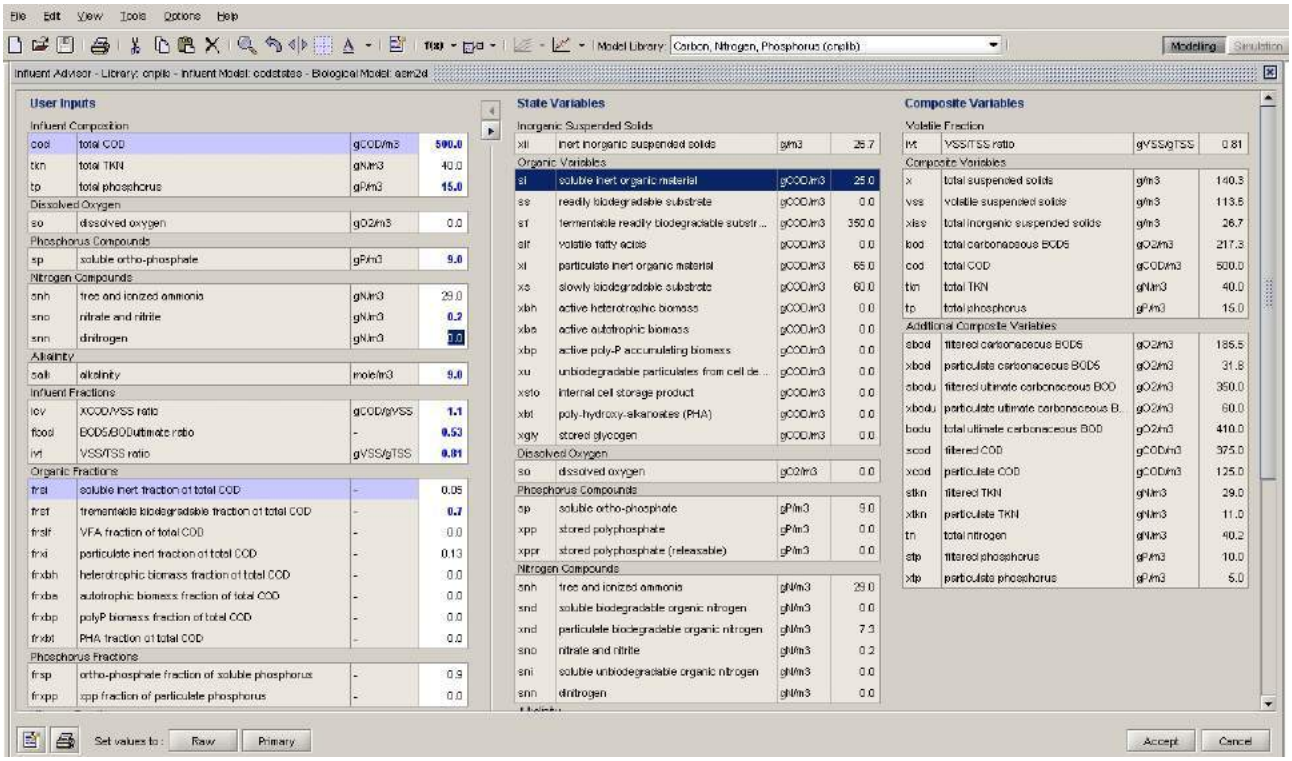

Fig. 9. Input data

Following the presentation of user inputs, state variables and composite variables, simulation will run.

3. Simulation of processes from WWTP

The process of simulation of waste water treatment plants begins, listing the values of waste water parameters monitored through simulation, before the evacuation (Fig. 10).

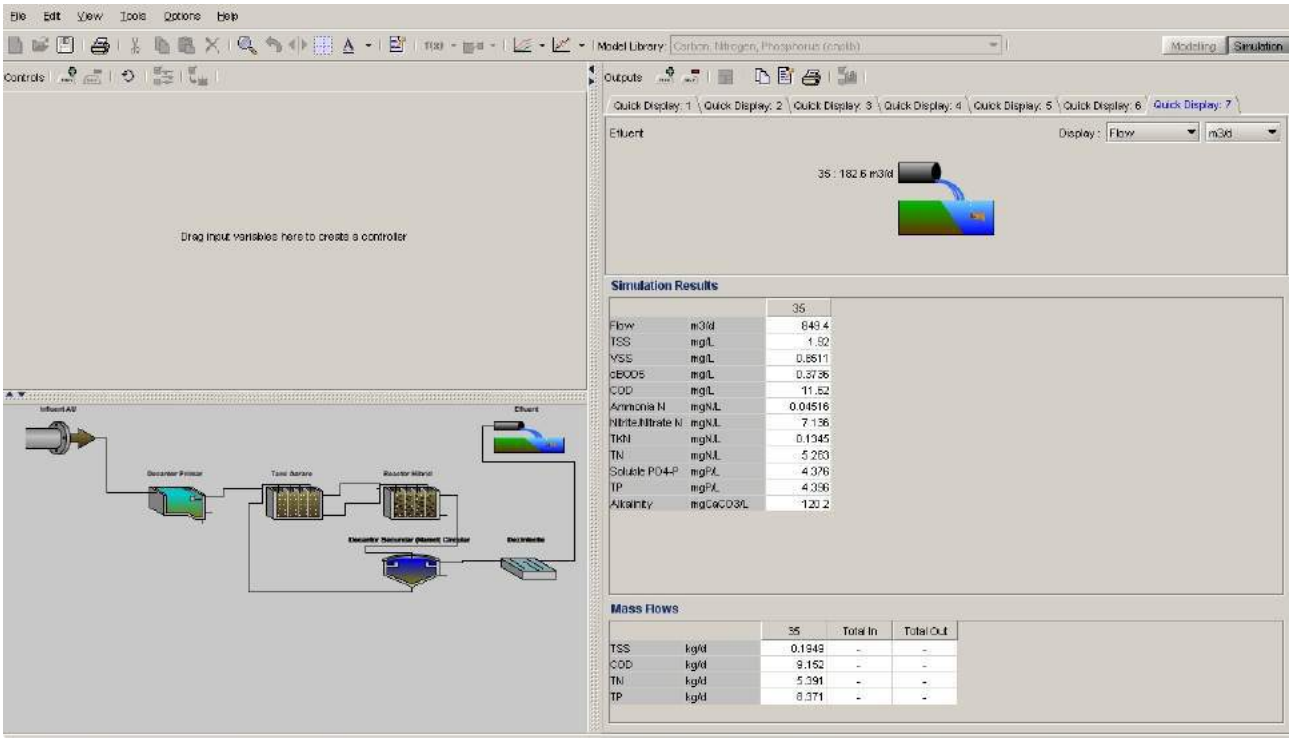

Fig. 10. The analyzed parameters of treated water

4. Results of simulation

The results of simulation are for: mass flow-influent (Fig. 11), primary settler (Fig. 12), operational data for primary settler (Fig. 13), operational results for aeration tank (Fig. 14), for hybrid reactor (Fig. 15), for biological reactor (Fig. 16), operational variables for secondary settler (Fig. 17), segregation mud in secondary settler (Fig. 18), operational data for disinfection (Fig. 19), effluent data in natural receiver (Fig. 20).

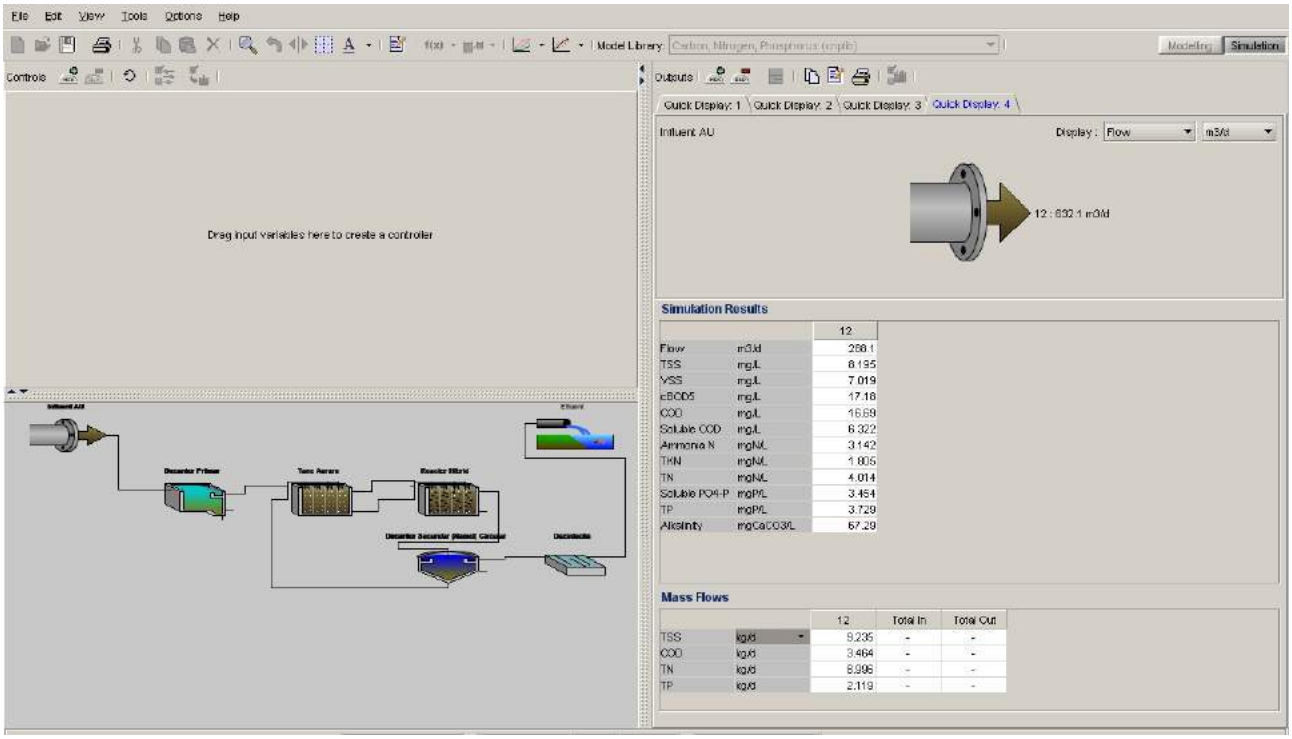

Fig. 11. Mass flow results

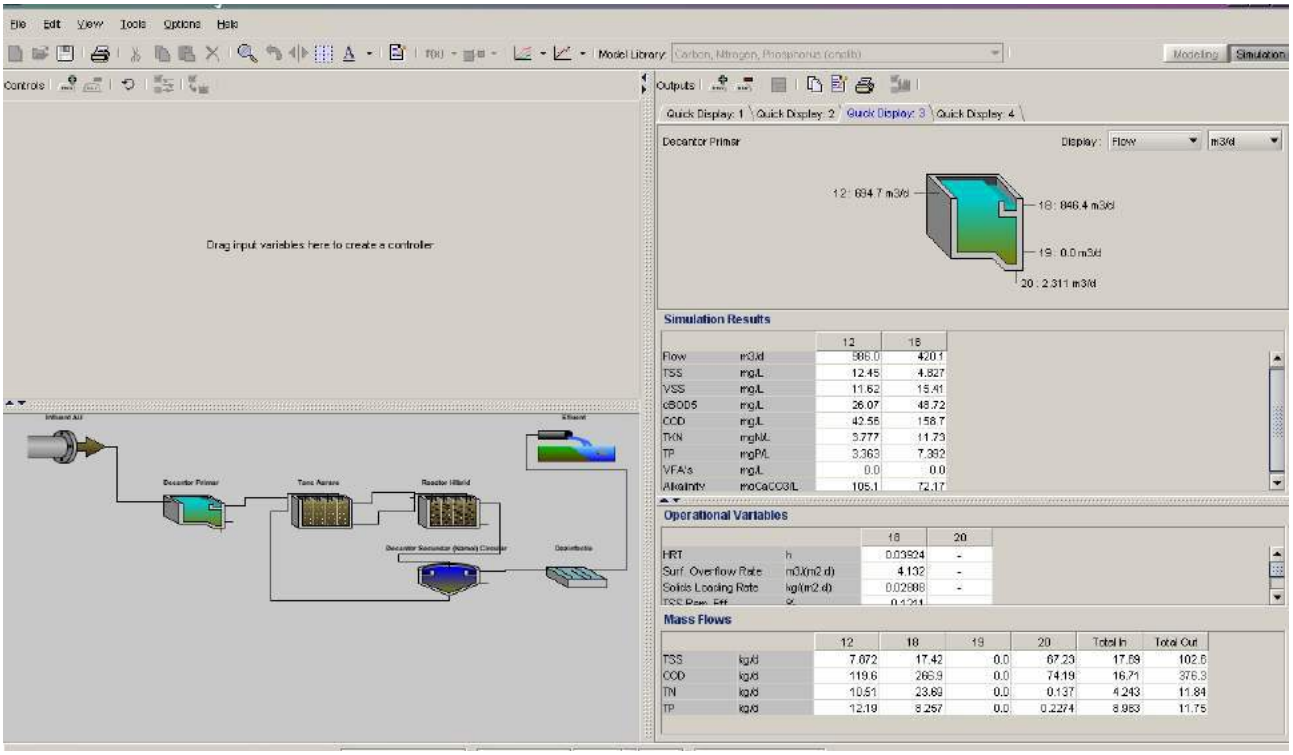

Fig. 12. Results for primary settler

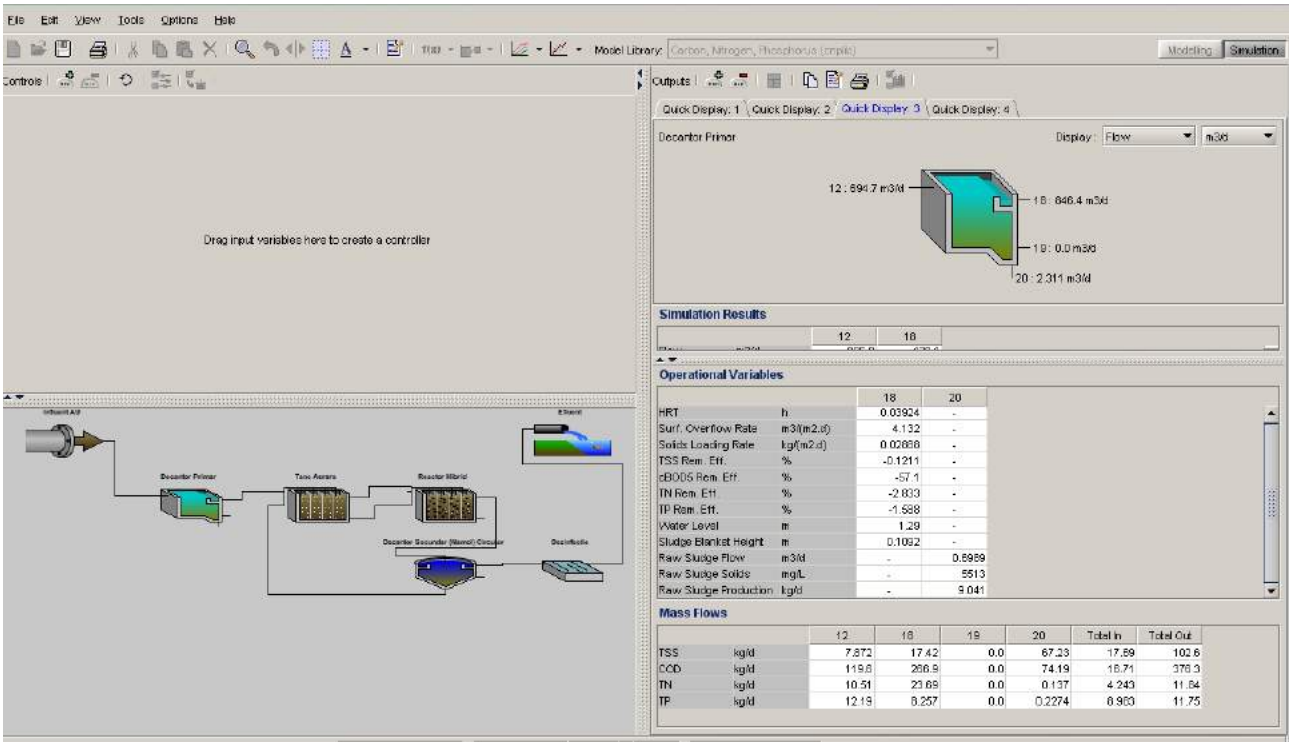

Fig. 13. Operational results for primary settler

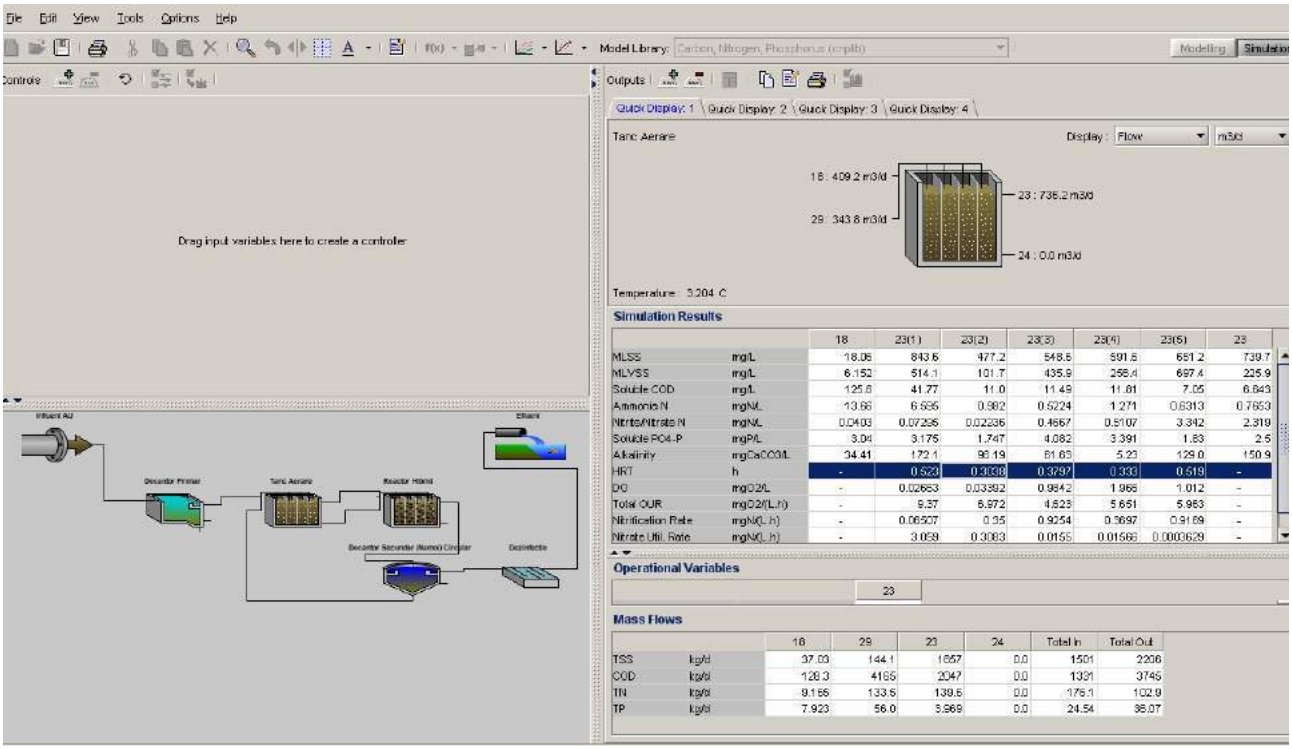

Fig. 14. Operational results for aeration tank

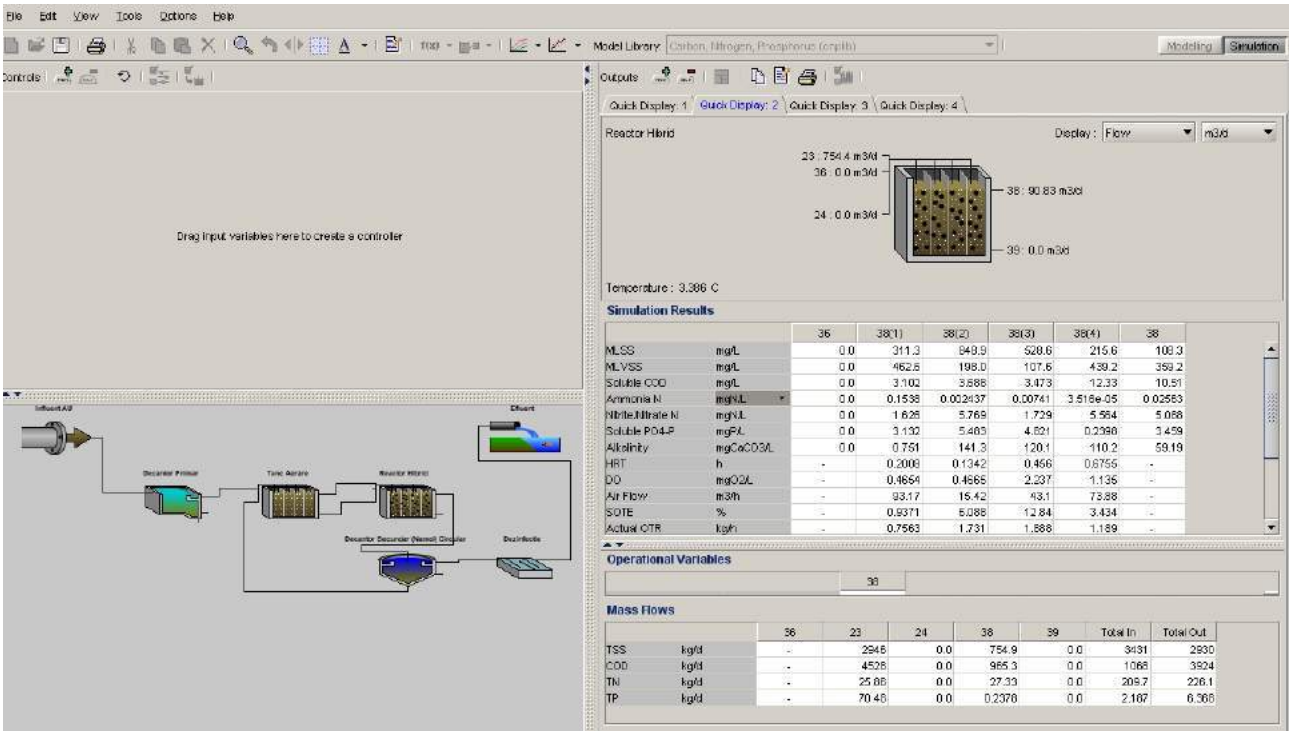

Fig. 15. Operational variables for hybrid reactor

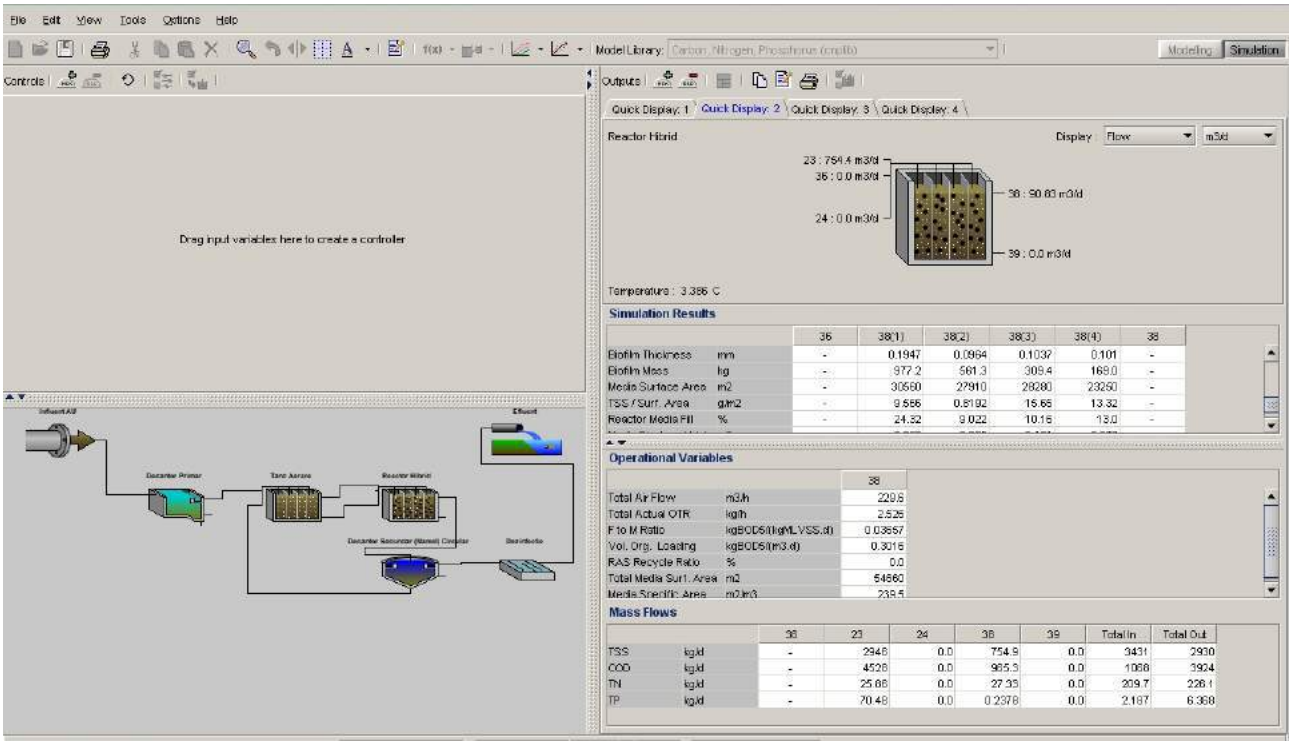

Fig. 16. Operational variables for biological reactor

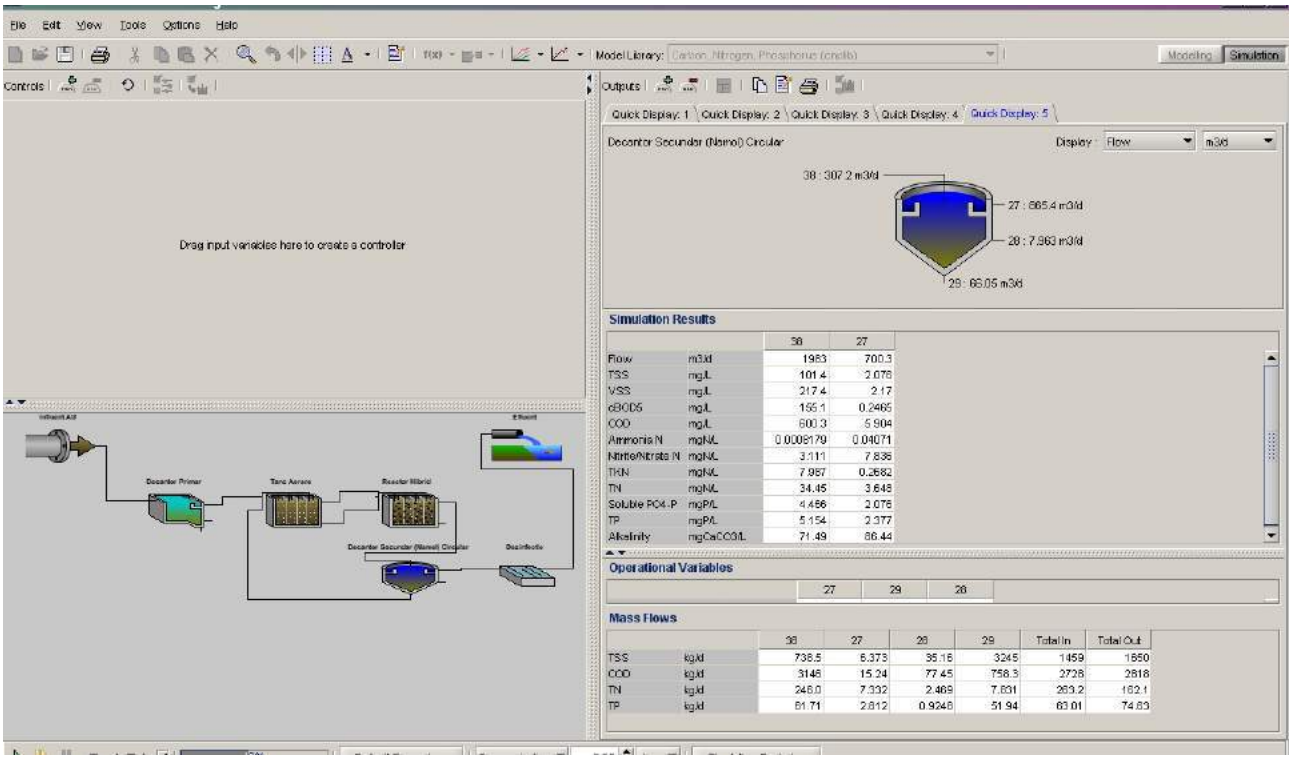

Fig. 17. Operational variables for secondary settler

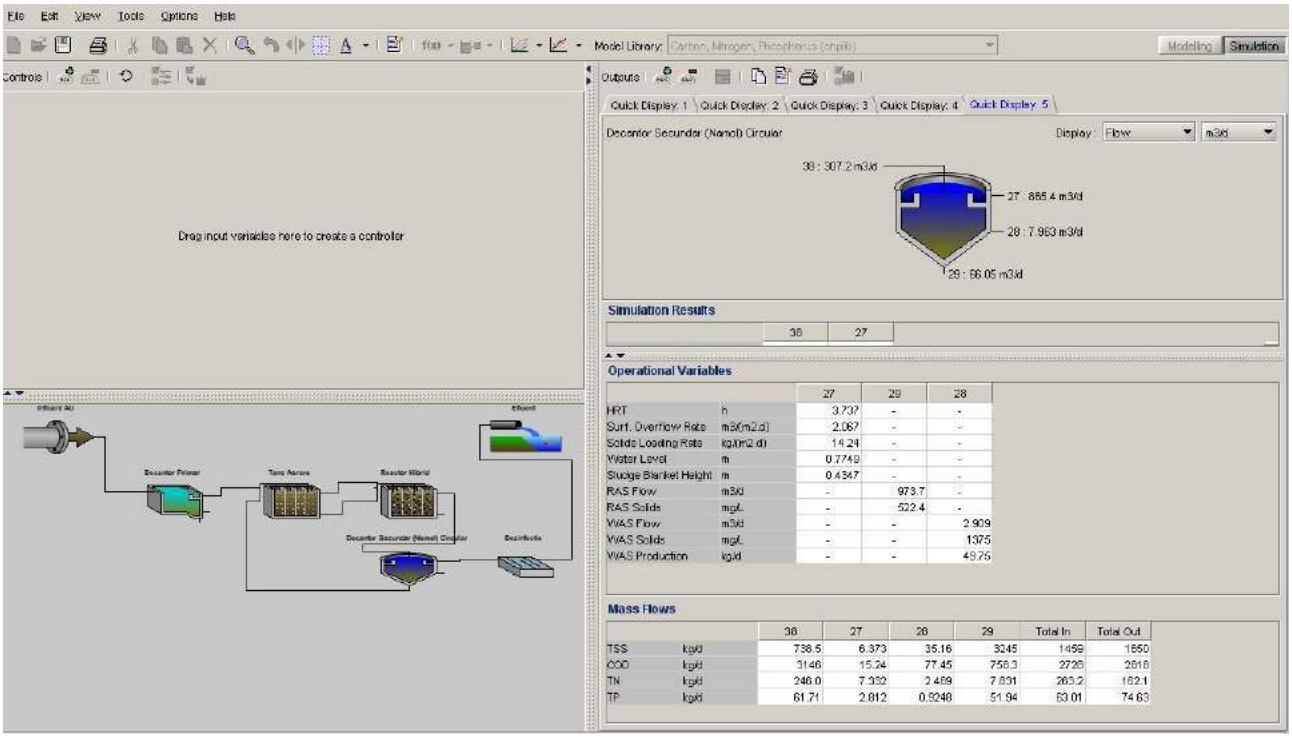

Fig. 18. Segregation mud in secondary circular settler

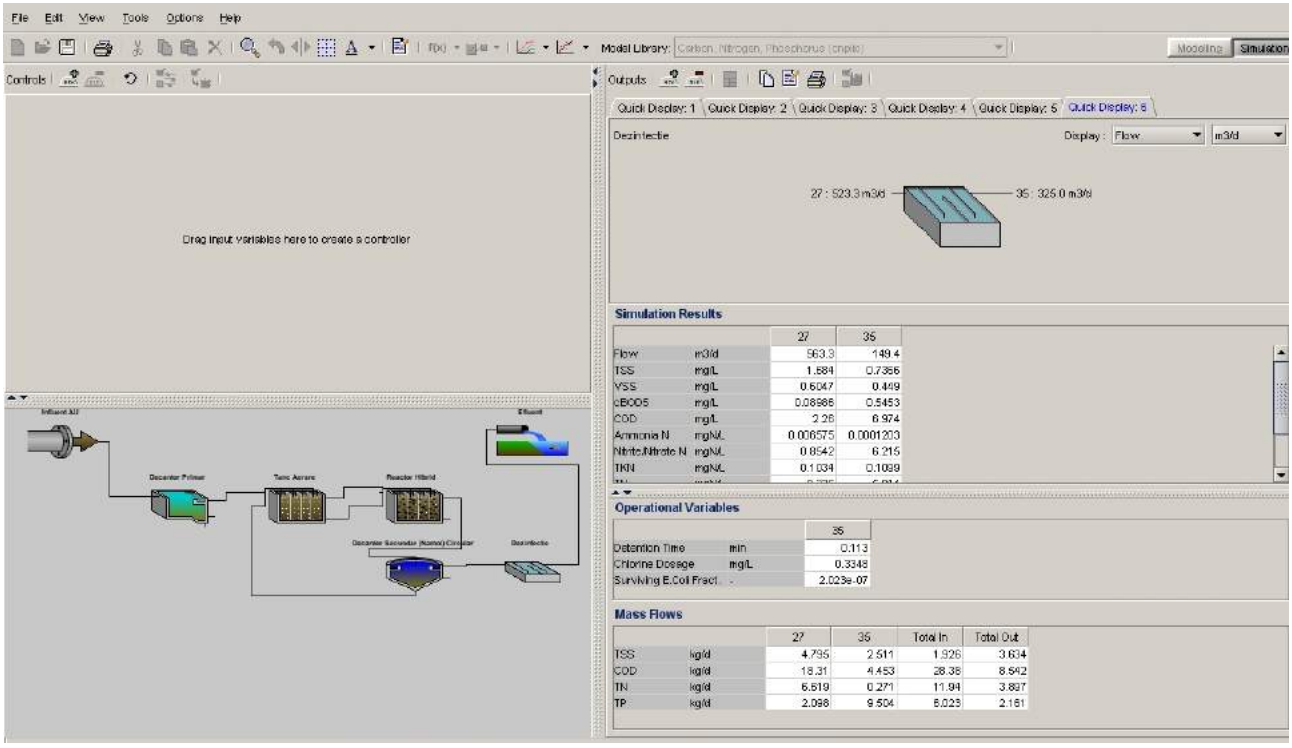

Fig. 19. Disinfection-operational data

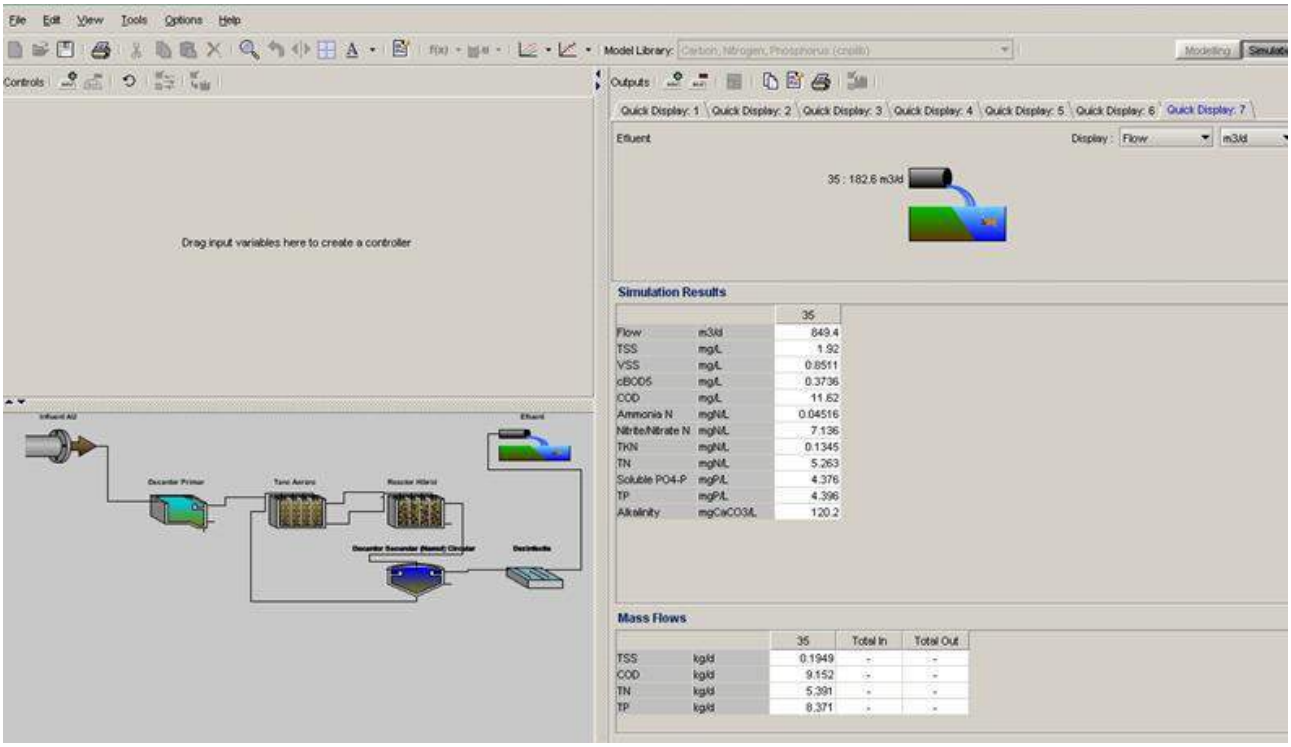

Fig. 20. Effluent data in natural receiver

5. Conclusions

It has been designed the flow station wastewater treatment plant.
Settings have been configured for installation components.
Subsequently input data have been changed according to the number of inhabitants, interchangeable.
Through simulation, it is an established type loading and subsistence change input data.
In the end, it runs the simulation process of waste water treatment plants, listing the values of waste water parameters monitored through simulation, before the evacuation into natural receiver.
Through this work it can be seen that the values of the analyzed parameters did waste water purified, to escape into natural receiver values are reduced from those set at the entrance of the plant, making it possible to obtain water purified according to standards in force.
Sustainable development implies the control of environmental pollution through the use of easy and efficient software tools.
GPS-X tools are very efficient tool for control of processes from waste water treatment plants and very useful instrument for operational training.

References

[1] D.Robescu, N.D. Robescu, "Modeling and simulation of the processes and treated technologies" („Modelarea si simularea proceselor si tehnologiilor de epurare"), Technical Publishing House, Bucharest, 2000;
[2] D.L. Robescu, "Similitudinea generală a proceselor de epurare a apei uzate", 2000, Bucharest, Romania; 26-27 May, 2000, *Proc. of First Confence of Hydroenergetics from Romania, vol. 2,* pp. 879-882;
[3] *** Wastewater Treatment Plant Optimization — November 2003, National Guide to Sustainable Municipal Infrastructure, Canada.

Increasing Energy Efficiency and Optimizing the Operation of Systems That Produce Clean Energy from Renewable Sources

PhD. Eng. **Corneliu CRISTESCU[1],** PhD. Eng. **Cătălin DUMITRESCU[1],**
Prof. PhD. Eng. **Valeriu DULGHERU[2],** PhD. Eng. **Teodor Costinel POPESCU[1]**

[1]Hydraulics and Pneumatics Research Institute INOE 2000-IHP, Bucharest; cristescu.ihp@fluidas.ro

[2]Technical University of Moldova, Chișinău; dulgheru@mail.utm.md

Abstract: *This paper presents some general issues regarding the development of research concerns in the field of renewable energy worldwide, as well as some research directions for increasing the efficiency of renewable energy conversion systems, addressed in the Institute INOE 2000-IHP in the field of energy efficiency and functional optimization of the systems that obtain clean energy from renewable resources. In the end, there are presented some techniques, methods and ways for optimization, in terms of structure and operation, of wind and hydraulic energy conversion parts and systems, and the paper denominates several practical achievements of the Technical University of Moldova in Chisinau, Republic of Moldova, which is the collaborator of the Institute in the implementation of a project on renewable energy.*

Keywords: *Renewable energy, energy efficiency, functional optimization, clean energy, wind energy, hydraulic energy*

1. Introduction

The concept of energy efficiency (or optimization of energy consumption) has currently become one of the main concerns of mankind across the globe.
Human society has become more aware of the need to develop a sustained strategy to increase energy efficiency and implement energy efficiency programs amid the worrying depletion of the Earth's fossil fuel reserves.
Today, we can talk about a global energy policy and a concerted strategy to reduce pollutant emissions into the atmosphere, both based on practical technical and economic solutions for the rational use of fossil fuel reserves (which still have the main share of energy production); we can also talk about increasing, on a wider scale, the use of renewable energy resources, the so-called "*clean*" energies or unconventional energies, an alternative to the current system of energy recovery of the Earth's fuel reserves. The environmentally friendly renewables (solar, wind, hydraulic, etc.) are today unable to cover these ever-increasing needs [1].
Renewable energy comes from natural resources that are constantly renewed over relatively short periods of time. Currently, the functioning of the world economy relies heavily on energy from non-renewable resources (coal, oil, natural gas). Factors such as greenhouse gas emissions that favour global warming (Figure 1), pollution, acid rain, all caused by the use of these conventional resources, but also the alarm signals that draw attention to the fact that oil - the main fuel source for transport - is about to run out, have triggered a significant global investment process in order to **capitalize on renewable energy resources** [2]. Renewable energy sources can be used both as centralized energy sources and, to a large extent, as decentralized sources. The latter are extremely advantageous especially for rural or isolated consumers, but there are special issues about operating stability and energy storage [1].
The year 2015 was an extraordinary one for renewable energy, with the largest global capacity additions seen to date, although challenges remain, particularly beyond the power sector. The year saw several developments that all have **a bearing on renewable energy**, including a **dramatic decline in global fossil fuel prices;** a series of announcements regarding the lowest-ever prices for renewable power long-term contracts; a significant **increase in attention paid to energy storage** [3].
Now, in the world annually there adds more renewable power capacity than it adds (net) capacity from all fossil fuels combined. In 2015, renewables accounted for an estimated more than 60% of net additions to global power generating capacity, and for far higher shares of capacity added in

several countries around the world. By year's end, renewables comprised an estimated 28.9% of the world's power generating capacity – enough to supply an estimated 23.7% of global electricity, with hydropower providing about 16.6%.
The top countries for total installed renewable electric capacity continued to be China, the United States, Brazil, Germany and Canada. China was home to more than one-quarter of the world's renewable power capacity–totalling approximately 495 GW, including about 296 GW of hydropower. Considering only non-hydro capacity, the top countries were China, the United States and Germany; they were followed by Japan, India, Italy and Spain, Figure 1.
Among the world's top 20 countries, for non-hydro renewable power capacity, those with the **highest capacity amounts per inhabitant** were: Denmark, Germany, Sweden, Spain and Portugal.

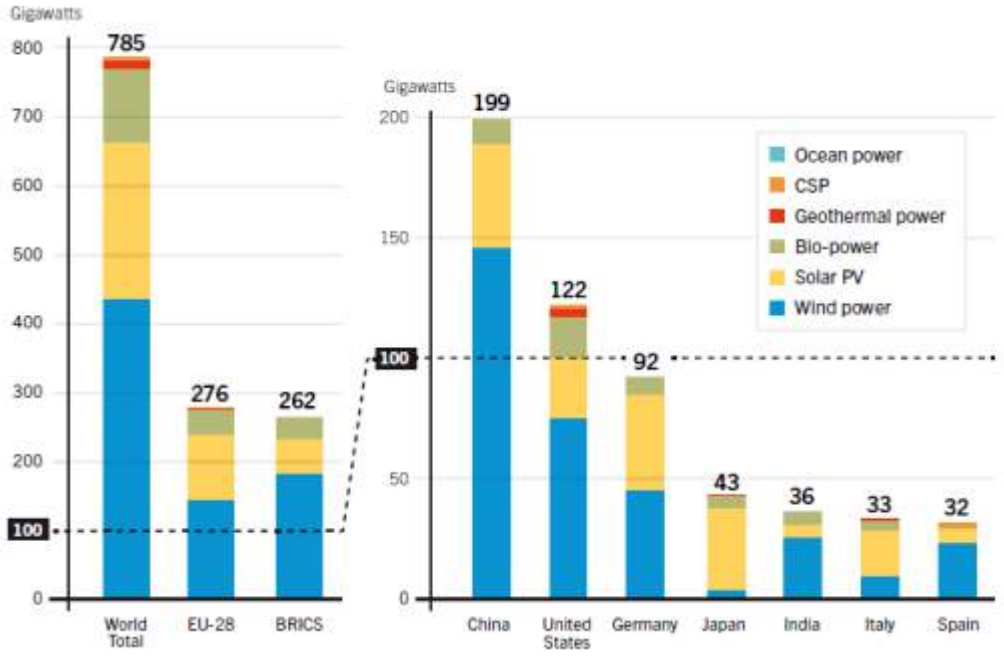

Fig. 1. Renewable Power Capacities in World, EU-28, BRICS and Top Seven Countries [3]

The **Wind and solar PV** both saw record additions for the second consecutive year, together making up about **77% of all renewable power capacity** added in 2015.
Renewables are now established around the world as **main-stream sources of energy**.
Emphasis on **activities to improve energy efficiency** in all sectors **increased during 2015** at all levels. There is growing recognition worldwide that **energy efficiency** can play **a key role** in reducing energy-related emissions and that it can provide multiple economy-wide benefit– such as enhanced energy security, reduced fuel poverty and improved public health [3].
In this context of the evolution of renewable energies, efforts of researchers in the field aim at **increasing the energy efficiency** of renewable energy conversion systems, identifying new technologies and improving the existing ones, through **analysis and optimization** of all technical and functional aspects, as we shall see below.

2. Research directions to increase the efficiency of renewable energy conversion systems

Given **the trend of continuous growth** of systems using renewable energy sources, respectively growth of the production of energy from these sources, a current but also prospective issue is, on the one hand, that of **increasing the efficiency of clean energy production systems,** and on the other hand, **optimizing their associated consumption**.
In this respect, for each type of system of obtaining energy from renewable sources, techniques, technologies and appropriate energy capture systems have been developed, but also **methods and techniques to increase the efficiency** and **optimize the associated consumption**.

To increase the efficiency, research has focused on **optimizing technical solutions of turbines and existing systems** which capture wind and hydraulic renewables, on the one hand, and on the other hand, on **identifying / designing new technical solutions of turbines and systems** which capture energy from wind and hydraulic sources.
Also there has been conducted research on **optimizing the associated consumption**, both to producers and consumers, in order to have, in the end, **higher energy efficiency. For the consumer,** it is essential **the amount of energy** delivered, the form of useful energy needed, how big energy losses are there and how much he has to pay for the energy delivered [1].
Energy, either fossil or renewable, **conversion methods** are characterized by **the efficiency factor *E*.** The higher the *E* efficiency, the less input primary energy will be spent to produce an output unit of energy [1].
The efficiency factor *E* is determined as the ratio:

$$E = (E_{useful} / E_{primary} \times 100 \quad [\%] \qquad (1)$$

Most of **the primary energy sources** on Earth are carbon-based fossil fuels. **Depletion of** oil and natural gas **reserves,** increased difficulties related to their capitalization, that will inevitably lead not only to **price increase** but also to awareness of **ecological disaster** to which mankind is heading, **will change the balance in favour of renewable energy sources** which are very environment friendly.
The issue of increased efficiency and **functional optimization** of renewable energy conversion systems **is very complex**; this is also due to the multitude of conversion technologies and equipment; therefore, only a few of them will be addressed in the following parts of the paper.
The main research directions for increasing efficiency and optimizing renewable energy conversion systems consist in:
- optimizing technical solutions for wind turbines and existing wind and hydraulic systems;
- optimizing hybrid systems provided with energy storage;
- designing new technical solutions for turbines and wind and hydraulic systems.

Here below are some of the world's concerns targeting increased efficiency and optimization of renewable energy conversion systems.

3. Optimizing the technical solutions for wind turbines and systems

Concerning the **generation and use of electricity** from **wind energy**, the world's undeniable leader is the EU-27 European community with a share of 65%, followed by the USA and India. No other global industry sector experiences such a spectacular development. *Wind energy is certainly one of the fastest growing technologies and it plays an important role, contributing to the creation of a sustainable and competitive energy policy in Europe* [1]. When settling a large number of wind turbines, the question that rises is related to **optimization of the wind farm** [4].
Thus, after **identifying a location** for the construction of a **wind farm**, we need to **analyze / verify the possibility for connection** or not of the wind farm to the electrical grid in the area. Another issue is related to **choosing the turbine type;** its **sizes**, and also **the number of turbines** are very important elements of optimizing a wind farm, figure 2.
It is also possible to **optimize the distances between the turbines**, to road access and to the grid. This optimization can reduce the cost of investment using **less material, shorter cable routing**; one can also better design the **access ways** and permanent or temporary **mounting platforms**.
The basic principle of a wind turbine has remained almost unchanged and consists of **two conversion processes** made by the main components, figure 3, [5]:
♦ **the rotor,** which **extracts the kinetic energy of the wind** and **converts it into generator torque**;
♦ **the generator,** which **converts this torque into electricity** and delivers it to the grid.

Fig. 2. Wind farm in California during winter [5]

Fig. 3. The structure of a wind power station [5]

The amount of electricity produced by a wind power station depends on the type and sizes of the turbine and also on the installation site. Although apparently unchanged, wind power station **technology** has received **a number of improvements**, being made both the **optimization of the basic components**, particularly the turbine, and the **optimization,** as a whole, of **operation of existing wind systems / power stations**. The latest achievements are equipped with a **tilt angle control device** which changes the angle of the rotor blade when there are unfavourable weather conditions.

3.1 Conversion of the kinetic energy of the airflow into mechanical energy. The Betz limit

As is known from the literature [1], actually, not all wind power can be converted into mechanical energy. When the air flows at a certain speed, the turbine converts only some of the kinetic energy of the air, and a considerable amount of energy will be retained in the air flow leaving the turbine, otherwise the turbine will not work. Figure 4 shows the variation in the specific power of a flow of air depending on the speed. The rated estimated wind speed for modern high-capacity turbines rages from 12.0 to 15.0 m/s (shaded area), and Figure 5 shows schematically an air flow at the initial speed *V0*, which crosses the circular area *A0* and interacts with the turbine rotor with the swept area *A1*. In the section *A1* the airflow encounters resistance, the pressure increases, and the speed drops to *V1*. Leaving some of the energy, the airflow leaves the turbine at speed *V2*, which is lower, resulting that *A2>A1>A0*.

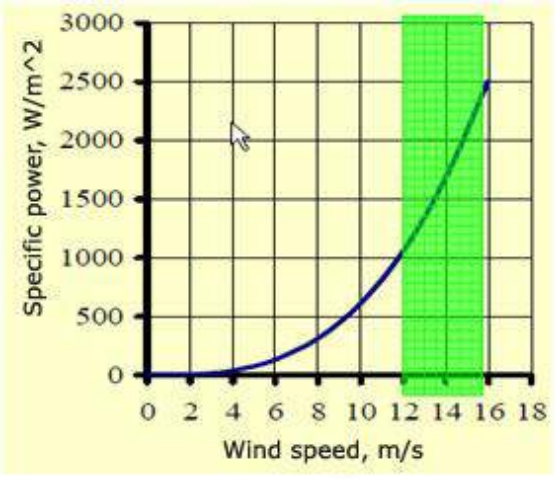

Fig. 4. Variation of specific airflow power [1]

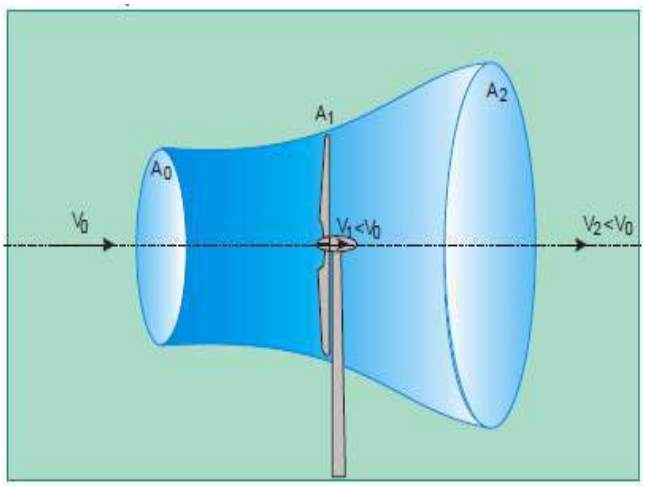

Fig. 5. Turbine effect on the airflow [1]

According to the theory of Betz (German physicist), the maximum theoretical power can be 59.3% of the flow power, but practically neither the best and optimized turbines can exceed 45-50%.

3.2 Determining the optimal number of blades in wind turbines

Betz's theory does not indicate the operation mode for the turbine or what construction the rotor should have so that the maximum power factor is reached. **Efficiency of airflow energy conversion** into mechanical energy will be **lower than the optimum value** if:

1. **The turbine rotor has a large number of blades** (the ratio of solidity is high) or the rotor rotates at a very high speed and each blade moves into an air flow disturbed (turbulent) by the blade in front of it;

2. **The turbine rotor has a small number of blades** (the ratio of solidity is low) or the rotor rotates at a very low speed and the air flow crosses the surface of the rotor without interacting with it.

It follows that, in order to obtain **maximum energy conversion efficiency**, **rotation speed of the rotor must be correlated with wind speed**.

To characterize wind turbines with different aerodynamic characteristics, the dimensionless parameter λ, called `tip speed ratio`, is used. Speed ratio connects in one formula three important turbine variables: rotation speed ω, the radius (or diameter) of the rotor R and wind speed V, and it is defined as the ratio of the linear velocity of the blade tip U and wind speed:

$$\lambda = \frac{U}{V} = \frac{\omega R}{V} \tag{2}$$

A turbine of some kind of structure can operate in a wide range of variation in tip speed ratio λ, but it will have maximum efficiency Cp only for an optimal value of tip speed ratio, in other words, if the linear speed U will be equal to the wind speed multiplied to the optimum value of the tip speed ratio.

Figure 6 presents the characteristics $Cp–\lambda$, taken from [6], for turbines with a different number of blades. Analyzing these features enables us to draw the following conclusions:

1. **The lower the number of blades**, the higher the optimal tip speed ratio for which the power factor or **the energy conversion efficiency is maximal**.

2. **Two turbines with equal power** but with a different number of blades differ in the fact that **the turbine with many blades will develop a high torque and will have lower rotational speed** and the other way around – the turbine with few blades will develop a small torque but will have a higher rotational speed.

3. **The three-bladed turbine** has **the highest efficiency factor**. The difference between the maximum efficiency factors of 2 to 5-bladed turbines is not significant. Advantages of turbines with a **small number of blades** consist of the possibility of operating in a **wider area of variation in tip speed ratio**, in which **the efficiency factor has a maximum value** or close to the maximum one.

4. The maximum efficiency factor (Betz) of the 12 to 18-bladed turbine is lower than the one of the 3-bladed turbine and does not exceed 0.35.

3.3 Optimizing the ratio of the power and the diameter of the turbine

The mechanical power generated by the turbine is proportional to the square of the rotor diameter. With increasing in diameter, respectively increasing in tower height, the wind speed will also increase. Small power turbines have towers with relatively greater heights than high power turbines. This is explained by the need to exclude the negative influence of the surface layer of the soil and the influence of obstacles on the wind speed. For rotor diameters between 5 and 10 m the ratio of the tower height to the rotor diameter is equal to 6 – 2. Starting with diameters equal to or greater than 30 m this ratio varies around number 1. Obviously, the specific costs of small turbines will be higher.

As said before, with increasing in diameter, respectively increasing in tower height, the wind speed will also increase. Usually, the increase in wind speed is considered proportional to the ratio of heights to the 1/7 degree [3, 5]. Thus the power of the turbine is proportional to the diameter of the rotor to the $(2+3\cdot1/7) = 2.42$ degree. For the turbines currently on the market a good approximation is given by the formula:

$$P = 0.06 \cdot D^{2.42} \tag{3}$$

in which *D* – is the diameter of the rotor, in m; *P* – power, in kW.
Figure 6 presents the qualitative and quantitative evolutions of power of modern turbines [1], [6]. The continuous line in Figure 7 corresponds to the analytical formula (3).

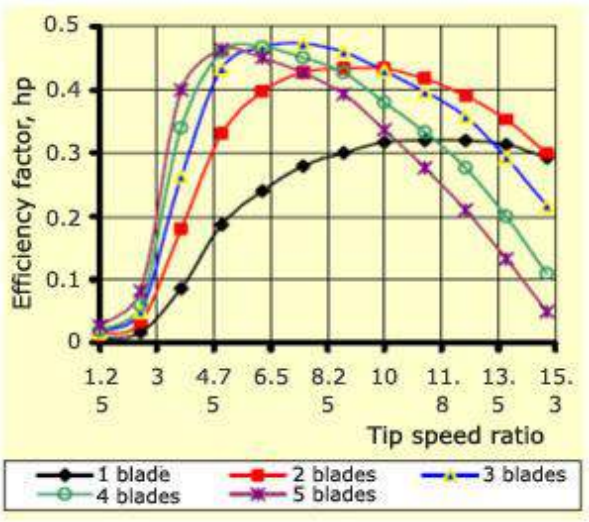

Fig. 6. Aerodynamic characteristics of wind turbines with different numbers of blades [1]

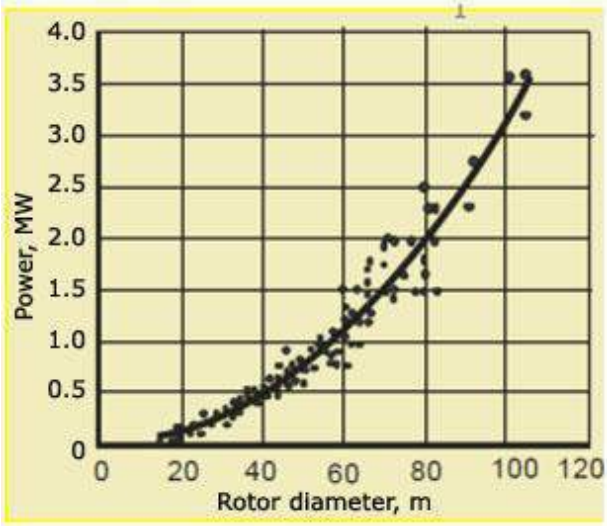

Fig. 7. The rated power of the turbines on the market relative to the rotor diameter [1]

Worldwide there is a tendency to increase the diameter of the rotor, even if the rated power remains the same.
The evolution of the wind turbine diameters over time is shown in Figure 8, [7].

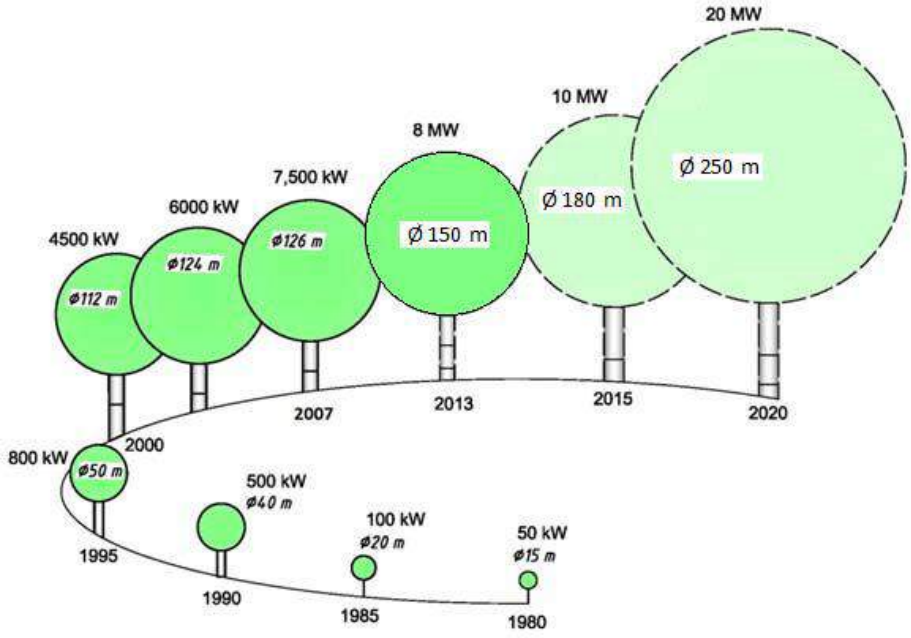

Fig. 8. Increase of the rotor diameter and the power of the turbines on the market [7]

Increasing rotor diameter leads to increased power extracted from the wind. But if the rated power remains the same, the estimated wind speed can be reduced. This increases the use of wind turbines, which may also include other areas with medium and low wind potential, where average wind speeds are somewhat lower, but can generate the same rated power, by using a larger wind turbine diameter.

Another important aspect, which should be optimized in functioning of wind turbines, is the noise that a careless design can generate. It is known that the linear speed of the blade tip is the product of the angular rotational speed of the turbine and the rotor radius. For example, for turbines with rated power of 0.6 – 3.6 MW the linear speed varies from 43.0 to 90 m/s (155 – 325 km/h).

Such linear speeds require a rigorous design of the aerodynamic profile, ensuring good blade surface quality and excellent rotor dynamic balancing. All these measures lead to a considerable reduction of noise, which allows the optimal location of modern wind turbines even around villages and towns.

3.4 Optimizing wind turbine operation by controlling power

The wind turbine will supply the rated power in the grid if the wind speed is equal to the calculation one, usually 11–15 m/s. For higher wind speeds, we need to limit the mechanical power, i.e. over-stress on the blades of the rotor, the multiplier, the generator, the tower, etc. This raises the need for turbine power control [1].

The most common are the following control methods:

1.- **Passive aerodynamic braking** (*passive stall control*);
2.- **Adjusting the angle of attack** (*active pitch control*);
3.- **Active aerodynamic braking** (*active stall control*);
4.- **Removing the turbine rotor from the direction of the wind** (*yaw control*)

1. Power control by using passive aerodynamic braking (passive stall control) is the simplest method and can be used for turbines with constant rotational speed, In other words, the speed of rotation does not depend on the wind speed or it varies insignificantly (1–2 %). The constant rotation speed of the turbine can be obtained in control systems equipped with asynchronous generators or synchronous generators connected directly to public electrical grids (Figure 9 b). The rotor blades are rigidly fixed and have an aerodynamic shape that ensures laminar flow of air for wind speeds ranging from the start speed *Vp* and the calculated one *Vc* (Figure 9 c). For wind speeds higher than *Vc* (Figure 9 a), the movement of the air flow above the blade becomes turbulent, the lift force decreases, and the resistance one increases, and respectively the mechanical power decreases.

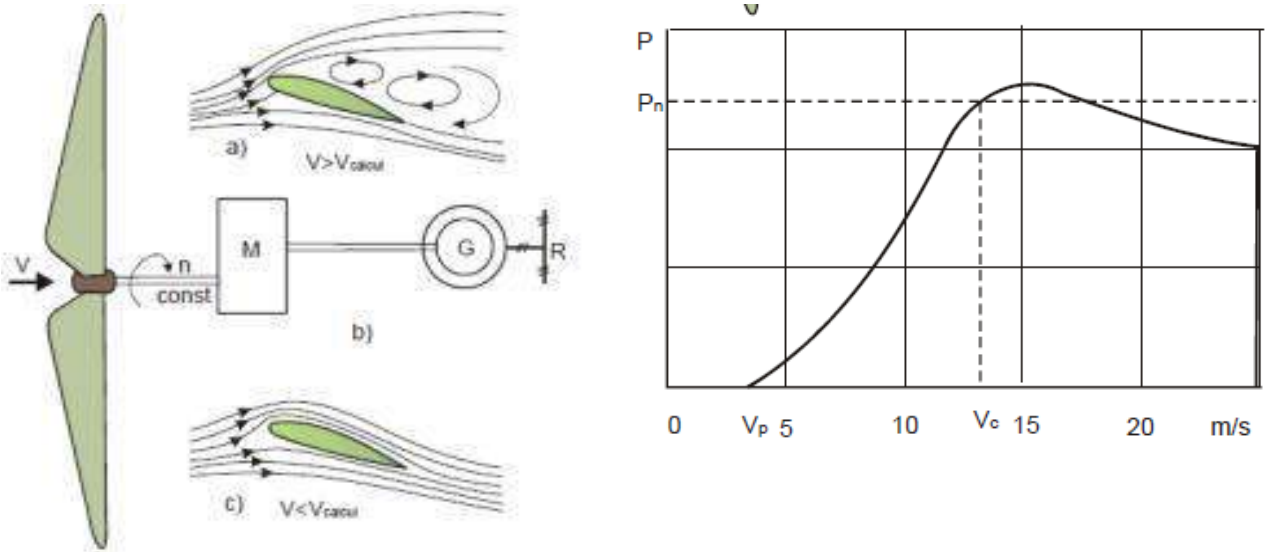

Fig. 9. The principle of controlling the power provided in the grid by using aerodynamic braking [1]

2. Power control by using adjustment of the angle of attack (active pitch control) is achieved by adjusting the angle of attack *α* (Figure 10 a). For this purpose the blade is rotated by a special mechanism around the longitudinal axis. The rotational speed of the turbine may be variable. To maintain constant frequency, the synchronous generator is connected to the grid via the frequency converter (Figure 10 b).

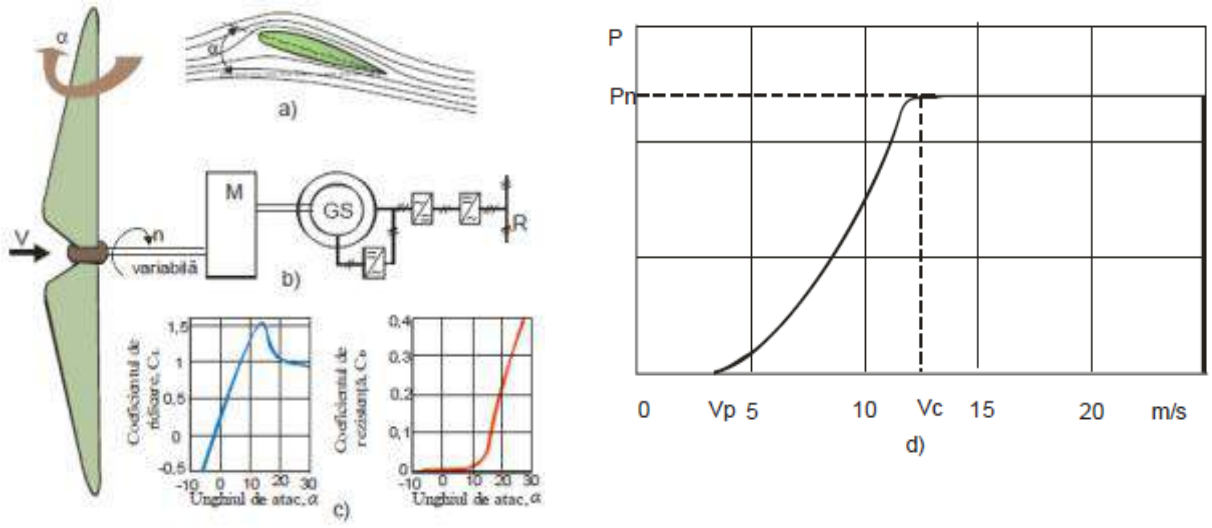

Fig. 10. The principle of controlling the power provided in the grid by using adjustment of the angle of attack [1]

For small attack angles ranging from 0 to 13 / 15 degrees, aerodynamic lift force increases linearly with increasing attack angles.
The main advantage of active angle adjustment is the reduction of mechanical stress on the blades, rotor and tower; at the same time it increases the efficiency of wind energy conversion at lower speeds than the nominal one by 2-4%.
Active aerodynamic braking is a combination of the two above-mentioned methods, namely aerodynamic braking and adjustment of the attack angle.

4. Optimizing the technical solutions for hydraulic turbines and systems

Hydraulic energy is the oldest form of renewable energy used by humans and currently has become one of the most commonly used renewable energy sources, being also one of the best, cheap and clean energy sources. **Hydraulic energy**, as a renewable energy source, can be captured under two extra-energy forms: **potential energy** (energy of freefall water) and kinetic **energy** (energy of water flows), with arrangements of different sizes [1].
Large hydropower is a **clean energy** source, uses **advanced technology**, being **the most efficient way to generate** electricity, as hydro power turbines **can convert up to 90% of the potential energy of the water** into electricity, but requires the construction of dams, which are very expensive, generating social and environmental problems as well.
For now, small hydropower plants, **micro hydropower,** are **not a major option** for the future in developed countries, for various reasons, such as the environment.
However, there is an increasing number of concerns in this regard.
More efficient use of hydraulic energy, in terms of ecological and social impact, is **conversion of the kinetic energy of flowing water of the rivers, without the construction of the dams**.
What are the main advantages of this type of energy? This is a **technology with enormous potential**, which must exploit the hydraulic resources to meet the needs, in the first place the needs of **rural consumers with low access** to conventional energy sources. The electric hydro micro-turbines are the most efficient and cheapest electricity generators.
Analysis of existing **micro-hydropower plants which convert the kinetic energy of flowing water** showed that **there are reserves to increase the efficiency** of the turbines used. The **Betz coefficient, equal to 0.593,** is **maximum theoretical efficiency of** hydraulic energy **conversion**. Most **existing systems provide** a coefficient of use of the kinetic energy of the water **within the range of 0.2.** Only some **modern systems exceed the efficiency of 30%.** In this line, there are **sufficient reserves to increase the efficiency of flow water turbines**, which are increasingly tempting for engineers and inventors in the field.

In this line, outstanding achievements have been made in the **Republic of Moldova**, which are a good example for **Romania** [1]. For this purpose, the Centre for the Development of Renewable Energy Conversion Systems (CESCER) has been established in the Technical University of Moldova; it benefits from **qualified human potential, high performance engineering design and research infrastructure.**

4.1 Micro-hydropower plant with vertical rotor shaft and hydrodynamic profile of blades

Of particular interest are floating micro-hydropower plants. In terms of costs, **the floating micro-hydropower plants** are more efficient because they do not include essential costs related to the construction of dams. To **avoid building a dam**, the kinetic energy of the river can be used by means of **water current turbines.** This type of turbine is easy to install, simple to operate and maintenance costs are convenient. The current speed of 1m / s represents an energy density of **500W/ m^2** of the cross section. **The main advantages** of these types of micro-hydropower plants are:
- low environmental impact;
- no civil engineering works are required;
- the river does not change its natural course;
- the possibility of using local knowledge to produce floating turbines.

Another important advantage is that it is possible to **install a series** of micro-hydropower plants along the river at short distances (about 30-50 m) as the influence of turbulence caused by neighbouring installations can be excluded. In order to increase the coefficient of conversion of the kinetic energy of water (the Betz coefficient) there have been **elaborated and patented a series of structural diagrams of floating micro-hydropower plants,** which include a **rotor with vertical axis** with **vertical blades** and **hydrodynamic profile** in the normal section. The blades are connected to each other by a mechanism for directing them towards the direction of the water currents. The nodes listed are fixed to a **platform** installed on floating bodies. **The platform is connected to the shore** via an articulated metal frame and strain relief cables, as one can see in the Figure 11.

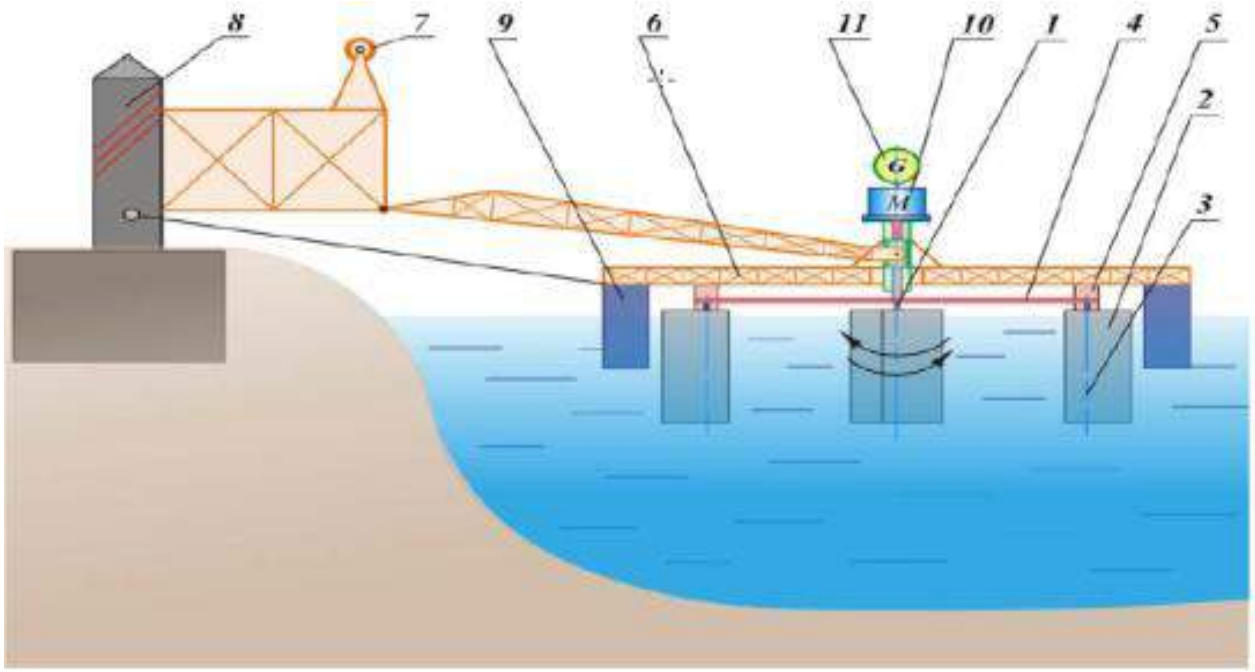

Fig. 11. Floating micro-hydropower plant with blade orientation mechanism [1]

Conceptual design of the rotor with hydrodynamic profile of the blades and adjustable to water currents is shown in the Figure 12, and positioning of the blade against the water currents - in the Figure 13.

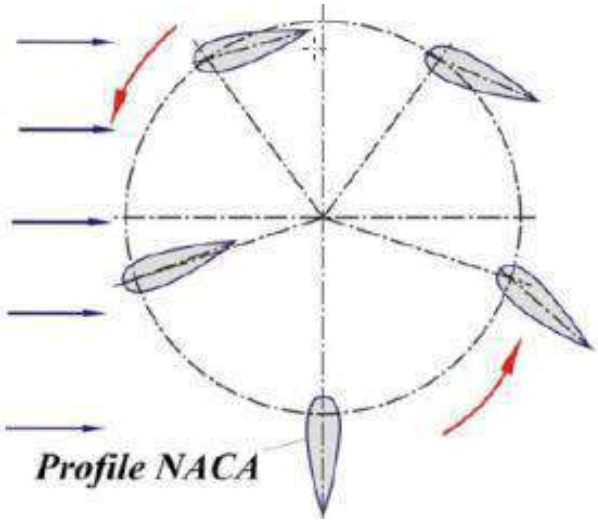

Fig. 12. Diagram of hydrodynamic profile adjustable blade rotor [1]

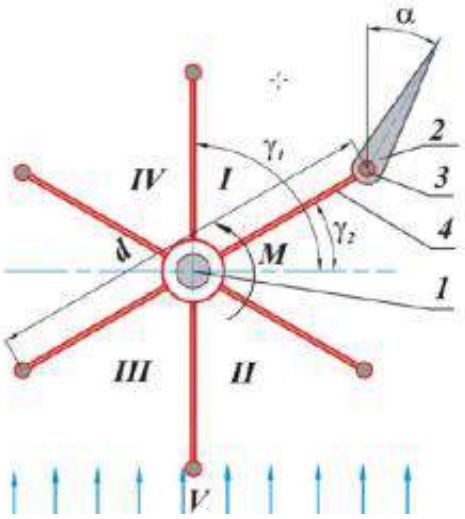

Fig. 13. Positioning of the blade against water currents [1]

The rotational movement of the rotor with a vertical axis is **multiplied** by means of a **mechanical transmission system** and it is conveyed to an **electric generator** or a **hydraulic pump** [1].

4.2 Structural and functional optimization of micro-hydropower plants

Structural and functional optimization of micro-hydropower plants is achieved by **choosing the optimal hydrodynamic profile of the blades**, which enables **increased conversion coefficient** (the Betz coefficient) due to **hydrodynamic buoyancy forces**. Increasing conversion rate is also achieved through **ensuring the optimal position of the blade** against water currents in various rotor rotation phases, using a blade orientation mechanism. Thus, virtually all blades (even those that move against water currents) **are simultaneously involved in generating torque** summary. The blades which move in the direction of the water currents use both hydrodynamic forces and water pressure exerted on the surfaces of the blades to generate the torque. The blades that move against the water currents only use hydrodynamic buoyancy forces to generate the torque. Due to the fact that the **relative speed of the blades** to the water currents **when the blades move against the water currents is virtually twice as big**, the hydrodynamic buoyancy force is relatively high, and the torque generated is commensurable with the one generated by water pressure [1].

In the micro-hydropower plant in the Figure 11**,** the turbine *1* includes the blades *2*, made with **hydrodynamic profile** and mounted on the axles *3*, fastened with the top in the extreme ends of the bars *4*, with the possibility of rotation around their axes. Position of the blades *2* at the angle α relative to the direction of flow of water is ensured by **the adjusting mechanism *5*.** The platform *6* is additionally secured with a winch *7*, fixed on the frame immovable on the shore pillar *8*. The turbine *1* together with the blades *2* is placed in the water stream of the river. The blade position relative to the water level is adjusted by the floating bodies *9* and by the blades *2* themselves, which are hollow. **The multi-blade rotor** is kinematically and coaxially connected through **the multiplier** *10* with the electric generator *11*. For technical servicing of the turbine *1*, which requires its removal from the water, the **winch** *7* is used. The blade *2,* in the Figure 13, is positioned against the water course at an angle *α,* which is variable depending on its position relative to the flow direction of the water.

As for the hydrodynamic rotor, to ensure for it maximum efficiency of kinetic energy conversion for each blade in different stages of rotation, there has been developed a **mechanism for blade orientation** relative to water currents; it has two configurations [8], as shown in the Figure 14:

1. Positioning of blades according to the angle of attack and the speed of water flows $V \leq 1.0$ *m/s* (Figure 14 a);
2. Positioning of blades according to the angle of attack and the speed of water flows $V > 1.0$ *m/s* (Figure 14 b)

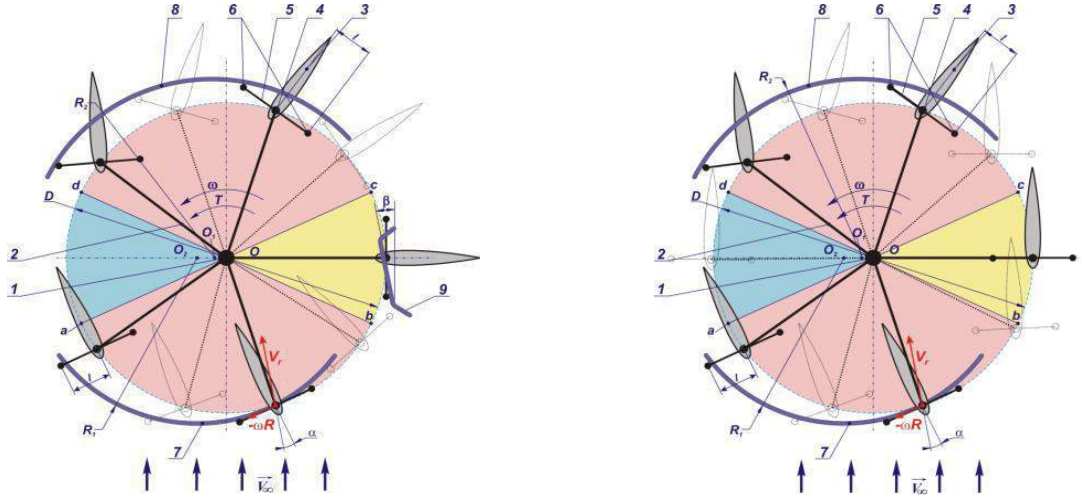

a) for a speed of water flows $V \leq 1.0$ *m/s* b) for a speed of water flows $V > 1.0$ *m/s*

Fig. 14. Diagram of the mechanism for continuous blade orientation relative to the direction of flow [8]

The difference is given by the positioning of the blade in the neutral zone, at the angle of attack **f**= 90^0*,* at a speed of water currents of $V \leq 1.0$ *m/s,* using the directrix *9* in the Figure 16 a, and in the latter case, the self-positioning of the blade in the neutral zone, at the angle of attack **f** = 0^0, takes place, and the directrix *9* is removed from the structure of the orientation mechanism. Thus, the orientation mechanism becomes a key mechanism in the optimal operation of the power plant.
In order to increase the coefficient of conversion of the kinetic energy of water a series of structural diagrams of floating micro-hydropower plants have been developed and patented; they include a rotor with a vertical axis with vertical blades and hydrodynamic profile in the normal section [8]. These optimized constructive solutions, some of them patented, have led to the **maximum energy efficiency** of turbines for running water. A series of theoretical and experimental research have also been carried out, resulting in optimization of the structural and functional parameters [9].
Following these theoretical and experimental research activities there has been achieved an experimental model of a hydrodynamic rotor micro-hydropower plant for converting the kinetic energy of the river into mechanical energy further used for pumping water, shown in the Figure 15, which has been located on the Prut River, Figure 16.

Fig. 15. Micro-hydropower plant with vertical rotor and blade with hydrodynamic profile [9]

Fig. 16. The industrial prototype of the micro-hydro power plant installed on the Prut River [9]

To achieve such performances, mathematical models, numerical methods and algorithms in CFD have been applied in the theoretical research for numerical simulation of turbulent flow in the hydraulic rotor area, especially near the hydrodynamic blades, namely through the boundary element method coupled with the Head model, implemented in the MATLAB software to simulate two-dimensional flow around the hydrodynamic blades, with preliminary determination of geometric, constructive and functional parameters [9]. Similar research has also been conducted in other areas of renewable energy sources, which also led to outstanding results in terms of increasing energy efficiency [7], [10], [11].

5. Conclusions

This paper has made an analysis of the methods of increasing energy efficiency and optimizing the operation of systems for clean energy production from renewable sources, being presented some practical examples in the sector of wind energy and hydraulic energy of running waters.
There has been presented the technical problem related to constructive solutions, methods and technologies for obtaining / capturing and storing energy from renewable resources, in order to increase the energy efficiency in capture, storage and reuse of renewable energies.
Worldwide, for each type of renewable energy system, appropriate energy capture techniques, technologies and systems have been developed, and also methods and techniques for increasing energy efficiency and optimizing their operation.
As a result of the global population growth and the decrease in oil and natural gas reserves, research and development have focused, in particular, on the field of renewable sources, which will ensure the energy future of mankind. In this line, the paper gives several research directions for increasing energy efficiency and optimizing renewable energy conversion systems, and in the end it presents some research and outstanding results achieved in the Technical University of Moldova in the Republic of Moldova, the collaborator of the Institute INOE 2000-IHP in the implementation of a project on renewable energy.

Acknowledgments

This paper has been developed in INOE 2000-IHP, as part of a project co-financed by the European Union through the European Regional Development Fund, under Competitiveness Operational Programme 2014-2020, Priority Axis 1: Research, technological development and innovation (RD&I) to support economic competitiveness and business development, Action 1.1.4 - Attracting high-level personnel from abroad in order to enhance the RD capacity, project title: *Establishing a high level proficiency nucleus in the field of increasing renewable energy conversion efficiency and energy independence by using combined resources*, project acronym: *CONVENER*, Financial agreement no. 37/02.09.2016.

References

[1] I. Bostan, V. Dulgheru, I. Sobor, V. Bostan, A. Sochireanu, "Renewable Energy Conversion Systems.- Wind, Solar, Hydraulic" („Sisteme de conversie a energiilor regenerabile - eoliană, solară, hidraulică"), Tehnica-Info Publishing House, Chişinău, 2017;
[2] E. Maican, "Renewable energy systems" („Sisteme de energii regenerabile"), Printech Publishing House, Bucharest, 2015;
[3] *** Renewables 2016 Global Status Report. REN21 Renewable Energy Policy Network for 21st Century. Paris, 2016; On: http://www.ren21.net/wp-content/uploads/2016/05/GSR_2016_Full_Report_lowres.pdf;
[4] *** Wind Power Energy. Cum se face optimizarea parcului eolian: Microsite-ing, 30 Oct. 2008; On: http://wpe.ro/cum-se-face-optimizarea-parcului-eolian-microsite-ing/;
[5] *** Wind and Solar. Why renewable Energy? In: Clean Line Energy Partners. http://www.cleanlineenergy.com/technology/wind-and-solar;
[6] T. Burton et al., "Wind Energy Handbook", John Wiley & Sons, New York, 2001, ISBN 0 471 48997 2; On: http://library.uniteddiversity.coop/Energy/Wind/Wind_Energy_Handbook.pdf;
[7] M. Guțu, "Optimization of aerodynamic blade resistance structure for wind turbines" („Optimizarea structurii de rezistenţă a palelor aerodinamice pentru turbine eoliene"), PhD thesis, Technical University of Moldova, Chişinău, 2017;
[8] Patent no. 601 Z, MD, F03B7/00; F03B13/18. Floating hydraulic power plant (Centrală hidraulică flotantă) / V. Bostan, O. Ciobanu, V. Dulgheru, A. Sochireanu, V. Gladîş, Published on 30.09.2013, BOPI no. 2/2013;
[9] O. Ciobanu, "Contributions regarding the research of the working body of the flow micro-hydropower plants" („Contribuţii privind cercetarea organului de lucru al microhidrocentralelor de flux"), PhD thesis, Technical University of Moldova, Chişinău, 2014;
[10] C. Cristescu, C. Dumitrescu, I. Ilie, L. Dumitrescu, "Hydrostatic transmissions used to drive electric generators in wind power plants", *Hidraulica Magazine,* No.1/2015, pp.60 – 72, ISSN 1453-7303;
[11] C. Cristescu, C, Dumitrescu, G. Vrânceanu, L. Dumitrescu, A-M. Popescu, "Combined energy systems for obtaining energy from renewable sources used in isolated areas", *Hidraulica Magazine*, No. 4/2016, pp.33 - 40, ISSN 1453 – 7303.